(A) SPIN AND SPIN REPRESENTATIONS

Spin is a fundamentally non-classical property of matter. It is like angular momentum in its algebraic properties, as well as its symmetries. In both cases one defines a vector operator ($\underline{L}$ or $\underline{S}$) which, when quantised, give a "ladder" of states. The crucial difference is that the ladder for spin is FINITE, and in the limit $\hbar \to 0$, spin disappears.

A.1 OPERATOR ALGEBRA for SPIN & ANGULAR MOMENTUM

We recall here the elementary results for angular momentum & spin algebra - these are covered in standard refs like Landau & Lifshitz [1], or Feynman [2]. The difference between spin & angular momentum is already clear in these fairly elementary results.

A.1.1 ANGULAR MOMENTUM

Angular momentum is a classical quantity - for a set of particles with canonical coordinates $\{ \underline{r}_j, \underline{p}_j \}$ in phase space we have

$$ \underline{L} = \sum_j \underline{r}_j \times \underline{p}_j \longrightarrow -i\hbar \sum_j \hat{\underline{r}}_j \times \underline{\nabla}_j \qquad (1) $$

where the second expression is the quantum-mechanical operator expression derived from the 1st classical expression.

From the usual result

$$ [\underline{r}_j, \underline{p}_j] = i\hbar \qquad (2) $$

which is equivalent to the result

$$ \underline{p}_j = -i\hbar \underline{\nabla}_j \qquad (3) $$

we derive the following set of results:

$$ \hat{L}_\alpha = \epsilon_{\alpha\beta\gamma} \hat{r}_\beta \hat{p}_\delta \qquad (e.g., \ \hat{L}_x = \hbar l_x = \hat{y}\hat{p}_z - \hat{z}\hat{p}_y) \ \Big\} \ (4) $$
$$ = \hbar l_\alpha $$

$$ [L_\alpha, r_\beta] = i\hbar \epsilon_{\alpha\beta\gamma} r_\gamma \qquad (e.g., [L_x, y] = i\hbar z) \qquad (5) $$

$$ [L_\alpha, p_\beta] = i\hbar \epsilon_{\alpha\beta\gamma} p_\gamma \qquad (e.g. \ [L_x, p_y] = i\hbar p_z) \qquad (6) $$

$$ [L_\alpha, L_\beta] = i\hbar^2 \epsilon_{\alpha\beta\gamma} L_\gamma \qquad (7) $$

where the subscripts α, β, γ.. label the directions x, y, z in orbital space/ real space. The angular momentum is quantized in units of $\hbar$. We also have

$$ [L^2, L_\alpha] = 0 \qquad (8) $$

$$ [L_\alpha^2, L_\beta] = i\hbar \epsilon_{\alpha\beta\gamma} [L_\alpha L_\gamma + L_\gamma L_\alpha] \qquad (e.g. \ [L_y^2, L_z] = i\hbar(L_x L_y + L_y L_x)) \qquad (9) $$

where the operator $\qquad L^2 = \sum_\alpha L_\alpha^2$ $\qquad\qquad\qquad\qquad$ (.10)

Thus the angular momentum components do not commute with each other, and this gives the algebra a quite different character from that of real space operators.

The "ladder operators" are
$$\left.\begin{aligned}\hat{L}_\pm &= \hbar \hat{l}_\pm = \hbar(\hat{l}_x \pm i\hat{l}_y) \\ &= \hat{L}_x \pm i\hat{L}_y\end{aligned}\right\} \quad (.11)$$

and they satisfy
$$[\hat{l}_+, \hat{l}_-] = 2l_z \qquad\qquad\qquad (12)$$
$$[\hat{l}_z, \hat{l}_\pm] = \pm l_\pm \qquad\qquad\qquad (13)$$

and we may write equivalently that
$$\left.\begin{aligned}\hat{l}_z &= \tfrac{1}{2}[l_+, l_-] \\ l_x = \tfrac{1}{2}(\hat{l}_+ + \hat{l}_-) \qquad l_y &= -i\tfrac{1}{2}(\hat{l}_+ - \hat{l}_-)\end{aligned}\right\} \quad (14)$$

and also note that
$$L^2 = L_z^2 + \tfrac{1}{2}(\hat{L}_+\hat{L}_- + \hat{L}_-\hat{L}_+) \qquad\qquad (15)$$

and that $\qquad [L^2, L_\pm] = 0 \qquad\qquad\qquad\qquad (16).$

Finally, note that we can also write, using (7), that
$$\hat{\underline{L}} \times \hat{\underline{L}} = i\hbar\hat{\underline{L}} \qquad\qquad\qquad\qquad (17)$$

A.1.2 ANGULAR MOMENTUM & ROTATIONS

$\qquad$ Starting again from the classical angular momentum we can discuss the angular momentum in terms of its canonical conjugate rotation variable. To properly derive this, we proceed, in classical mechanics, by noting that the angular momentum is the generator of rotations: if we rotate the system by an infinitesimal angle $\delta\underline{\phi}$, then the radial coordinate changes according to
$$\left.\begin{aligned}\underline{r} \to \underline{r}'(\delta\underline{\phi}) &= \underline{r} + (\underline{r} \times \delta\underline{\phi}) = \underline{r} + \delta\underline{r}\end{aligned}\right\} \quad (18)$$
and undo a finite rot^n $\underline{\phi}$, $\qquad r \to r'(\underline{\phi}) = \underline{r} - (\underline{r} \times \underline{\phi})$

which we write as $\qquad \underline{r}'(\phi) = \hat{R}(\underline{\phi})\underline{r} \qquad\qquad\qquad (19)$

where $\hat{R}(\underline\phi)$ is a rotation operator.

How then does a wave-function transform? Under $\delta\underline{\phi}$ we have
$$\left.\begin{aligned}\psi(\underline{r}) \to \psi(\underline{r}') &= \psi(r) + \delta\underline{r}\cdot\nabla\psi(\underline{r}) = \psi(r) - (\underline{r}\times\delta\underline{\phi})\cdot\nabla\psi(r) \\ &\equiv U(\delta\underline{\phi})\,\psi(\underline{r})^{\cdot}\end{aligned}\right\} \quad (20)$$

where the infinitesimal rot^n operator is

$$\hat{U}(\delta\underline{\phi}) = 1 - (r \times \delta\underline{\phi}).\underline{\nabla}$$
$$\equiv 1 + \delta\underline{\phi}.(\underline{r}\times\underline{\nabla}) = 1 + \frac{i}{\hbar}\underline{L}.\delta\underline{\phi} \qquad (21)$$

which we can also write in the form

$$-i\hbar\frac{\partial\psi}{\partial\underline{\phi}} = \underline{L}\psi \qquad (22)$$

showing that the angular momentum $\underline{L}$ is conjugate to the angle ϕ. We can if we wish write out this result in terms of the polar & azimuthal angles:

$$\hat{L}_z = -i\hbar\,\partial_\phi \qquad (23)$$

$$\hat{L}_\pm = i\hbar e^{\pm i\phi}\left[\cot\theta\,\partial_\phi \pm \partial_\theta\right] \qquad (24)$$

and, using (15),

$$L^2 = -\hbar^2\left[\frac{1}{\sin^2\theta}\,\partial_\phi^2 + \frac{1}{\sin\theta}\,\partial_\theta(\sin\theta\,\partial_\theta)\right] \qquad (25)$$

From (23) we can immediately show that the numbers arising from equations like (4), or (12)-(14), are integers. Consider the eigenvalue eqtn (22) written along the $\hat{z}$-axis:

$$-i\hbar\frac{\partial\psi}{\partial\phi} = \hat{L}_z\psi \qquad (26)$$
$$= \hbar\hat{l}_z\psi$$

The solution to the eqtn $-i(\partial_\phi\psi) = l_z\psi$ must have form $\psi = e^{il_z\phi}u(r,$
so that we immediately come to the conclusion that

$$l_z = m \qquad (m = 0, \pm1, \pm2, \dots)$$
$$L_z = \hbar m = M \qquad (27)$$

because ψ has to be single-valued.

It is fairly easy to demonstrate that the following results also derive from what we have so far. First, the eigenvalue of L^2 is uniquely given by

$$\hat{L}^2\psi = L(L+1)\psi = \hbar^2 l(l+1)\psi \qquad (28)$$
$$\text{where } l = 0, \pm1, \pm2, \dots$$

and for a given l, the values of m range over

$$-l \leq m \leq l \qquad (29)$$

so that for a given l, there are $(2l+1)$ possible values of m. Next, one can show that a complete set of states for the system is given

by a set of eigenfunctions $|L,M\rangle$, such that

$$\hat{L}^2 |L,M\rangle = L(L+1) |L;M\rangle$$
$$\hat{L}_z |L,M\rangle = M |L;M\rangle \tag{30}$$

These states are simply vectors in a $(2\ell+1)$-dimensional Hilbert space. More familiar to most is the inner product of these states with a set of states $|\theta,\phi\rangle$, which are localised at points on the unit sphere, according to

$$\langle \theta\phi | \theta'\phi' \rangle = \delta(\phi-\phi')\delta(\theta-\theta') \tag{31}$$

and where

$$\langle \theta\phi | L,M \rangle = Y_{\ell m}(\theta,\phi) \tag{32}$$

where $Y_{\ell m}(\theta,\phi)$ is the normalised spherical harmonic:

$$Y_{\ell m}(\theta,\phi) = \Theta_{\ell m}(\theta) \Phi_m(\phi)$$
$$= (-1)^m i^\ell \left[\frac{2\ell+1}{2} \frac{(\ell-m)!}{(\ell+m)!} \right]^{\frac{1}{2}} P_{\ell m}(\cos\theta) \frac{1}{\sqrt{2\pi}} e^{im\phi} \tag{33}$$

where we normalise $\Phi_m(\phi)$ as

$$\Phi_m(\phi) = \frac{1}{\sqrt{2\pi}} e^{im\phi} \tag{34}$$

and the $P_{\ell m}$ are the associated Legendre polynomials:

$$P_{\ell m}(\mu) = (1-\mu^2)^{m/2} \frac{d^m}{d\mu^m} P_\ell(\mu)$$
$$P_\ell(\mu) = \left(-\frac{1}{2}\right)^\ell \frac{1}{\ell!} \frac{d^\ell}{d\mu^\ell} (1-\mu^2)^\ell \tag{35}$$

in terms of the Legendre polynomials P_ℓ. The $Y_{\ell m}(\theta,\phi)$ satisfy the differential eqn

$$\hat{L}^2 \psi(\theta,\phi) = L(L+1) \psi(\theta,\phi) \tag{36}$$

from (30), which when written out using (25) becomes

$$\left[\frac{1}{\sin\theta} \partial_\theta (\sin\theta \, \partial_\theta) + \frac{1}{\sin^2\theta} \frac{\partial^2}{\partial\phi^2} + \ell(\ell+1) \right] \psi(\theta,\phi) = 0 \tag{37}$$

For a general understanding of angular momentum we do not need to remember the detailed form of these functions. Note the "orthogonality" relation

$$\langle L'M' | LM \rangle \equiv \langle L'M' | \theta\phi \rangle \langle \theta\phi | LM \rangle$$
$$= \int d\theta \sin\theta \int d\phi \, Y^*_{\ell'm'}(\theta,\phi) Y_{\ell m}(\theta,\phi) = \delta_{\ell\ell'} \delta_{mm'} \tag{38}$$

where we use the usual Dirac bra/ket notation & the "summation convention", according to which repeated indices or variables are summed/integrated over. Note also that an area element dS on the Bloch sphere is given by

$$dS = d\mu \, d\phi = \sin\theta \, d\theta \, d\phi \tag{39}$$

One can go on from here to study the algebra of pairs of angular moments, and so on.

Note finally that the classical limit for angular momentum, starting from a finite L^2, is given by

$$\left. \begin{array}{l} \underline{L} = \text{const} \\[2mm] \hbar \to 0 \qquad |\underline{\ell}| \cdot \ell \to \infty \end{array} \right\} \tag{40}$$

A.1.3 SPIN ALGEBRA

A lot of what is said above for angular momentum is also true for spin, except that the spin is entirely quantum-mechanical:

$$|\underline{S}| \xrightarrow[\hbar \to 0]{} 0 \tag{41}$$

Spin is not associated with an extended set of rotating particles – instead, it is considered to be a property of "elementary" particles, and these have definite values of spin.

We may therefore write

$$[\hat{S}_\alpha, \hat{S}_\beta] = i\hbar^2 \epsilon_{\alpha\beta\gamma} \hat{S}_\gamma \tag{42}$$

$$\hat{\underline{S}} = \hbar \underline{s} \tag{43}$$

$$[\hat{S}^2, \hat{S}_\alpha] = 0 \qquad\qquad [\hat{S}_\alpha^2, \hat{S}_\beta] = i\hbar \epsilon_{\alpha\beta\gamma} (\hat{S}_\alpha \hat{S}_\gamma + \hat{S}_\gamma \hat{S}_\alpha) \tag{44}$$

Moreover, all the relations in (10)-(17) also hold for $\underline{S}$ and $\underline{s}$, with the obvious substitutions $\underline{L} \to \underline{S}$ and $\underline{\ell} \to \underline{s}$.

However, an important part of the theory for angular moments is not directly applicable to spin states, just because we cannot simply write eqtns. like (22) or (26); spin is not considered to exist in real space.

In fact, one finds experimentally that spin is quantized in units of ONE HALF; we have

$$m_s = 0, \pm \tfrac{1}{2}, \pm 1, \pm \tfrac{3}{2}, \ldots \tag{45}$$

$$S_z = \hbar s_z = \hbar m_s \equiv M_s \tag{46}$$

Analogous results to (28)-(30) also follow, but we cannot treat the spin states in terms of the real space angular states as before.

Thus we have a set of states $|\chi(\underline{S})\rangle \equiv |S, M_s\rangle$, where

$$\hat{S}^2 |S, M_s\rangle = S(S+1) |S, M_s\rangle$$

$$\hat{S}_z |S, M_s\rangle = M_s |S, M_s\rangle$$

(47)

with
$$S = 0, \tfrac{1}{2}, 1, \tfrac{3}{2}, \ldots$$

$$-S \leq M_s \leq S$$

(48)

and we also have orthogonality of these states:

$$\langle S' M_s' | S M_s \rangle = \delta_{SS'} \delta_{M_s M_s'}$$

(49)

However, it should be noted that if we do perform a rotation in space, the spin state (usually called a "SPINOR") will transform. Since experimentally one finds that spin & angular momentum just add, to give a total angular momentum

$$\underline{J} = \underline{L} + \underline{S}$$

(50)

it follows that we still have
$$-i \partial_\phi \chi(\underline{S}) = m_s \chi(\underline{S})$$

(51)

in analogy with (22), but since m_s can take half-integer values, the spinor wave-function is not necessarily single-valued as before.

Of particular interest is the spin-$\tfrac{1}{2}$ system, with $m_s = \tfrac{1}{2}$, for which we have

$$\hat{S}_\alpha = \tfrac{1}{2} \hat{\sigma}_\alpha$$

$$[\hat{\sigma}_\alpha, \sigma_\beta] = i \epsilon_{\alpha\beta\gamma} \sigma_\gamma$$

$$\underline{S}^2 |\chi\rangle = \tfrac{3}{4} |\chi\rangle$$

(52)

where the $\{\hat{\sigma}_\alpha\}$ are the famous "Pauli spin operators". Note the following useful result, valid for any 2 vectors in "spin space", for spin-$\tfrac{1}{2}$ systems:

$$(\hat{\underline{S}} \cdot \underline{V}_1)(\underline{S} \cdot \underline{V}_2) = \tfrac{1}{4}(\underline{V}_1 \cdot \underline{V}_2) + \tfrac{i}{2} \underline{S} \cdot (\underline{V}_1 \times \underline{V}_2)$$

(53)

A.1.4. MATRIX REPRESENTATION & MATRIX ELEMENTS

Finally, we can evaluate the matrix elements of these various operators between the different states. The operators $\underline{L}^2$, L_z, $\underline{S}^2$, and S_z are diagonal in the representation given above, so we already have these results in eqtns. (30), (47), & (48). However we also need the matrix elements of other operators. These are easily derived and found to be as follows [next page]:

$$\langle M+1|L_x|M\rangle = \langle M|L_x|M+1\rangle = \frac{1}{2}\left[(\ell+m+1)(\ell-m)\right]^{\frac{1}{2}} \left.\right\} \quad (54)$$
$$\langle M+1|L_y|M\rangle = -\langle M|L_y|M+1\rangle = \frac{-i}{2}\left[(\ell+m+1)(\ell-m)\right]^{\frac{1}{2}}$$

and

$$\langle M+1|L_+|M\rangle = \langle M|L_-|M+1\rangle = \left[(\ell+m+1)(\ell-m)\right]^{\frac{1}{2}} \quad (55)$$

with analogous results for spin. In the special case of the spin-$\frac{1}{2}$ particle, we have $\hat{S}_\alpha = \frac{1}{2}\hat{\sigma}_\alpha$ from (52), with

$$\sigma_x = \begin{pmatrix} 0 & 1 \\ 1 & 0 \end{pmatrix} \qquad \sigma_y = \begin{pmatrix} 0 & -i \\ i & 0 \end{pmatrix} \qquad \sigma_z = \begin{pmatrix} 1 & 0 \\ 0 & -1 \end{pmatrix} \left.\right\}$$
$$\sigma_+ = \begin{pmatrix} 0 & 1 \\ 0 & 0 \end{pmatrix} \qquad \sigma_- = \begin{pmatrix} 0 & 0 \\ 1 & 0 \end{pmatrix} \qquad\qquad\qquad\quad (56)$$

as the representation of the Pauli matrices in the basis where $\hat{S}_z$ is diagonal.

A.2. COHERENT STATES for SPIN & ANGULAR MOMENTA

Although we introduced an abstract set of states $|\theta,\phi\rangle$ that were supposed to pick out a particular direction, these are not terribly useful because for any finite ℓ or S, we cannot form them using a set of spin wave-functions (this is obvious, since we have at most $(2\ell+1)$ or $(2s+1)$ orthogonal states, and there is no way we can make a δ-function on the Bloch sphere with these).

For this reason one defines a set of states which are peaked around a given direction, and which in fact give the best way of representing a "wave-packet" localised in some particular direction.

One way to define these is to start off with a state which is quite well localised along the $\hat{z}$-direction, and then rotate it around the sphere. Thus we start with the state

$$|S,S\rangle \equiv |S, M_s = S\rangle \quad (57)$$

and we rotate it to the direction we want by applying a rotation operator:

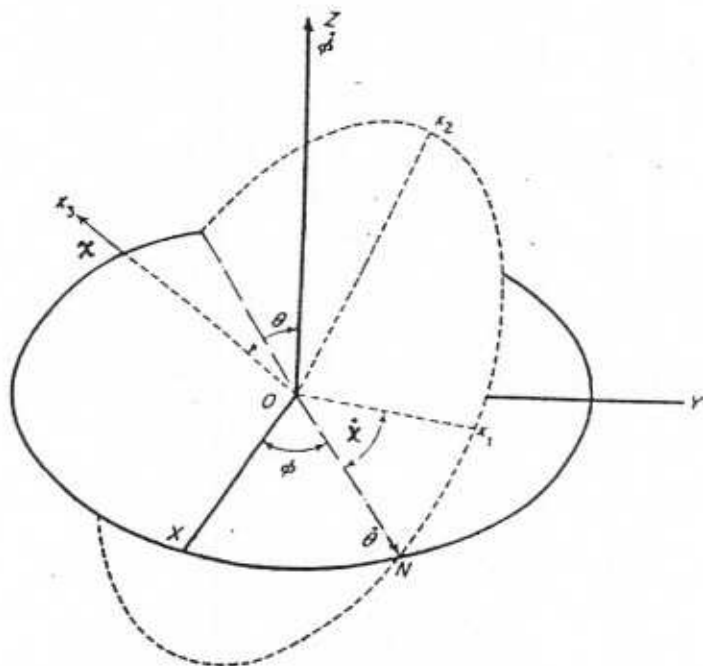$$|\underline{\Omega}_s\rangle = R(\hat{\underline{\Omega}})|S,S\rangle \quad (58)$$

where $\hat{\underline{\Omega}} = (\theta,\phi)$ is the direction of the state on the Bloch sphere.

The standard way of parametrizing rotations, in either spin or

orbital space, is to use the Euler angles — see Figure. The rotation operator can then be written in the form

$$R(\hat{\underline{n}}) = e^{iS_z \phi} e^{iS_y \theta} e^{iS_z \chi} \qquad (59)$$

in terms of the 3 Euler angles ϕ, θ, and χ. Note that the S_z operator is applied twice in this rotation operator.

There are various ways of deriving explicit expressions for the coherent states. Before beginning it is useful to recall some salient features of coherent states that are usually derived for the harmonic oscillator. Suppose we have an oscillator with ground state $|0\rangle$ and excited state $|n\rangle$. The entire set $\{|n\rangle\}$ with $n = 0, 1, \ldots \infty$ forms a complete set of states for the SHO.

THE EULER ANGLES

The the coherent states $|z\rangle$ for the SHO are defined as

$$|z\rangle = \frac{1}{\sqrt{\pi}} e^{-\frac{1}{2}|z|^2} e^{z a^+} |0\rangle \qquad (59)$$

and if we call that the SHO state $|n\rangle = \frac{1}{\sqrt{n!}} (a^+)^n |0\rangle$, we also have

$$|z\rangle = \frac{1}{\sqrt{\pi}} e^{-\frac{1}{2}|z|^2} \sum_{n=0}^{\infty} \frac{z^n}{(n!)^{1/2}} |n\rangle \qquad (60)$$

Note that $z = x + iy = z_0 e^{i\phi}$ is just a complex number — we have now moved the action to the z-plane, where in fact the coherent state functions look just like 2-d SHO wave-functions:

$$|z\rangle = \sum_{n=0}^{\infty} \psi_n(z) |n\rangle$$

$$\psi_n(z) = \frac{1}{\sqrt{\pi}} e^{-\frac{1}{2} z_0^2} \frac{z_0^n}{\sqrt{n!}} e^{in\phi} \qquad \left.\right\} \qquad (61)$$

It is easily verified that the z-states form a complete set of states — in fact they are overcomplete, since we not only have

$$\sum_{n=0}^{\infty} |n\rangle\langle n| = \int d^2z \, |z\rangle\langle z| = 1 \qquad (62)$$

but we also have a non-zero overlap between states of different z :

$$\langle z_1 | z_2 \rangle = \frac{1}{\pi} e^{-\frac{1}{2}(|z_1|^2 + |z_2|^2)} e^{z_1^* z_2} \tag{63}$$

Note that the completeness follows simply because the $\psi_n(z)$ are orthogonal, and so would happen no matter what set of $\{\psi_n(z)\}$ was chosen to make the $\{|z\rangle\}$ functions. The OVER-completeness follows because the dimension of z is larger than that of the original 1-d oscillator.

These are various reasons for choosing the $\psi_n(z)$ in the form given, which I won't go into here. Let us now turn to spin coherent states, which we develop first by direct analogy with oscillator coherent states. We define the _normalised_ states

$$|Z\rangle = \frac{1}{(1+|Z|^2)^S} e^{Z\hat{S}_-} |S,S\rangle \tag{63}$$

where $|S,S\rangle$ now acts as the vacuum state. If we write this as a sum over the states with different M we get

$$|Z\rangle = \frac{1}{(1+|Z|^2)^S} \sum_{m=-S}^{S} \left(\frac{(2S)!}{(S-m)!(S+m)!} \right)^{1/2} Z^{S-m} |S,M\rangle \tag{64}$$

To get a proper complete set relationship we must include a weighting function in the integration over Z; we have

$$\frac{2S+1}{\pi} \int \frac{d^2Z}{(1+|Z|^2)^2} |Z\rangle\langle Z| = \sum_{m=-S}^{S} |S,M\rangle\langle S,M| = 1 \tag{65}$$

At first glance it is not clear what this complex variable Z is supposed to represent, but it becomes clearer once we make the standard Riemann construction

$$Z = \tan \frac{\theta}{2} e^{i\phi} \tag{66}$$

which maps the Z-plane onto the unit sphere. We then find that on this Bloch sphere we can define a unit vector $\underline{n}$ with coordinates θ, ϕ as defined by (66), so that now

$$|\underline{n}\rangle = (\cos \frac{\theta}{2})^{2S} \exp\left[\tan \frac{\theta}{2} e^{i\phi} \hat{S}_- \right] |S,S\rangle \tag{67}$$

which, when written as a sum over M-states, gives

$$|\underline{n}\rangle = \sum_{m=-S}^{S} \left(\frac{2S!}{(S-m)!(S+m)!} \right)^{1/2} (\cos \frac{\theta}{2})^{S+m} (\sin \frac{\theta}{2})^{S-m} e^{im\phi} |S,M\rangle \tag{68}$$

with a completeness relation

$$(2S+1) \int d\underline{n}\, |\underline{n}\rangle\langle \underline{n}| \equiv (2S+1) \int \frac{d\phi\, d\theta}{4\pi} \sin\theta\, |\underline{n}\rangle\langle \underline{n}| \left. \right\} \tag{69}$$
$$= 1$$

14

All of this looks fairly complicated but will become clearer. From (68) we can calculate the overlap between 2 different states $|n_1\rangle$ and $|n_2\rangle$:

$$\langle \underline{n}_1 | \underline{n}_2 \rangle = \left[\cos\frac{\theta_1}{2} \cos\frac{\theta_2}{2} + \sin\frac{\theta_1}{2} \sin\frac{\theta_2}{2} e^{-i(\phi_1-\phi_2)} \right]^{2S}$$

$$\equiv \left(\frac{1 + \underline{n}_1 \cdot \underline{n}_2}{2} \right)^S e^{iS\beta_{12}} \qquad \qquad (70)$$

where

$$\tan\frac{\beta_{12}}{2} = \tan\left(\frac{\phi_1-\phi_2}{2} \right) \frac{\cos\left(\frac{\theta_1+\theta_2}{2}\right)}{\cos\left(\frac{\theta_1-\theta_2}{2}\right)} \qquad (71)$$

We see again that the coherent states are overcomplete. Now, suppose calculate the expectation value of the spin operators on these states. It is a useful exercise to show that

$$\langle \underline{n} | \hat{S}_z | \underline{n} \rangle = S \cos\theta$$
$$\langle \underline{n} | \hat{S}_\pm | \underline{n} \rangle = S \sin\theta \, e^{\pm i\phi} \qquad (72)$$

from which we immediately have

$$\langle \underline{n} | \hat{\underline{S}} | \underline{n} \rangle = S\underline{n} \qquad (73)$$

and one can show that more generally we can calculate expectation values of any spin operator $f(\underline{S})$ in the basis of coherent states :

$$\langle f(\hat{S}) \rangle = \sum_{MM'} \langle S,M | f(S) | S, M' \rangle$$
$$= (2S+1) \int d\underline{n} \, \langle \underline{n} | f(\hat{S}) | \underline{n} \rangle \qquad (74)$$

From these results the meaning of these functions starts to become a little clearer. From (73) it will be no surprise to find that if we apply the rotation operator in (59) to the state $|\underline{n}\rangle = |\hat{\underline{z}}\rangle \equiv |S,S\rangle$, we get

$$R(\hat{\underline{\Omega}}) | \hat{\underline{z}} \rangle = | \underline{n}_\Omega \rangle \qquad (75)$$

with $|\underline{n}\rangle$ pointed along the vector $\hat{\underline{\Omega}}$. A direct calculation of this result is lengthy, but we will see shortly how it can be made a little simpler.

From equation (70) we see that we can think of the spin associated with the coherent states as being attached to a region on the Bloch sphere around the direction $\underline{n}$, and spread out over an area of roughly $4\pi/S$. Alternatively we can think of expanding the sphere to a radius S, in which case the state extends over an area $\sim 4\pi$.

This spreading reflects the finite-dimensional nature of our Hilbert space — we only have a finite number $(2S+1)$ states available to properly define a given position on the Bloch sphere. Thus the "smearing" of the spin

coherent states $|n\rangle$ around the direction n on the Bloch sphere simply reflects the QM uncertainty in the definition of the spin.

I emphasize immediately that this does not mean that the actual coherent state wave-function is localised around the direction n on the Bloch sphere - only the spin is. To see this it is useful to draw a few pictures; we consider a spin $S = 10$ system.

$|Y_{10}^{10}(\theta,\phi)|^2$ $\qquad n$ $\qquad\qquad\qquad S(\theta,\phi)$ $\qquad\qquad n$
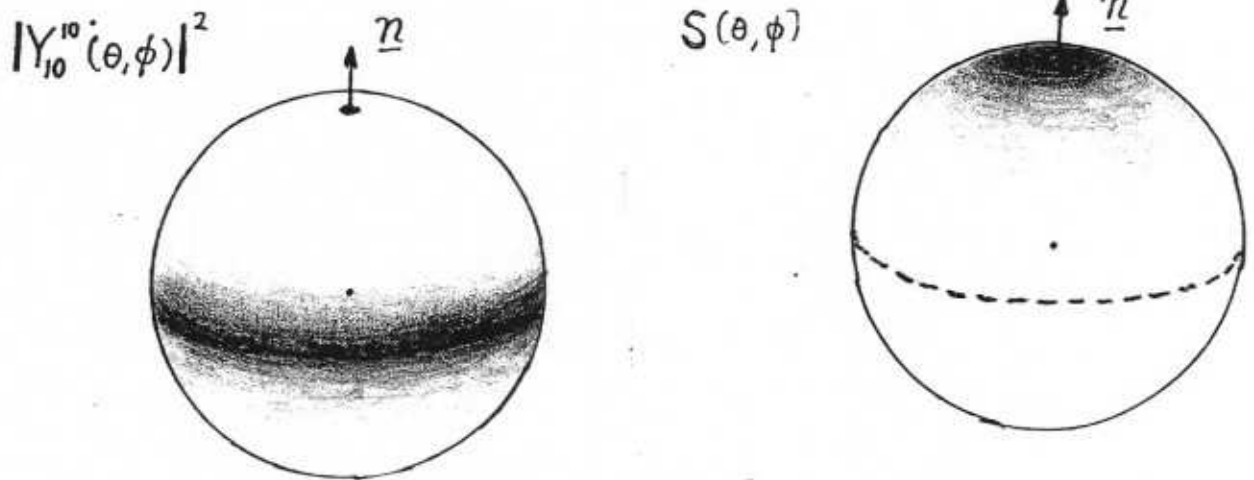
(a) Consider first the vacuum state $|S,M\rangle = |10,10\rangle$; this has the magnitude shown at left, with the spin density shown at right. We have a "current" circulating around the equator.

$S_{\uparrow+\downarrow}(\theta,\phi)$ $\qquad \hat{z}$ $\qquad\qquad\qquad |Y_{10}^{10} + Y_{-10}^{10}|$

$-\hat{z}$
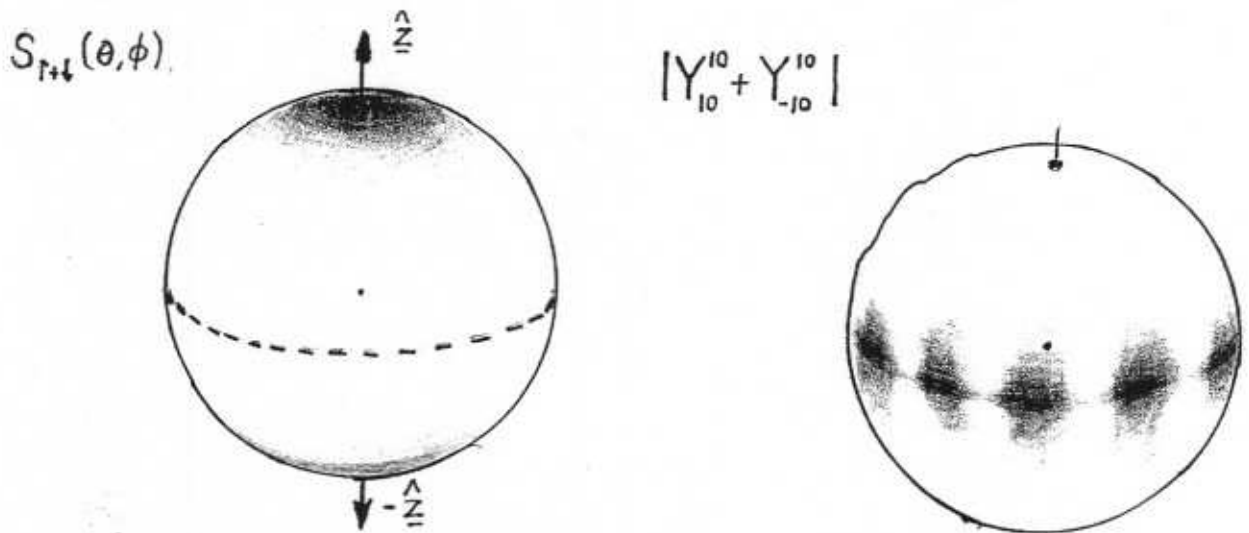
(b) Now suppose we form a superposition of states:

$$|\psi_{\uparrow+\downarrow}\rangle = \frac{1}{\sqrt{2}}\left(|10,10\rangle + |10,-10\rangle\right) \qquad\qquad (76)$$

From the point of view of spin, we are simply adding states which are polarised along $\hat{z}$ and $-\hat{z}$, hence the spin density shown at left. The actual coherent state wave-function is still concentrated around the equator, but now with a 'standing-wave' interference pattern between the 2 states.

We can of course superpose coherent states which are oriented in arbitrary directions; an example is shown at left. Although I have not drawn it, the coherent state wave-function for the sum of these is easily visualised — it is a sum of currents orbiting the 2 vectors $\underline{n}_1$ and $\underline{n}_2$, along the "equators" for these 2 vectors, and with interference between the two appearing where they overlap.

$S(\theta, \phi)$
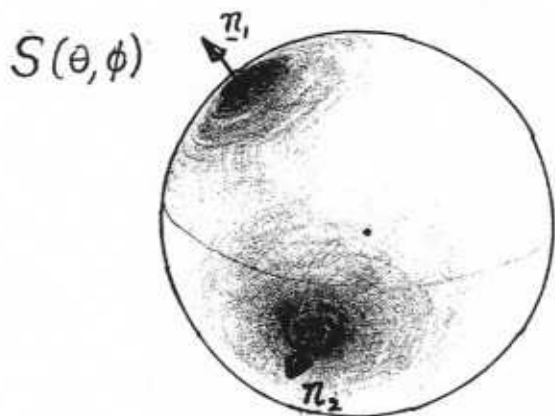
We shall see that the coherent state representation is particularly useful when we come to do semiclassical calculations for spin. In this context it is useful to look at the limit of large S, and look at bosonic representations for spin, which we now do.

A.3   BOSONIC REPRESENTATIONS for SPIN & ANGULAR MOMENTA

It is very tempting to try and construct either bosonic or fermionic reps. for spin degrees of freedom. As we shall see, certain problems arise when we try & do this, but nevertheless under the right circumstances these constructions are very useful, and when employed as part of a theory, lead to powerful methods of analysis.

We begin with 2 fairly well known representations, which we discuss for a single spin or angular momentum.

A.3.1   HOLSTEIN-PRIMAKOFF REPRESENTATION :

Suppose we again assume that our vacuum state is the "maximally up" state $|S, S\rangle$. Then it seems intuitively natural model small fluctuations about this state as though they were like small fluctuations of an oscillator. This tactic was first used in the very early days of quantum mechanics, and a particularly useful formulation was given by Holstein & Primakoff in 1940. We write

$$\hat{S}_z = S - b^+ b$$

$$\hat{S}^+ = (2S)^{1/2}\left[1 - \frac{1}{2S}b^+ b\right]^{1/2} b$$

$$\hat{S}^- = (2S)^{1/2} b^+ \left[1 - \frac{1}{2S}b^+ b\right]^{1/2}$$

$$(77)$$

where the bosonic operators satisfy the usual commutation relationships:

$$[b, b^+] = 1 \qquad\qquad [b, b] = 0 \qquad\qquad (78)$$

These expressions should only be used if the occupation number $n = \langle b^+ b\rangle$ is small, ie., $n \ll 2S$ (although in many applications it is actually found that accurate calculations can be done for quite large n). In this case it

makes sense to expand the square roots in $\hat{S}_{\pm}$, to get

$$\hat{S}_+ = (2S)^{1/2}\left[1 - \frac{1}{4S}b^+b - \frac{1}{32S^2}b^+bb^+b + \cdots\right]b$$

$$\hat{S}_- = (2S)^{1/2}b^+\left[1 - \frac{1}{4S}b^+b - \frac{1}{32S^2}b^+bb^+b + \cdots\right] \tag{79}$$

This "$1/S$-expansion" forms the basis of spin wave expansions and the theory of interacting magnons.

In passing, we note that these bosonic oscillator states are also obtained directly from the coherent spin states of the last sub-section. Suppose we write

$$z_s = (2S)^{1/2} z \tag{80}$$

where z is the complex variable which appears in the coherent spin state in (63). Now, if we take the lowest order term in the $1/S$ expansion (79) for S_- (i.e., that $\hat{S}_- = (2S)^{1/2}b^+$) we get for the coherent state in (63) that

$$|z\rangle \rightarrow |z_s\rangle \equiv \frac{1}{\left(1 + |z_s|^2/2S\right)^S}\, e^{z_s b^+}\,|0\rangle \tag{81}$$

where we have now renamed the vacuum state $\equiv |S,S\rangle \equiv |0\rangle$. In the large S limit

$$\left(1 + |z_s|^2/2S\right)^S \xrightarrow{S\to\infty} e^{\frac{1}{2}|z_s|^2} \tag{82}$$

so that $\quad |z_s\rangle \xrightarrow{S\to\infty} e^{-\frac{1}{2}|z_s|^2}\, e^{z b^+}\,|0\rangle \tag{83}$

so that we recover the SHO coherent state in (59) (apart from a normalization factor).

A.3.2 SCHWINGER BOSONS

We have already seen how it is possible to map between spin & oscillator states in one way, and in fact it is quite fun to play around with different possible ways of doing this. For example, you can verify quite easily that by writing some component of angular momentum $L_k = \epsilon_{ijk}\, r_i P_j$, and then writing this in terms of oscillator states, we end up with an expression like $L_k \propto i(b_j^+ b_i - b_i^+ b_j)$, in terms of 2 different bosons b_i and b_j.

The treatment of Schwinger is a refinement of this idea. We consider two sets of bosons, created by operators a^+ and b^+, and represent the spin operators as

$$\hat{S}_x = a^+b + b^+a \qquad\qquad \hat{S}_y = -i(a^+b - b^+a)$$

$$\hat{S}_z = \tfrac{1}{2}(a^+a - b^+b) \tag{84}$$

so that $\qquad \hat{S}_+ = a^+b$

$\qquad\qquad\quad \hat{S}_- = b^+a \tag{85}$

18

The vacuum state here is a little different, as we see if we construct the spin states that we are used to. The point is that we are not allowed to have no bosons in the system — some of the states must always be occupied. In fact we must have, from (86), a set $2S$ bosons at any time in the system, whereas the vacuum state has none. From (84) we have

$$|S, M_s\rangle = \frac{1}{\left[(S+m)!\,(S-m)!\right]^{1/2}} \left(a^+\right)^{S+m} \left(b^+\right)^{S-m} |0\rangle \qquad (87)$$

where $|0\rangle$ is the vacuum state.
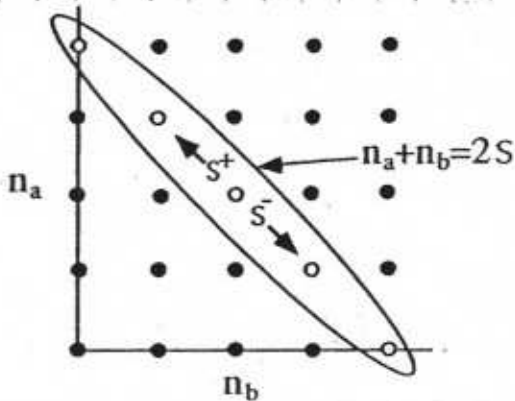
The rather peculiar construction of the Hilbert space is shown in the commonly-used diagram shown at left. Any ladder operator automatically increases one set of bosons, taking away from the other.

If we eliminate the "a" bosons using the constraint (86), we just get back the Holstein-Primakoff bosons, with $b_{\text{schwinger}} \leftrightarrow b_{HP}$, and

$$a = (2S)^{1/2} \left[1 - \frac{1}{2S} b^+ b\right]^{1/2} \equiv a^+ \qquad \Big\} (88)$$

A.3.3 SPIN ROTATIONS IN THE BOSONIC REPRESENTATIONS:

There is a very unwieldy algebra associated with rotations in spin space, but things are not quite so bad when dealing with bosonic representations. From what you know about spin algebra the following results may seem fairly obvious, but it is useful to derive them.

Consider again the rotation defined by the operator in (58). We wish to apply this either to a state like $|S, S\rangle$ (or perhaps even $|S, M_s\rangle$), or perhaps applied directly to one of the "excited" states. One way to do this is to start from the Schwinger boson representation itself, and ask how these operators transform. This must be a unitary transformation, and the standard result is that

$$R(\Omega) \begin{pmatrix} a \\ b \end{pmatrix} R^{-1}(\Omega) = \begin{pmatrix} \cos\frac{\theta}{2}\, e^{i\phi/2} & \sin\frac{\theta}{2}\, e^{-i\phi/2} \\ -\sin\frac{\theta}{2}\, e^{i\phi/2} & \cos\frac{\theta}{2}\, e^{-i\phi/2} \end{pmatrix} \begin{pmatrix} a \\ b \end{pmatrix} \qquad (89)$$

so that a pair of Schwinger bosons transforms as $a \to (u(\Omega)a + v(\Omega)b)$, and $b \to (-v^+(\Omega)a + u^+(\Omega)b)$, with

$$\begin{aligned} u(\Omega) &= \cos\frac{\theta}{2} e^{i\phi/2} \\ v(\Omega) &= \sin\frac{\theta}{2} e^{-i\phi/2} \end{aligned} \Bigg\} \qquad (90)$$

Actually this result is not quite the most general we can write down, as can be seen if we start from the form for $R(\Omega)$ in terms of Euler angles given in (59). Suppose, for example, we rotate from $\hat{z}$ to $\hat{n}$, so that we want to know what happens to operators like S_z. This transforms in the usual way

As $\hat{S}_z \rightarrow R(\hat{u})\,\hat{S}_z\,R^{-1}(\hat{u})$

$$\left.\begin{array}{l}\\[4pt]= \hat{\vec{S}}\cdot\hat{n} \equiv [\hat{S}_x\sin\theta\cos\phi + \hat{S}_y\sin\theta\sin\phi + \hat{S}_z\cos\theta]\end{array}\right\} \quad (91)$$

If we now compare this with what we get by direct application of (59), we see that we can actually have the more general result

$$\left.\begin{array}{l} u(\hat{u}) = \cos\tfrac{\theta}{2}\,e^{i\phi/2}\,e^{i\chi/2} \\[6pt] v(\hat{u}) = \sin\tfrac{\theta}{2}\,e^{-i\phi/2}\,e^{i\chi/2} \end{array}\right\} \quad (92)$$

This extra degree of freedom, the angle variable χ, is usually of no interest-. It is a "gauge variable", corresponding to rotations about $\hat{S}$, and usually we will fix $\chi = 0$.

Using these results we can now also re-derive our previous result for the form of the coherent state vector $|n\rangle$ [see eqns (67) and (68)]. To do this, we note that in Schwinger boson language, using (87), we have

$$\left.\begin{array}{l}|\bar{n}\rangle = \dfrac{(\hat{u}\hat{a}^{+} + v\hat{b}^{+})^{2S}}{(2S!)^{1/2}}\,|0\rangle = \dfrac{(\tilde{a}^{+})^{2S}}{(2S!)^{1/2}}\,|0\rangle \\[12pt] = \displaystyle\sum_{s}^{m=-s} u^{S+m}\,v^{S-m}\left(\dfrac{2S!}{(S-m)!\,(S+m)!}\right)^{1/2}|S,M_s\rangle\end{array}\right\} \quad (93)$$

where $\tilde{a} = R\,\hat{a}\,R^{-1}$ is the transformed operator, and the u and v are as in (90).

Note that the result (93) is precisely what we derived in (68).

A.3.4 MAJORANA SPINS or BLOCH SPHERE :

Finally I discuss quite briefly a rather cute representation of a general spin state for a spin-S system, due to Majorana in 1932.; it seems to be very little known. (and should not be confused with the Majorana spins commonly used in the theory of strongly correlated systems).
The general idea can be expressed by taking a single spin, and writing the general state:

$$|\psi\rangle = \sum_{s}^{m=-s} \alpha_m\,|S,M_s\rangle \quad (94)$$

where the $\{\alpha_m\}$ are all complex, and $\sum_m |\alpha_m|^2 = 1$. Now define the polynomial

$$P(x) = \sum_{s}^{m=-s} C_m\,x^{S-m} \equiv C_0 + C_{-1}x + C_{-2}x^2 + \cdots C_S\,x^{2S+1} \quad (95)$$

$$C_m \equiv \left(\dfrac{2S+1}{S-m}\right)^{1/2}\alpha_m \quad (96)$$

which has the complex roots $\{z_j\}$:

$$P(x) = (x-z_1)(x-z_2)\cdots(x-z_{2S+1}) \quad (97)$$

In equations (95) and (96), the number C_m^{2S+1} is just a binomial coefficient, i.e.,

$$C_m^n = \frac{n!}{m!\,(n-m)!} \tag{98}$$

Thus the polynomial $P(x)$ is a type of generating function for the state $|\psi\rangle$ and its coefficients.

Now we can take the $2S+1$ complex roots of $P(x)$ and map them back onto the Bloch sphere using the Riemann construction in (66). This then defines our original state as a set of $2S+1$ points on the Bloch sphere (rather than a single point, as was done for the coherent state $\hat{n}$).

The inner product between 2 states $|\psi_A\rangle$ and $|\psi_B\rangle$ is then given by

$$\langle \psi_A | \psi_B \rangle = \sum_M A_m (C_m^A)^* (C_M^B) \left.\vphantom{\begin{array}{c}a\\a\\a\end{array}}\right\} \tag{99}$$

$$A_t = (-1)^{S-m}\, 1/(C_{S-m}^{2S+1})^2$$

We may at some stage use this representation later on, in which case I will develop its properties further.

REFERENCES to (A)

L.D. Landau · E.M. Lifshitz : "Quantum Mechanics"

R.P. Feynman : "Feynman Lectures in Physics, vol. 3"

A. Auerbach : "Interacting Electrons & Quantum Magnetism"

R. Penrose : "Shadows of the Mind"

J.M. Radcliffe : J. Phys $\underline{A4}$, 313 (1971).

The books by Landau & Lifshitz & by Feynman are well-known, extremely good, and need no comment. The book of Auerbach is rather specialised, & a little too focussed on certain formal techniques, but worth looking at. The book of Penrose is a highly speculative discussion of the problems associated with Q.M., a mixture of quite amazing insights along with some real nonsense when he goes outside his own field. It contains the only easily accessible I know of the Majorana spin representation. The paper of Radcliffe first introduced coherent spin states, & is well worth studying.

Ⓑ | SPIN HAMILTONIANS |

Magnetism in general, & Quantum magnetism in particular, are topics in which the models used range from very well-defined models with a long and distinguished history in statistical mechanics, to much more phenomelogical models whose justification is often rather problematic, and often appeals to or rests unreasonably on experiments.

In both cases the underpinnings of these models sometimes rests more on historical longevity than any good theoretical base. Thus in this section we take a somewhat critical look at the important models, and try to understand their basis.

B.1 The HIERARCHY of MAGNETIC INTERACTIONS
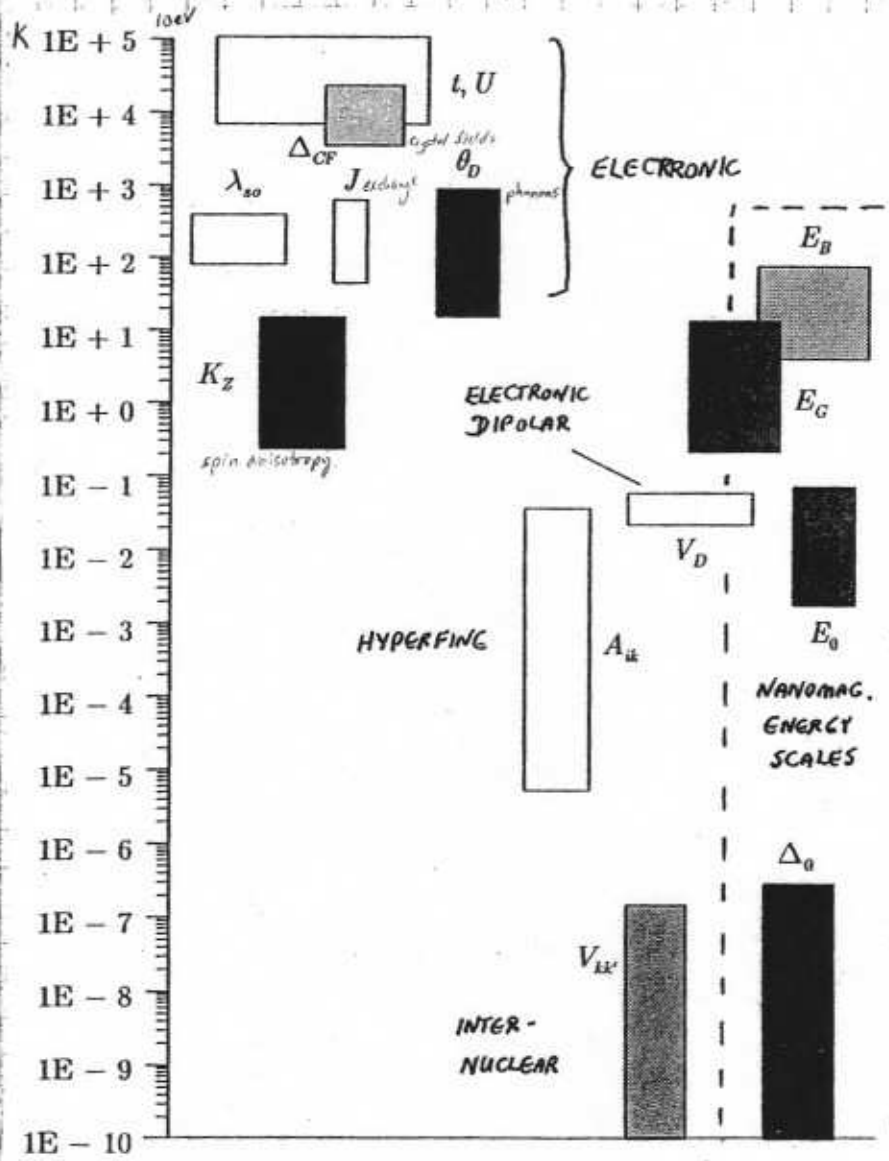
We begin with a look at the various interactions in a typical magnetic insulator. Insulators are easier to understand then conductors, for several reasons, the main one being the separation between spin & charge degrees of freedom.

The figure shows the energy scales characteristic of the important interactions in these systems - energies are given in units of temperature. For future reference you should note the following conversions:

$$1 \text{ eV} = 11,604 \text{ K}$$
$$= 2.418 \times 10^{14} \text{ Hz} \Big\} \text{(1)}$$

$$1 \text{K} = 20.837 \text{ GHz.}$$

For those used to optics,

$$1 \text{ cm}^{-1} = 1.439 \text{ K}$$
$$= 29.98 \text{ GHz} \Big\} \text{(2)}$$
$$= 1.240 \times 10^{-4} \text{ eV.}$$
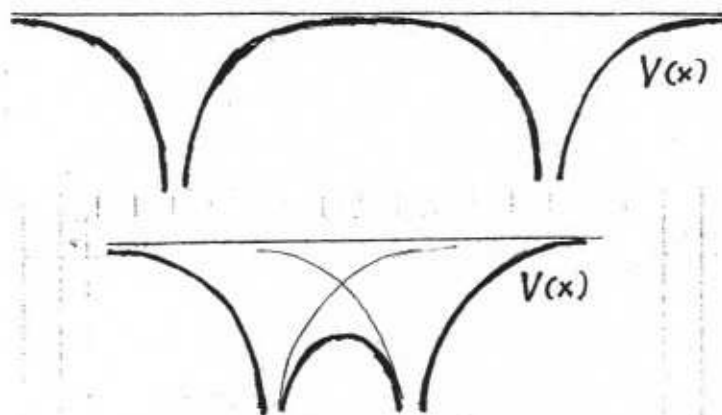
$$1 \text{ Ry} = 13.6 \text{ eV}$$

Now consider what are these various energy scales. Starting from high energies, we have

(1) The "HOPPING ENERGY" t: This is typically in the eV range; for some systems like C atoms in a diamond lattice it can exceed 5 eV, but more typically it is $1-$ eV. The reasoning underlying the typical band Hamiltonian

$$H_{Band} = -t \sum_{\langle ij \rangle, \sigma} (c_{i\sigma}^+ c_{j\sigma} + H.c.)$$

$$\equiv \sum_{k\sigma} \epsilon_0(k) c_{k\sigma}^+ c_{k\sigma} \qquad (3)$$

is fairly simple. We consider a set of atomic orbitals localised around individual atoms, and then imagine the atoms in some crystalline array, with separation R_0. Now suppose we start off with a_0 very large, and plot the tunneling amplitude t for a particle between the orbitals on 2 nearest-neighbour atoms. In this picture of non-interacting electrons we can do an elementary analysis. We consider the tunneling amplitude $t(E, R_0)$ as a function of the distance R_0 and the energy E of the tunneling particle; we have

$$t_{12}(E) \sim \hbar\omega_0(E) e^{i/\hbar S_{12}}$$

$$= \hbar\omega_0(E) e^{i/\hbar \int_1^2 p(x)dx} \qquad (4)$$

$$= \hbar\omega_0(E) \exp\left\{ \frac{i}{\hbar} \int_1^2 dx [2m(V(x)-E)]^{1/2} \right\}$$

where the prefactor $\omega_0(E)$ is sometimes called the "attempt frequency", and is typically of order the small oscillation frequency in the potential well. Here we shall simply assume that the particle is tunneling between 2 levels, each of energy E_n (where n labels the relevant atomic orbital). Then $\hbar\omega_0 \sim |E_n|$, and we can also estimate that the energy $(V(x)-E)$ over most of the trajectory between the points x_1 and x_2 is roughly $(V(x)-E) \sim |E_n|$. Then we have

$$t_{12}(E_n) \sim |E_n| \exp\left\{ -(2m|E_n|)^{1/2} R_0/\hbar \right\} \qquad (5)$$

$$\equiv |E_n| e^{-\bar{R}_0 A_n} \qquad (6)$$

where we define $\bar{R}_0 = R_0/a_0$, $\qquad A_n = \left|\frac{E_n}{E_0}\right| \left(\frac{2me^2 a_0}{\hbar^2}\right)^{1/2} \qquad (7)$

in terms of the Bohr radius a_0 and the Rydberg energy $E_0 \sim 13.6$ eV, which is the ionization energy of a H atom. Note that this result will under-estimate the tunneling amplitude as $\bar{R}_0$ decreases towards 1, because the barrier height will $< |E_n|$ over most of the trajectory.

Equation (3) is written assuming only nearest-neighbour hopping (this is what $\langle ij \rangle$ signifies). In this case, and for a cubic lattice, the

Fourier transform gives

$$\epsilon_0(k) = -t \sum_{\alpha=1}^{3} \cos(k_\alpha R_0).$$

(8)

with a bandwidth $W_n = 6t$. For a different lattice symmetry, and for more than just nearest-neighbour hopping, one gets a more complicated band structure.

Actually if one calculates the bandwidths for real solids, one gets quite different results, as we see below. There are 2 things to notice here:
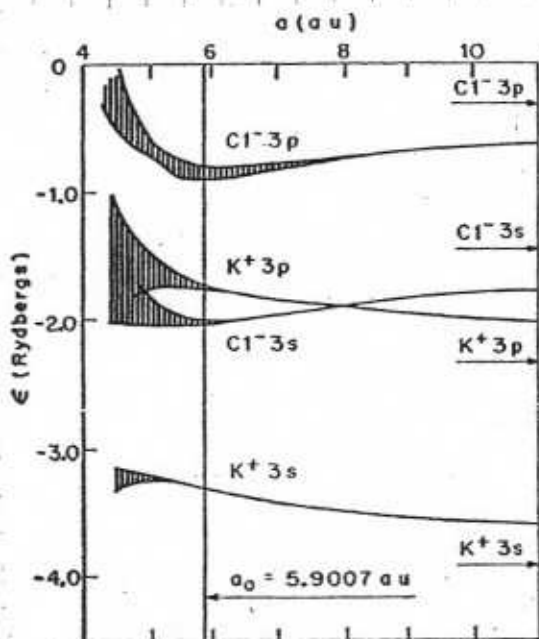
LEFT: ENERGY BANDS CALCULATED FOR KCl AS FN OF R_0

BELOW: ENERGY OF LOWEST LEVELS AS FN OF R_0, FROM (6)
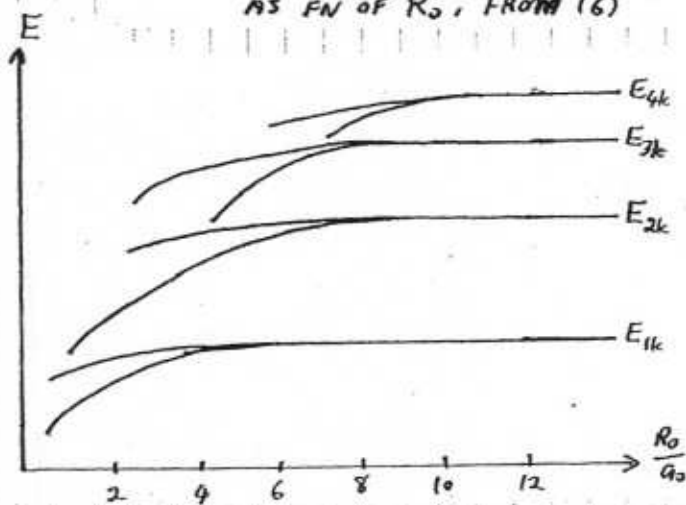
First, we see from the figure on the left that the bandwidths are much smaller for small $\bar{R}$, than might be expected; and second, if we calculate the energy at the centre of the band, it behaves in a rather peculiar way, not at all as would be expected from a simple tunneling calculation (in which the levels are simply split by tunneling, with no change in the mean energy). The reason for this is interactions, to which we now turn:

(ii) <u>The "ON-SITE INTERACTION" ENERGY</u> U_0 : This is also commonly referred to as the Hubbard energy. In its simplest form it is written as a term

$$\mathcal{H}_{int} = \frac{1}{2} \sum_j \sum_\sigma U_0 n_{j\sigma} n_{j-\sigma}$$

(9)

in the Hamiltonian. This is a simplification, because it assumes that there is only one orbital on each site (so that the 2 possible states on this orbital have opposite spin). A more realistic form will range over many orbitals, and have the form

$$\mathcal{H}_{int} = \frac{1}{2} \sum_j \sum_{\substack{m \\ m'}} \sum_{\substack{\sigma \\ \sigma'}} \left[U_0 \delta_{mm'} \delta_{\sigma,-\sigma'} + U_{mm'}^{\sigma\sigma'} \right] n_{jm\sigma} n_{jm'\sigma'}$$

(10)

In these equations $n_{jm\sigma}$ represents the occupation of the m-th orbital with spin σ, and all occupation is on site j. Thus $n_{jm\sigma} = c_{jm\sigma}^+ c_{jm\sigma}$. The energies U

can vary over quite a range, and typical they satisfy $\lesssim 4eV \lesssim U \lesssim 15 eV$, depending on the ions concerned.

If we combine (3) and (9) we get the simplest form of the famous Hubbard model:

$$\mathcal{H}_{Hubb} = -\sum_{<ij>} t\left(c_i^\dagger c_j + H.c\right) + \tfrac{1}{2} U_0 \sum_j n_{j\sigma} n_{j-\sigma} \qquad (11)$$

which has been the subject of many papers.

The ultimate origin, in a non-relativistic theory, for these interaction terms is the Coulomb interaction. We shall look at this in a little more detail later on — a proper discussion is rather lengthy.

The interaction forms (9) and (10), and the Hubbard model in (11), assume that we are dealing with a single set of degenerate levels on each site which then amalgamate into a band. However in real solids the bands can overlap and interact with each other. Then one must generalize to include more than one band. The simplest such generalisation, very widely used, is the famous "Anderson lattice" model, which we write here for the case of hybridized p- and d-bands (appropriate to transition metal compounds):

$$\left.\mathcal{H}_{And} = \sum_{k\sigma} \epsilon_k\, c_{k\sigma}^\dagger c_{k\sigma} \;+\; \sum_{kj\sigma} V_k \left(c_{k\sigma}^\dagger d_{j\sigma} + H.c.\right) \;+\; E_d \sum_{j\sigma} d_{j\sigma}^\dagger d_{j\sigma} \\ \;+\; \tfrac{1}{2} U_0 \sum_{j\sigma} n_{j\sigma}^d\, n_{j-\sigma}^d \right\} \qquad (12)$$

In this Hamiltonian, the s- or p-conduction band term is written in a k-space representation, as in (3), whereas the d-band states, which are assumed to lie much deeper in the atomic wells and thus nearly localized, are written in a site representation (with the number of electrons in the d-orbital on site j being $n_{j\sigma}^d = \sum_\sigma n_{j\sigma} = \sum_\sigma d_{j\sigma}^\dagger d_{j\sigma}$).

Without the interaction term (ie., with $U_0 \to 0$), the Hamiltonian (12) is exactly soluble — the hybridization term V_k mixes the band states $|k\sigma\rangle$ with the "flat band" formed by the localised d-states. The net result is to give a heavy band and a light band, as shown.
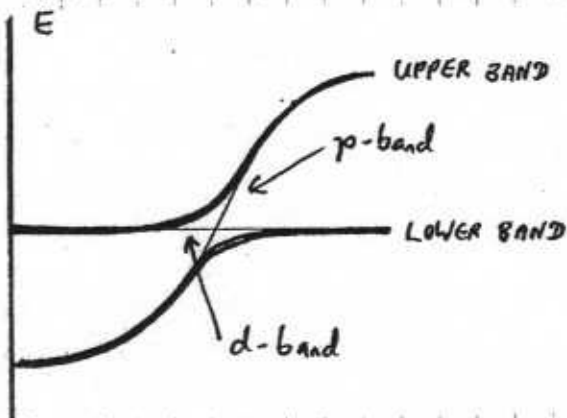

The model (12) is rather simplified — in reality the d-band itself will have some dispersion, and it is more appropriate to write

$$E_d \sum_{j\sigma} d_{j\sigma}^\dagger d_{j\sigma} \longrightarrow \sum_{p\sigma} E_p\, d_{p\sigma}^\dagger d_{p\sigma} \qquad (13)$$

with a finite bandwidth for E_p. However if the localised states are actually f-electrons, as is the case in the rare earths, eqn (12) is quite appropriate, although again, a practical Hamiltonian must include all the relevant sub-orbitals of the f-orbital (corresponding to the different polarisations m_L of the electrons along the angular momentum axis of quantisation). Typical hybridisation strengths $V_k \sim 0.5-1$ eV in transition metals, and more like 0.1 eV in rare earth systems.

BAND STRUCTURE of Cu
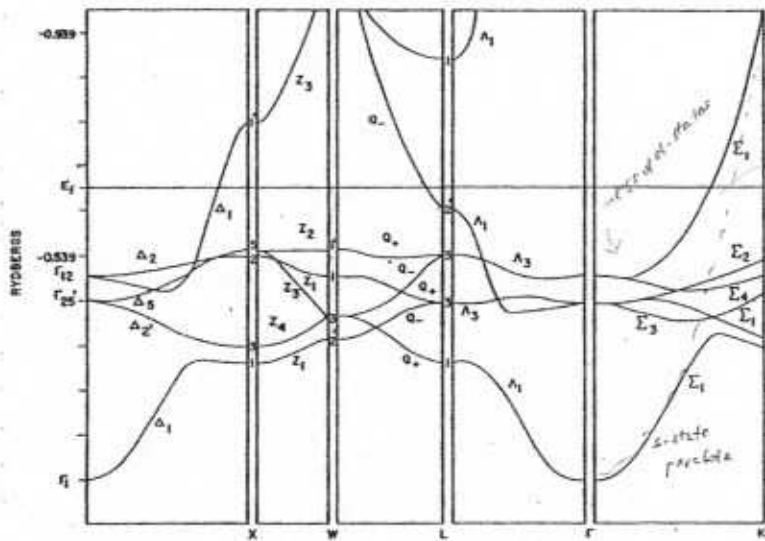
Without the Hubbard interaction U_0, one then gets a "band structure" which for a simple transition metal has the form shown at left.

The effect of U_0 is profound, as first noted by Peierls in 1937, and further studied by Mott in 1949. It can block electrons from hopping between sites, typically if $U_0 > t$. We will discuss this in more detail when we come to study the Hubbard and Anderson models.
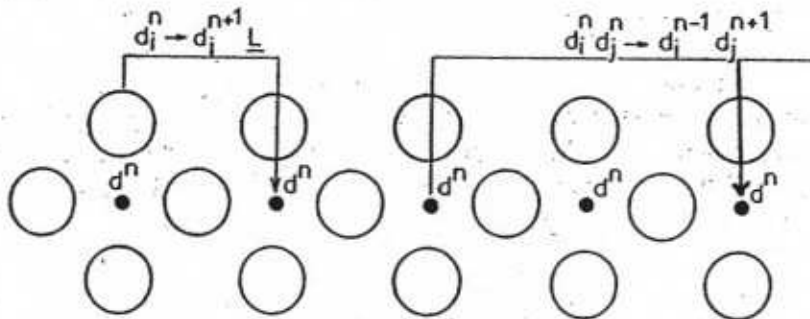
Unfortunately very few textbooks in solid-state theory deal properly with this — exceptions are the recent book of Fazekas, and the older book of Mott.

The whole subject is very intricate, and many questions are still not properly understood.

The energy scales t and U_0 are quite high, much higher than the temperature at which solids condense! Thus at ambient T, their effects are renormalized, as well see below.

There is a nice way to see how the Anderson lattice Hamiltonian arises, which was given in the "ZSA" paper — it provides a helpful link between the underlying atomic physics and the somewhat phenomenological Anderson form. Consider the scheme shown at left, where we have a lattice of d-state ions (representing, e.g., transition metal ions) and an accompanying lattice of p states (these could be quasi-localised around another lattice of anions, making a transition metal compound like CuO or NiO; or we could

LATTICES OF d- and p-STATES, AND THE PROCESSES DESCRIBED BY (14) AND (15)

be dealing with p-states on the same ions, in which case we are looking at a simple elemental solid such as Cu or Ni). Now consider the following two processes:

(a) We take an electron from one d-shell on site i, and transfer it to site j. Then the change in energy of the system is

$$U_0 = \left(E_0(d^{n+1}) - E_0(d^n) \right) + \left(E_0(d^{n-1}) - E_0(d^n) \right) \qquad \Bigg\} \quad (14)$$
$$= E_0(d^{n+1}) + E_0(d^{n-1}) - 2E_0(d^n)$$

where $E_0(d^m)$ is the lowest energy state for an ion in the lattice with m electrons in the d shell, and each ion has n d-electrons before transfer.

(b) Now transfer an electron out of the p-shell, leaving behind a hole, and add it to a d-shell on the i-th ion. The p-shell state with one hole

is usually written as $|L\rangle$ (where the L refers to a "ligand" hole) and so we have an energy change

$$\Delta = E_0(d^{n+1}L) - E_0(d^n) \tag{15}$$

In eqn (14) it was assumed that ions i and j are widely separated. We have not assumed the same in (15), but if we did, we could write the final state energy in the form

$$E_0(d^{n+1}L) = E_0(d^{n+1}) + E_0(L) \tag{16}$$

In both (15) and (16) we have somewhat arbitrarily taken the filled p-shell energy to be zero.

We can use these parameters directly in (12) if we assume that both the p- and d-orbitals have flat bands; then Δ is just the difference

$$\Delta \equiv E_d - \epsilon^0 \tag{17}$$

(a) Mott–Hubbard : Insulating

(b) Charge Transfer : Insulating

However if we add back the finite bandwidths we get the picture shown schematically above. In the first "Mott-Hubbard" case the p-bands are irrelevant, and the d-band is split into 2 parts by the Hubbard U. Since the Fermi energy E_F lies between them, the system is insulating if the original band is half-filled, with N electrons occupying the "lower Hubbard band", and N holes in the unoccupied "upper Hubbard band".

In the second "charge transfer" insulator, we have a filled p-band with $2N$ electrons in the whole system.
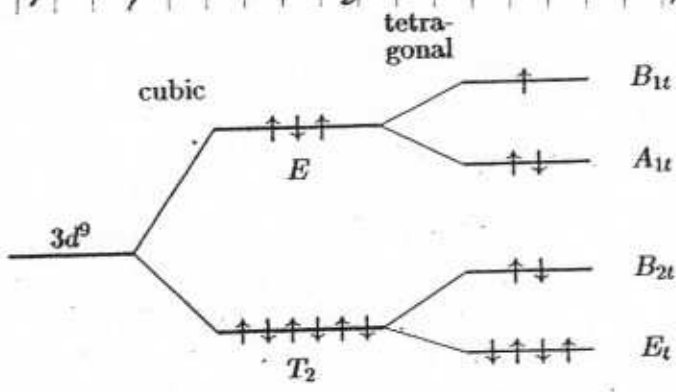
(iii) CRYSTAL FIELD and SPIN-ORBIT COUPLING ENERGIES $\Delta_{CF}, \lambda_{so}$: We now go

to the next set of energy scales of importance in solids. The terms we have just looked at can be derived very simply by considering the bare non-relativistic Coulomb problem, i.e., a set of ions with a simple kinetic term and the Coulomb interaction between electrons & ions. The Hubbard Hamiltonian, & offshoots of it, result from the original Coulomb Hamiltonian when we truncate down to energy scales ~ 0.0 eV, assuming a lattice structure - then the kinetic energy term truncates to the hopping term, and the Coulomb interaction, including screening, truncates to the Hubbard interaction.
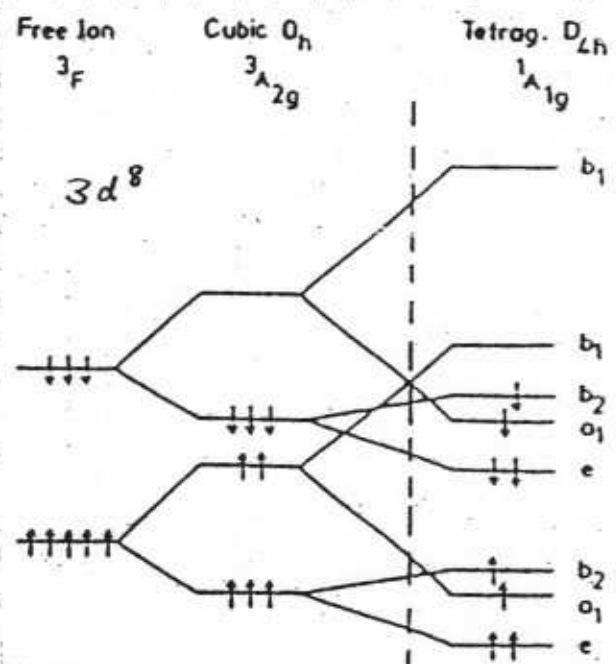
If we now lower our energy scale to the range 0.01 - 0.5 eV (i.e., 100 - 5000 k), we find 3 new terms of importance. In what follows we look at the crystal field and spin-orbit couplings together, since they both lead to static "potential" terms acting on single ions, and their strengths are similar (to within an order of magnitude).

The crystal field terms are a simple consequence of the electron clouds surrounding a given ion in a lattice. Since the surroundings of a given ion in a crystal are no longer isotropic (as they would be for an atom

in free space), the atomic levels of a given ion will be split by the electric fields from the "cage" of surrounding ions, in a way which depends on the symmetry of the cage (which, in a crystalline lattice, means the lattice symmetry).

In the figure at left we see 2 examples of this, for a d^9 ion and for a d^8 ion. In these pictures we not only see the effect of the crystal field Hamiltonian itself, which has the form

$$V_{CF}(\underline{r}) = V_{ion}(\underline{r}) + \sum_{(j)} V_{lig}(\underline{r}-R_j) \qquad (18$$

at position $\underline{r}$ near the ion in question (here V_{ion} is the potential from the ion itself, and V_{lig} from the ions at site j surrounding the ion). We also see the spin states in the various crystal field split levels. To determine these states we need to know more than just the crystal field - we also require knowledge of the various exchange terms in the Hamiltonian, to which we come below.
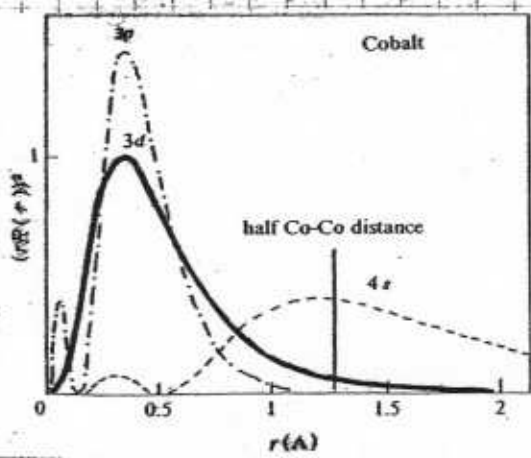
The strength of crystal field interactions depends very much on the nature of the central ions. For transition metal ions, we have

$$\Delta_{CF} \sim 0.8 - 1.5 \text{ eV} \qquad (TM) \qquad (19)$$

although this is quite rough. On the other hand for rare earth ions one has

$$\Delta_{CF} \sim 0.04 - 0.06 \qquad (RE) \qquad (20)$$

The reason for this difference is to be found in the different radial wave-fns of the 3d and 4f states in these systems, shown in the figure below. The 4f electrons are more deeply buried inside

cubic / tetragonal

$3d^9$ — E — B_{1t}, A_{1t} ; T_2 — B_{2t}, E_t

SPLITTING OF LEVELS BY CRYSTAL FIELD FOR $3d^9$ & $3d^8$ FIELDS

Free Ion	Cubic O_h	Tetrag. D_{4h}
^3F	$^3A_{2g}$	$^1A_{1g}$

$3d^8$

b_1 ; b_1, b_2, a_1, e ; b_2, a_1, e

PLOT OF THE "MODULUS SQUARED" OF THE RADIAL PARTS OF THE ATOMIC WAVE-FUNCTIONS IN THE TRANSITION METAL Co AND THE RARE EARTH Gd. THE ELECTRONS WHICH GIVE MAGNETISM ARE THE 3d AND 4f RESPECTIVELY.
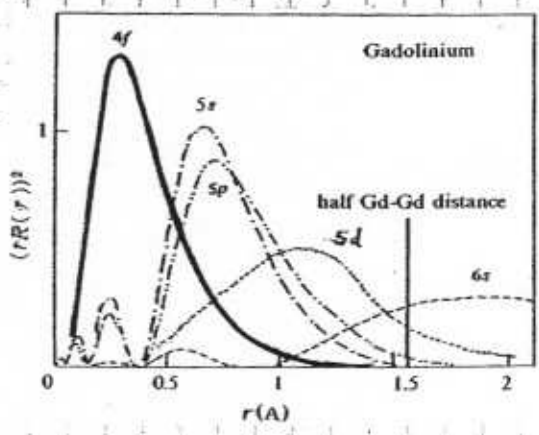
their respective ions, and hence better protected from their surroundings.

When one comes to spin-orbit interactions, the opposite is true. The typical values for the spin-orbit coupling

$$\mathcal{H}_{so} = \lambda_{so} \, \hat{L} \cdot \hat{S} \qquad (21)$$

in TM and RE systems is

$$\lambda_{so} \sim \begin{cases} 0.4 - 0.6 \text{ eV} & (RE) \\ 0.01 - 0.03 \text{ eV} & (TM) \end{cases} \qquad (22)$$

The spin-orbit coupling is of course of relativistic origin: for a completely unscreened nucleus it increases very rapidly with atomic number Z, as the electronic velocities increase.

Typically the following classification is used:

Weak Crystal fields : $\lambda_{so} \sim 0.5 \text{ eV} \quad >> \quad \Delta_{CF} \sim 0.05 \text{ eV}$
  (RE : 4f)

Intermediate Crystal fields : $\Delta_{CF} \sim 0.8-1.5 \text{ eV} \quad >> \quad \lambda_{so} \sim 0.02 \text{ eV}$ (23)
  (TM : 3d)

Strong Crystal fields : $\Delta_{CF} \sim 2-2.5 \text{ eV} \quad >> \quad \lambda_{so} \sim 0.2-0.5 \text{ eV}$
  (TM : 4d, 5d)

The last "strong CF" category includes heavy TM systems (compounds of metals like Pd, Ag in the 4d, or Ir, Pt, Au in the 5d series).

How one analyses these interactions depends on their relative strength. Consider, eg., a 3d TM system. One begins by classifying the levels as in the pictures on the previous page, according to their symmetry, and then $\mathcal{H}_{so}$ is added as a perturbation. The result of combining these 2 procedures is to produce an effective spin Hamiltonian for the system. We deal with this below when we discuss magnetic anisotropy.

To actually calculate these effects is a complicated business. The level structure given by the crystal field Hamiltonian is conveniently analyzed using group theory — a subject covered in many texts. However to calculate the size of the crystal field splittings is messy for transition metals, because the matrix elements of the ligand field term in (18) between different atomic orbitals can be almost as large as the charge transfer gap energy between these orbitals. When perturbation theory does work, we just have expressions like

$$\Delta_{CF} \sim \frac{|\langle p | V_{lig} | d \rangle|^2}{\Delta} \qquad (TM) \qquad (24)$$

where Δ is the charge transfer gap defined in (17). If not, more complex numerical schemes are required.

The size of the spin-orbit coupling λ_{so} is ultimately calculated from matrix elements of the spin-orbit interaction

$$\mathcal{H}_{so} = \frac{\gamma_e}{2m} \, \underline{S} \cdot \nabla V(r) \times \underline{p} \qquad (25)$$

where γ_e is the gyromagnetic ratio for the electron, and $V(r)$ is the

total potential field through which it is moving. In transition metals, where the spin-orbit coupling is $\ll \Delta_{CF}$, we add H_{SO} as a perturbation, calculating matrix elements of H_{SO} between the crystal field levels. In RE systems we do the opposite, first calculating

$$\lambda_{SO} \sim \frac{|\langle p|H_{SO}|d\rangle|}{\Delta} \qquad (RE) \qquad (26)$$

and then adding the crystal field effects.

(iv) <u>EXCHANGE ENERGIES</u> J : The basic reason for exchange terms is the relation discovered by Dirac in 1927 between the permutation operator and the exchange term. Thus for 2 spin-½ particles one has

$$\hat{P}_{12} = 1 + \hat{\sigma}_1 . \hat{\sigma}_2 \qquad (27)$$

and in any calculation involving Coulomb interactions between electrons this will lead to exchange terms of form $J_{12} \sigma_1 . \sigma_2$.

However it turns out that there are various ways in which exchange can happen in a real solid, each having different energy scales. Here we will focus on those that are important in TM systems, with some attention also to RE.

(a) <u>Atomic Hund's Rule coupling</u> : In elementary courses on atomic physics one learns about Hund's rules, which we repeat here for good measure:

<u>1st Hund's rule</u>: In an angular momentum shell of angular momentum $L = \hbar \ell$, which can fit $2(2\ell+1)$ electronic states, the system chooses the maximum S consistent with the Pauli principle. This gives an S value of

$$S = \frac{\hbar}{2}\left\{ (2\ell+1) - |2\ell+1-N| \right\} \qquad (28)$$

if we have N electrons in the shell. This reaches a maximum of $S_{max} = \frac{\hbar}{2}(2\ell+1)$ for a half-filled shell (an example being the Fe^{+2} ion with $S = 5/2$, with 5 of the 10 d-shell states filled).

<u>2nd Hund's rule</u>: In filling up the states with differing L_z in the L-shell, the system will also try to have the maximum total L, while still consistent with the 1st rule (which takes priority) and the exclusion principle. This implies that

$$L = |2\ell+1-N| S \qquad (29)$$

for N electrons. Since the system begins for $N \le 2\ell+1$ by filling up states with parallel spin (see rule 1) this means that it fills in turn states with $L_z = \hbar\ell, \hbar(\ell-1), \hbar(\ell-2)$, etc. For a half-filled shell this means that states from $L_z = \hbar\ell$ to $-\hbar\ell$ are filled, and the total $L = 0$ (as in the Fe^{+2} example above).

<u>3rd Hund's rule</u> : The first 2 rules do not tell us the relative orientation of $\underline{L}$ and $\underline{S}$, i.e., we do not know $\underline{J} = \underline{L} + \underline{S}$. This is decided by the

spin-orbit coupling $\lambda \underline{L} \cdot \underline{S}$; however we need to know the sign of λ. The 3rd rule says that

$$J = |2\ell - N| \, S \qquad (30)$$

ie., that when $N < 2\ell+1$ (less than $\frac{1}{2}$-filled), we have $J = |L-S|$ (ie., $\lambda > 0$, or AFM coupling between L and S); but for $N > 2\ell+1$, we have $J = |L+S|$, ie., $\lambda < 0$ (or FM coupling between L and S). For $N = 2\ell+1$, we have $L=0$ by the 2nd rule.

These rules are very useful: the first two almost always work. The underlying mechanism causing rule 3 is obvious, but to understand the first two we need to look at how the exchange interaction is calculated. The following is a standard calculation but deserves to be repeated.

Suppose we have managed to find a set of wave functions for the atomic electrons, properly symmetrised, but without the Coulomb interactions. Consider 2 one-electron states $|\psi\rangle = |\phi\sigma\rangle$ and $|\psi'\rangle = |\phi'\sigma'\rangle$, so that their Slater determinant, including spin, is

$$\langle r_1 r_2 | \Psi_{\sigma\sigma'}\rangle = \frac{1}{\sqrt{2}} \begin{vmatrix} \langle r_1 | \phi\sigma\rangle & \langle r_2 | \phi\sigma\rangle \\ \langle r_1 | \phi'\sigma'\rangle & \langle r_2 | \phi'\sigma'\rangle \end{vmatrix} \qquad (31)$$

Thus there are 4 different states possible here, depending on what are σ and σ'. Now let's order these spin states as follows:

$$|\sigma\sigma'\rangle = \left(|\uparrow\uparrow\rangle, \ |\uparrow\downarrow\rangle, \ |\downarrow\uparrow\rangle, \ |\downarrow\downarrow\rangle \right) \equiv |\mu\rangle \qquad (32).$$

It is then easy to see that we have the following matrix elements of the Coulomb interaction $U(r_1 - r_2)$ (which is spin-independent) between these states:

$$\langle \Psi_\mu | U(r_1 - r_2) | \Psi_\nu\rangle = \begin{pmatrix} C-J_H & 0 & 0 & 0 \\ 0 & C & -J_H & 0 \\ 0 & -J_H & C & 0 \\ 0 & 0 & 0 & C-J_H \end{pmatrix} \qquad (33)$$

where the numbers C and J_H are

$$C = \int d^3 r_1 \int d^3 r_2 \ U(r_1 - r_2) \ |\langle r_1 | \phi\rangle|^2 \ |\langle r_2 | \phi'\rangle|^2$$
$$J_H = \int d^3 r_1 \int d^3 r_2 \ U(r_1 - r_2) \ \langle \phi | r_1\rangle \langle r_1 | \phi'\rangle \langle \phi' | r_2\rangle \langle r_2 | \phi\rangle \qquad \Big\} \quad (34)$$

In the case of the Coulomb interaction, C is known as the Coulomb integral, and J_H is called the "direct exchange" or "Atomic Hund's rule" exchange integral. Noting that for spin-$\frac{1}{2}$ systems we have

$$(1 + 4 \hat{s}_1 \cdot \hat{s}_2) \begin{cases} |\text{singlet}\rangle \\ |\text{triplet}\rangle \end{cases} = \begin{array}{l} -2 |\text{singlet}\rangle \\ +2 |\text{triplet}\rangle \end{array} \qquad \Big\} \quad (35)$$

(compare eqn (27)), we have the very simple result given by Dirac - that

We can write the effect of $U(r_1 - r_2)$ in the subspace of these 2-particle states as

$$U(r_1 - r_2) \rightarrow \mathcal{H}_{int}^{eff} = \frac{E_{tr} + E_{sing}}{2} + \frac{1}{2}(E_{tr} - E_{sing})\left[\frac{1}{2} + 2\hat{S}_1 \cdot \hat{S}_2\right]$$

$$\equiv const. - 2J_H S_1 \cdot S_2 \tag{36}$$

We have not used the explicit form of the Coulomb interaction here, and a proper calculation requires the complex screening effects in a real system. A rough guide to the size of J_H is as follows:

$$\left.\begin{array}{llll}
4f \text{ electrons:} & J_H & \sim & 1.0 \text{ eV} \\
3d \quad " \quad : & " & \sim & 0.7 \quad " \\
4d \quad " \quad : & " & \sim & 0.5 \quad " \\
5d \quad " \quad : & " & \sim & 0.3 \quad "
\end{array}\right\} \tag{37}$$

The interesting this is how slowly these exchange integrals depend on the "spreading" of the electron clouds in the atomic states as we move from $4f$ (very tight clouds) to $5d$ (quite spread out). I will say more about this in an Appendix.

The Hund's rule exchange is which is responsible for the 1st rule - this is kind of obvious. It has a very simple physical origin - the electrons want to avoid each other because of the Coulomb interaction, and parallel spin states make it easier for them to do this because they already avoid each other by the Pauli principle (whereas nothing about anti-parallel spins makes them avoid each other, in the absence of interactions).

The 2nd Hund's rule can be understood in a similar way, as avoidance of electrons. The energies involved are a little smaller, roughly ⅓ to ½ of the J_H given above.

(b) "Kinetic" Intersite Exchange: The Hund's rule exchange mechanism is responsible for the existence of spin moments in solids. We now ask - how will moments on different sites interact? This depends very much on how these moments can communicate with each other. As we'll discuss later, the dipole-dipole interaction between them is very small ($< 1K$). However, if electrons can hop from one atomic site to another, we get another very important exchange mechanism. In real solids, this is complicated, so we start with a toy model.

Consider 2 electrons, on sites A and B, which can occupy a single orbital state on each site. The Hamiltonian is

$$\mathcal{H} = -t \sum_\sigma (c_{A\sigma}^\dagger c_{B\sigma} + H.c.) + \frac{U}{2} \sum_{j=A,B} \sum_\sigma n_{j\sigma} n_{j-\sigma} \tag{38}$$

from (11), where we ignore hybridisation, charge transfer, etc., and ignore all electron-electron except the on-site U.

Consider first the problem with $t, U = 0$. We can see quickly that there are 6 possible low-energy states, once the Pauli principle is incorporated. These states are

$$\left.\begin{array}{l}
\frac{1}{\sqrt{2}}|AA; \uparrow\downarrow - \downarrow\uparrow\rangle \\
\frac{1}{\sqrt{2}}|BB; \uparrow\downarrow - \downarrow\uparrow\rangle
\end{array}\right\} \begin{array}{l} 2 \text{ states;} \\ 1 \text{ site doubly} \\ \text{occupied} \end{array} \qquad |AB\rangle|B\sigma'\rangle\left.\begin{array}{l} 4 \text{ states,} \\ \text{each site} \\ \text{singly occupied} \end{array}\right. \tag{39}$$
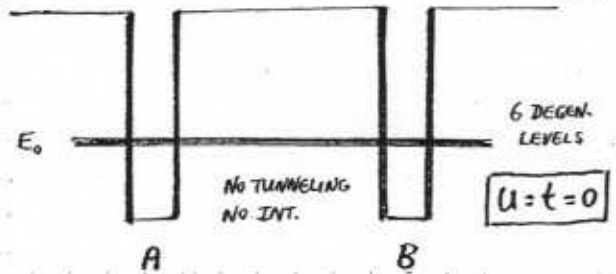
The states are shown schematically at left. The shape of the potential wells around each atom is irrelevant.

Now consider what happens when we switch on t and U. It is of real methodological interest to look at difference between doing this in a different order. So first we switch on U, leaving $t=0$. The result is shown below — the two doubly occupied states have their energies increased to

$V(x)$

E_0 — NO TUNNELING / NO INT.

6 DEGEN. LEVELS

$U = t = 0$

A   B

values U above the 4 singly occupied states. Otherwise the eigenstates are unchanged.

Note, incidentally, that it is quite reasonable to assume that the doubly-occupied states are still bound the system. Consider, e.g., the problem of 2 H atoms, which is a useful example of our present problem. The doubly-occupied state with energy U above the

$E_0 + U$ ———— 2 LEVELS

E_0 ———— 4 LEVELS

$t = 0$ / $U \neq 0$

A   B
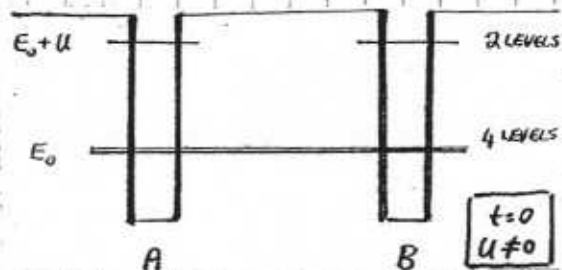
singly-occupied state corresponds to the H$^-$ ion, i.e., a single proton with 2 electrons. These 2 electrons can both bind to the proton by distorting their wave-functions somewhat so that the electrons stay as much as possible on opposite sides of the proton — so that the attractive protonic force outweighs the repulsive force from the other electron.

The energy of the doubly-occupied state, measured from the unbound continuum, is called the

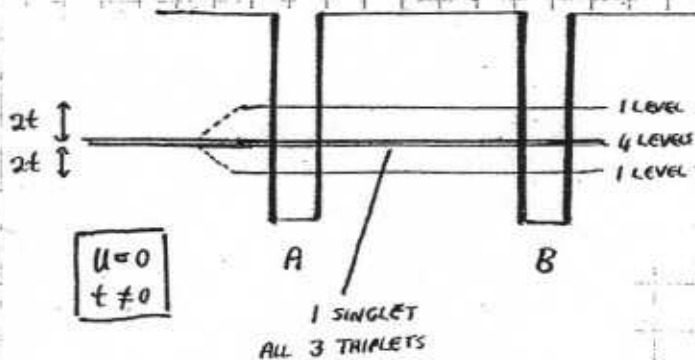| Electron affinity energy, in eV		
Atom	Theory	Experiment
H	0.7542	0.77 ± 0.02
Li	0.58	—
C	1.17	1.25 ± 0.03
N	−0.27	—
O	1.22	1.465 ± 0.005
F	3.37	3.448 ± 0.005
Na	0.78	—
Al	0.49	—
Si	1.39	—
P	0.78	—
S	2.12	2.07 ± 0.07
Cl	3.56	3.613 ± 0.003
Br	—	3.363 ± 0.003
I	—	3.063 ± 0.003
W	—	0.50 ± 0.3
Re	—	0.15 ± 0.1

"electron affinity". Some values for it are given above.

Now consider the effect of the hopping term (which becomes important if the two H atoms approach each other, in our example). If we ignore the on-site U, then this is also a simple problem. As we saw previously, for a single electron we just get a splitting between the states

$$|\psi_{\pm}\rangle = \frac{1}{\sqrt{2}}(|A\sigma\rangle \pm |B\sigma\rangle) \qquad (40)$$

with energies

$$E_{\pm} = \mp t \qquad (41)$$

$2t \updownarrow$ $2t \updownarrow$ ———— 1 LEVEL / 4 LEVELS / 1 LEVEL

$U = 0$ / $t \neq 0$

A   B

1 SINGLET / ALL 3 TRIPLETS

For non-interacting electrons, the problem of 2 hopping electrons on the 2 sites is best dealt with by dividing the states up into singlets and triplets, as follows:

Singlet States :

Double occupancy

$$|\psi_{AA}^{S}\rangle = \frac{1}{\sqrt{2}}|AA; \uparrow\downarrow - \downarrow\uparrow\rangle$$

$$|\psi_{BB}^{S}\rangle = \frac{1}{\sqrt{2}}|BB; \uparrow\downarrow - \downarrow\uparrow\rangle$$

Single Occupancy

$$|\psi_{AB}^{S}\rangle = \frac{1}{2}|(AB+BA); \uparrow\downarrow - \downarrow\uparrow\rangle$$

(42)

Triplet States ,

All singly occupied.

$$|\psi_{1}^{T}\rangle = \frac{1}{\sqrt{2}}|(AB-BA); \uparrow\uparrow\rangle$$

$$|\psi_{0}^{T}\rangle = \frac{1}{2}|(AB-BA); \uparrow\downarrow + \downarrow\uparrow\rangle$$

$$|\psi_{-1}^{T}\rangle = \frac{1}{\sqrt{2}}|(AB-BA); \downarrow\downarrow\rangle$$

(43)

We can now see how we get the level scheme shown on the last page. Note first that the hopping has no effect on the triplet states; this is because if we act on a triplet state with the hopping operator we get a doubly-occupied triplet on one of the 2 sites — this is impossible, so the matrix element is zero. On the other hand the 3 singlet states are split into 3 levels, with energies $\pm t, 0$.

If we now proceed to the full problem, we find

Triplet states : $E_T = 0$ ∀ three states   (44)

Singlet states :   See below

The singlet states divide into upper one, which are repelled upwards still further as U is switched on, and a lower one which lies below the triplet for all values of U. The eigenstates and eigenvalues are found by diagonalizing the Hamiltonian as written in the subspace of the 3 singlet states only, where it takes the following form as a function of the dimensionless coupling

$$g = U/4t$$ (45)

E

UPPER 2
SINGLET STATES

EIGENSTATES of
2-ELECTRON, 2-SITE
HUBBARD MODEL

3 TRIPLET STATES

LOWER
SINGLET STATE $\Delta E \sim t/g \equiv 4t^2/U$

$\Delta E \sim (2t - U/2 + \cdots)$

$g = \frac{U}{4t}$

we have $\mathcal{H}_{sing} = 2t \begin{pmatrix} 0 & -\frac{1}{\sqrt{2}} & -\frac{1}{\sqrt{2}} \\ -\frac{1}{\sqrt{2}} & 2g & 0 \\ -\frac{1}{\sqrt{2}} & 0 & 2g \end{pmatrix}$ (46)
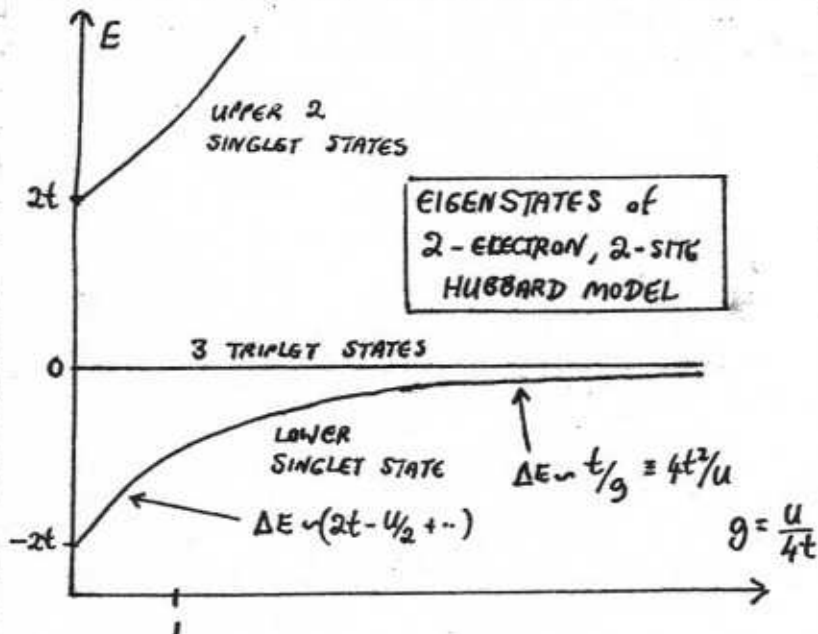
singlet

We are only interested here in the lowest singlet state, which has energy

$$E_0 = 2t\left[g - (1+g^2)^{1/2}\right]$$
$$\equiv \tfrac{1}{2}\left[U - (U^2 + 16t^2)^{1/2}\right] \qquad \left.\rule{0pt}{40pt}\right\} \qquad (47)$$

which has the limiting behaviour

$$E_0 \longrightarrow \begin{cases} -4t^2/U & (U \gg t) \\[10pt] -(2t - U/2) & (U \ll t) \end{cases} \qquad (48)$$

The large U/t limit ($g \gg 1$) is easily understood by perturbing away from $U = \infty$ (where no double occupancy is allowed); in 2nd-order pert. theory, we get a kinetic energy lowering by a weak tunneling, and

$$\Delta E = \sum_{\alpha} \frac{|V_{0\alpha}|^2}{E_0 - E_\alpha} = -4t^2/U \qquad (49)$$

where $|\alpha\rangle$ is the intermediate state with a doubly-occupied state. The small U/t limit is similarly understood by perturbing away from the $U = 0$ limit.

If we calculate the ground state singlet wave-function we can see how the double-occupancy probability falls as g increases.

The size of these inter-atomic exchange terms varies considerably. We now have an exchange term

$$J \equiv \Delta E = -E_0 \qquad (50)$$

whose values range from

$$J \sim 5\text{-}150 \text{ meV} \qquad (51)$$

$$P(g) = |\langle \Psi_0 | AA \rangle|^2 + |\langle \Psi_0 | BB \rangle|^2$$

$$P(g) \sim \frac{1}{8g^2} \equiv \frac{2t^2}{U^2}$$

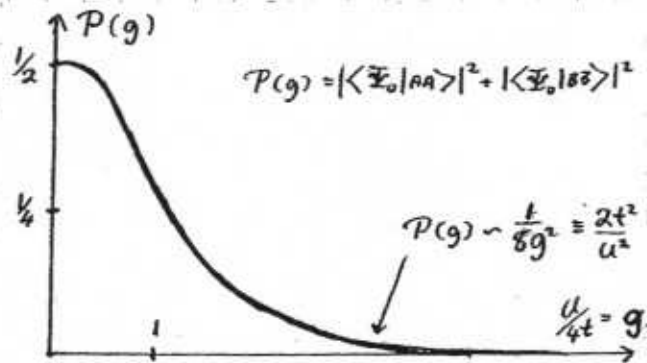THE PROBABILITY OF DOUBLE OCCUPATION OF A SITE IN THE GROUND STATE WAVE-FUNCTION

depending on which 3d system we are interested in (and we consider here interactions between lattices of a single species of ion).

Note finally that we can write our result here in the form of a new low-energy effective Hamiltonian

$$H_{tJ}^{eff} = -t \sum_{\delta} (1 - n_A^{-\delta})(c_{A\delta}^+ c_{B\delta} + \text{h.c.})(1 - n_B^{-\delta}) + \tfrac{1}{2} J \underline{S}_A \cdot \underline{S}_B \qquad (52)$$

where the terms $(1 - n_A^{-\delta})$, etc, prevent double occupancy. This form is only valid if we ignore the higher states. This the terms $(1 - n_A^{-\delta})$, etc are projection operators, projecting out singly occupied states.
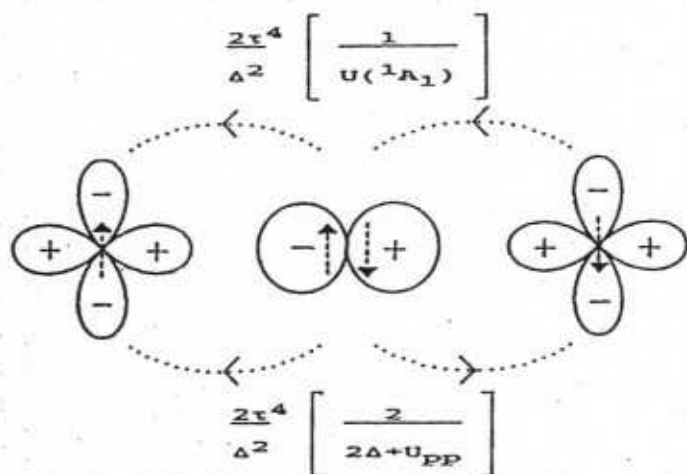
(c) Super-exchange Terms : The preceding discussion of kinetic exchange was tutorial in nature. In almost all insulators one deals with compounds in which the interaction between spins has to pass through ligand orbitals. Thus we have to consider processes where an electron hops from a magnetic orbital (d- or f-) on one site, via

a p- or s-orbital on some neighbouring ligand ion, and then on to another magnetic orbital, on some other site (or perhaps back to the same site).

An example of such a process is shown in the Figure. We imagine electrons hopping from a specific sub-orbital of the d-shell on a TM ion (the orbital shown here is the $d_{x^2-y^2}$ orbital), onto a p sub-orbital on an intermediate anion; from there it goes to the $d_{x^2-y^2}$ orbital on a different TM cation.

There are actually processes that contribute to lowest order perturbation theory for this problem, as follows:

(i) a particle can leave one TM ion, hop through the intervening p-state to the other TM ion, and then return to the first ion along the same path. The energy of the 3 successive intermediate states here are Δ, U, and Δ respectively, relative to the initial & final states. This process can happen either from left → right, or vice-versa, so the final energy of interaction we get is

$$\Delta E_1 = \frac{2t^4}{\Delta^2 U} \tag{53}$$

$$\frac{2t^4}{\Delta^2}\left[\frac{1}{U(^2A_1)}\right]$$

$$\frac{2t^4}{\Delta^2}\left[\frac{2}{2\Delta+U_{PP}}\right]$$

Note that for this process to go, it has to occur between opposite spins on the 2 TM ions, and this ensures it has the symmetry of an exchange interaction.

(ii) One electron hops from one TM to the central anion — then another particle hops to the same anion from the other TM ion. The energy of the successive intermediate states is Δ, $2\Delta+U_p$, Δ (where the intermediate state energy with 2 electrons on the central ion includes both the charge transfer energy and a local Hubbard U_p on the p-orbitals). These processes can also occur in either direction, so we get

$$\Delta E_2 = \frac{2t^4}{\Delta^2}\left(\frac{2}{2\Delta+U_p}\right) \tag{54}$$

Adding these processes then, gives, for this superexchange process, the exchange coupling

$$J = \frac{2t^4}{\Delta^2}\left[\frac{1}{U} + \frac{2}{2\Delta+U_p}\right] \tag{55}$$

We see that both of these processes only involve singlet, and so by the same arguments as for direct kinetic exchange, we get an AFM coupling.

The description given here is somewhat simplified, since a proper calculation needs to look properly at the matrix elements between different orbitals, which depends on the details of the wave-functions (here we have just written a single number t for this matrix element). This point is discussed in more detail in the Appendix, where we see that the interaction does not necessarily have the AFM sign given here - depending on bond angles, it can even be FM in sign. The superexchange interaction is also in general _anisotropic_ (which is hardly surprising

given the existence of crystal fields and spin-orbit coupling), taking the more general form

$$\mathcal{H}_{SE} = \frac{1}{2} J_{ij}^{\alpha\beta} S_i^\alpha S_j^\beta \tag{56}$$

with the allowed terms depending on the double point-group symmetry group of the system.

The size of the superexchange contributions depends enormously on which system we are dealing with (particularly if the superexchange paths involve more steps than the processes described above), particularly on the value of t that we choose. In TM compounds one has

$$J_{SE} \sim 50-2000 \, K \tag{57}$$

for the dominant superexchange paths, although one often finds values outside these rough values. For RE systems $\underline{U_{SE}}$ is much smaller, often $< 1K$.

There are other kinds of exchange coupling, but we will not discuss them here. these include double exchange, which is important in the manganites.

(v) <u>SPIN ANISOTROPY ENERGY K</u> : Suppose now we descend further in energy, to temperatures $\lesssim 50 K$ or less. These energy scales, only a couple of meV or less, are far below the values we have seen for crystal fields, spin-orbit, and exchange energies, in most systems. The electrons have long since settled into states of definite spin S, and angular momentum L and/or total J, and the underlying structure of the $|S, M_S\rangle$ and $|L, M_L\rangle$ states has also been determined by the large energies $\Delta_{CF}, \lambda_{SO}$, and J. At least that is what one might naively expect.

If this were true then magnetic systems would behave quite differently at low T then they do. The most important thing missed by the naive argument is the existence of <u>single-ion anisotropy</u>, i.e., forces acting on the individual spins, which try to orient them in spin space. The basic idea is fairly simple, and was mentioned already on p. 28.

Suppose we consider a TM ion, for which $\Delta_{CF} \gg \lambda_{SO}$, and first classify the levels in a crystal field - the splitting between the levels is of order $0.1-1 \, eV$. Now add the spin-orbit coupling perturbatively; we must then calculate the matrix elements of $\mathcal{H}_{SO}$ between different levels, ie., matrix elements like the 2nd-order term

$$\langle 0; S, M_s | \hat{\mathcal{H}}^{eff} | 0; S, M_s' \rangle = E_0 \delta_{M_s, M_s'} + \langle 0; SM_s | \lambda \underline{L} \cdot \underline{S} | 0; SM_s' \rangle$$
$$+ \sum_{\mu} \sum_{M_s''} \frac{\langle 0; SM_s | \lambda \underline{L} \cdot \underline{S} | \mu; SM_s'' \rangle \langle \mu, SM_s'' | \lambda \underline{L} \cdot \underline{S} | 0, SM_s' \rangle}{E_0 - E_\mu} \tag{58}$$
$$+ \text{etc.}$$

In this equation, which defines an effective spin Hamiltonian $\hat{\mathcal{H}}_{eff}$ up to 2nd order in the dimensionless parameter λ/Δ_{CF}, we label the different crystal field levels by μ, with energies E_μ; all of these levels refer to a given L shell, as in the pictures on p. 27, and E_0 is the lowest level. The 1st-order term in (58) gives 0, and the 2nd-order term gives

$$\langle 0 \, S M_s | \hat{H}_{eff} | 0; S M_s' \rangle = -\lambda^2 \langle 0; S M_s | S^\alpha \Lambda_{\alpha\beta} S^\beta | 0; S M_s' \rangle \tag{59}$$

where

$$\Lambda^{\alpha\beta} = \sum_\mu \frac{\langle 0 | L_\alpha | \mu \rangle \langle \mu | L_\beta | 0 \rangle}{E_\mu - E_0} \tag{60}$$

In other words, if we write $\hat{H}_{eff}$ as

$$\hat{H}_{eff}^K = | M_s \rangle K_{M_s M_s'} \langle M_s' | \tag{61}$$

then

$$K_{M_s M_s'} = -\lambda^2 S^\alpha \Lambda_{\alpha\beta} S^\beta \equiv -\lambda^2 \underline{S} \cdot \underline{\underline{\Lambda}} \cdot \underline{S} \tag{62}$$

At these energy scales it is important to also consider the Zeeman coupling of the system to an external field $\underline{H}_0$; this coupling is just

$$\hat{H}_{Zeeman} = \mu_0 (\underline{L} + 2\underline{S}) \cdot \underline{H}_0 \tag{63}$$

If we make the same 2nd-order expansion for H_{Zeeman} as for H_{SO}, we finally end up with a "spin Hamiltonian" valid for energy scales $\ll 50 K$ for most systems:

$$\begin{aligned} \hat{H}_{eff}^K &= E_0 - \lambda^2 \underline{S} \cdot \underline{\underline{\Lambda}} \cdot \underline{S} + \mu_0 \underline{S} \cdot \underline{\underline{g}} \cdot \underline{H}_0 - \mu_0^2 \underline{H}_0 \cdot \underline{\underline{\Lambda}} \cdot \underline{H}_0 \\ &\equiv E_0 - \lambda^2 S^\alpha \Lambda_{\alpha\beta} S^\beta + \mu_B S^\alpha g_{\alpha\beta} H_0^\beta - \mu_0^2 H_0^\alpha \Lambda_{\alpha\beta} H_0^\beta \end{aligned} \left. \right\} \tag{64}$$

Thus we have 3 terms: a spin anisotropy term H_{eff}^K in (61), (62), a modified Zeeman coupling between $\underline{S}$ and $\underline{H}_0$ which involves an anisotropic g-tensor $g_{\alpha\beta}$, and the 3rd term modifies the spin susceptibility. Let us examine the first 2 terms a little more closely:

(a) **Spin Anisotropy** $\hat{K}$: The result in (61), (62) for the spin anisotropy is 2nd-order in λ; one can continue the perturbation expansion up to order λ^{2S+1}, to get a final form

$$\hat{H}_{eff}^K = K(\hat{\underline{S}}) = K_{\alpha\beta}^{(2)} \hat{S}_\alpha \hat{S}_\beta + K_{\alpha\beta\gamma\delta}^{(4)} \hat{S}_\alpha \hat{S}_\beta \hat{S}_\gamma \hat{S}_\delta + \cdots \tag{65}$$

$$= \frac{K_{\alpha\beta}^{(2)}}{S} S_\alpha S_\beta + \frac{K^{(4)}}{S^3} \hat{S}_\alpha \hat{S}_\beta \hat{S}_\gamma \hat{S}_\delta + \cdots \tag{66}$$

where the $K^{(n)} \propto \lambda^n$, and $K^{(n)} \propto \lambda^n S^{n-1}$; we shall see later on the reason for writing this "spin potential" in the form (66).

The easiest way to think about (65) and (66) is on the Bloch sphere; $K(\hat{\underline{S}})$ defines a potential on the surface of the Bloch sphere, which because of time reversal symmetry is even in $\underline{S}$. Even at 2nd order in $\underline{S}$ the results can be interesting. The form of $K(\underline{S})$ obviously depends on the symmetry of the lattice (via (60)), and at 2nd order a typical form has biaxial symmetry, with 2 axes picked out by the crystal field; one writes

$$\mathcal{H}_{eff}^{K} \sim k_z^{(2)} S_z^2 + k_\perp^{(2)} S_x^2$$

$$\equiv \frac{1}{S}\left[K_z^{(2)} S_z^2 + K_\perp^{(2)} S_x^2 \right] \qquad \text{(Biaxial)} \qquad \Big\} \qquad (66)$$
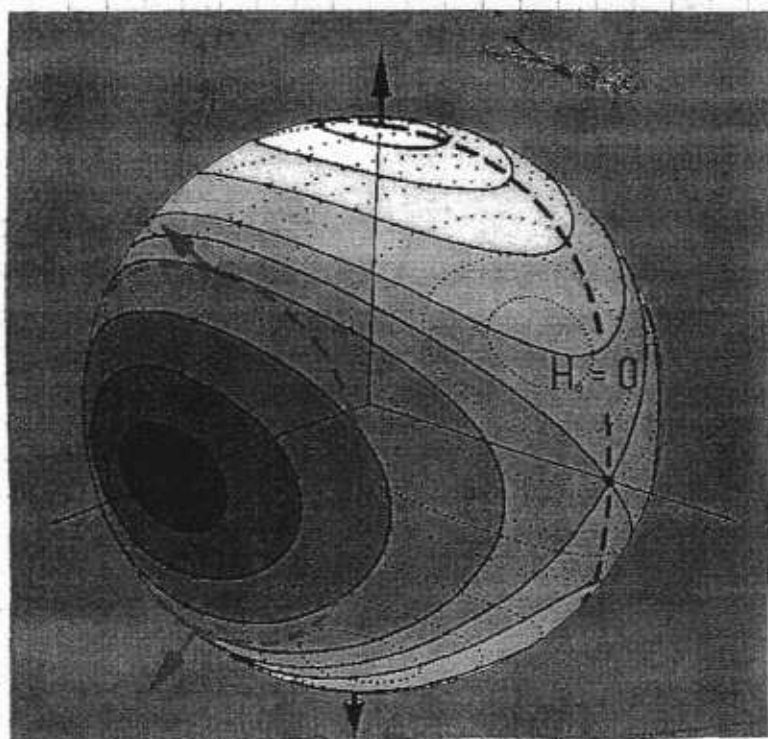
BIAXIAL (EASY AXIS, HARD AXIS) POTENTIAL ON THE BLOCH SPHERE, IN ZERO FIELD. HIGH POTENTIAL IS DARK, LOW IS LIGHT. $\mathcal{H} = -DS_z^2 + ES_x^2$

In the literature common forms like these have acquired their own notation, and (66) is usually written

$$\mathcal{H}_{eff}^{K} \sim DS_z^2 + ES_x^2 \qquad (67)$$

The size of these terms is of crucial importance. In TM systems one finds that

$$|K^{(n)}| \sim 0.1 - 10\,K \qquad (68)$$

which means that the orienting effect of the spin anisotropy potential first begins to be strongly felt at an energy

$$E_B \sim S|K^{(n)}| \qquad (69)$$

For single electronic spins this means that spin anisotropy is usually important for $T \lesssim 10K$. However as we will discuss later, there are many high-spin molecules, where S can be as high as 50, and in that case E_B can be over 100 K.

(2) <u>Anisotropic Zeeman coupling g</u>: In the form (64), with $\mathcal{H}_{eff}^{K}$ evaluated up to $O(\lambda^2)$, we have an expression for $g_{\alpha\beta}$ given by

$$g_{\alpha\beta} = 2(\delta_{\alpha\beta} - \lambda\Lambda_{\alpha\beta}) \qquad (70)$$

with a field-independent anisotropic g-factor. Because typically $\lambda/\Delta_{CF} \ll 1$ in TM compounds, this means that usually $g_{\alpha\beta}$ is fairly isotropic and close to 2 in these systems. In this case it makes sense to ignore higher-order terms in λ (which will just make $g_{\alpha\beta}$ weakly field-dependent). We can then imagine adding the Zeeman term to our effective potential $\mathcal{H}_{eff}^{K}$, as a term linear in $\underline{S}$, which tries to orient the spin. The strength of this Zeeman coupling is then

$$S|g_{\alpha\beta} H_o^\beta| \sim (0.7K/T) \times S \qquad (71)$$

We see that this competes with the magnetic anisotropy at fields ranging from $\sim 0.1 - 10$ Tesla.

All of the above discussion was for TM systems. As noted on p. 28, in RE systems $\lambda_{so} > \Delta_{CF}$, and we have to calculate the spin Hamiltonian by first diagonalizing the spin-orbit interaction, and then adding crystal field terms. The net result is the same, ie., we again get a spin Hamiltonian of the form in (64),

except that it is written in terms of $J = L+S$ rather than S; the strong spin-orbit interaction locks L and S rigidly together. Typical anisotropy energies in RE systems can be quite a lot larger than in TM systems; one has

$$|K^{(n)}| \sim 1-100 \text{ K} \qquad \text{(RE)} \qquad (72)$$

The expression for the g-factor is somewhat different — we shall not go into it here — and it can be much more anisotropic than for TM ions.

Finally, note that all this discussion was for single ions. An obvious question to be asked is — what about the exchange interactions — don't they mess up the spin Hamiltonian completely?

The answer to this clearly yes, if $J \gtrsim \lambda$; we must then include the exchange interaction in our derivation of H_{eff}. The result of this is to (a) make J anisotropic, as discussed above (cf eqn (56)), and also to mix together the eigenstates of $H_{cf}^K(S_j)$ for different spins. We do not discuss this in detail here, but we will look later on at an example. Some interesting terms are generated when one does a more thorough analysis of this kind; one well-known one is the Dzyaloshinskii - Moriya term

$$H_{DM} = D \cdot (S_i \times S_j) \qquad (73)$$

which explicitly breaks time-reversal symmetry; typical values of D in TM systems are $|D| \sim 0.1 - 1 \text{ K}$.

(vi) ELECTRONIC DIPOLAR INTERACTION V_D : We have seen that there are really quite strong exchange interactions between different ionic spins, which come from a combination of Coulomb interactions and the Pauli principle. There is a much weaker inter-spin interaction, which however has great importance because it is long-ranged. This is the dipolar interaction, which is a photon-mediated coupling between spins:

$$H_{dip} = \frac{1}{2} \sum_{(i \neq j)} \sum \frac{1}{R_{ij}^3}\left[m_i \cdot m_j - 3\frac{(m_i \cdot R_{ij})(m_j \cdot R_{ij})}{R_{ij}^2} \right] \qquad (74)$$

where the magnetic moment of the "spin" is

$$m_i = m_i^L + m_i^S ; \qquad \begin{matrix} m_i^L = -\mu_B L_i \\ m_i^S = -2\mu_B S_i \end{matrix} \qquad (75)$$

and $\mu_B = e\hbar/2m_e$ is the usual Bohr magneton. In TM systems this is often purely an interaction between the $\{S_j\}$, since the crystal fields "quench" the angular momentum in many cases. In RE it is an interaction between the $\{J_i\}$.

The long-range nature of H_{dip} in $1/R_{ij}^3$ is seen in the integral

$$\frac{1}{L_0^3}\int d^3r \, H_{dip} \sim M_0^2 \ln|L_0/a_0| \qquad (76)$$

where a_0 is the size of the unit cell and L_0 the system size (of volume L_0^3). This

answer should worry you — it says that the energy density of the system grows without limit like $\ln|L_0/a_0|$; and note that the magnetisation density M_0 per unit volume is not all that small (in field units, $M_0 \sim 1000$ Gauss in TM systems like Fe or Ni).

Above a certain size the system can relieve this "demagnetisation energy" by forming domain walls — we will look at these in more detail later. These cost energy but cut off the divergence in (76) at a length scale L_D, the typical distance between walls.

The typical energy scale of the nearest-neighbour interaction between dipoles is

$$\left| \mathcal{H}_{dip}^{nn} \right| \sim \frac{m^2}{a_0^3} \cong \mu_B^2 \frac{(L+2S)^2}{a_0^3} \left.\rule{0pt}{40pt}\right\} \quad (77)$$
$$\sim 0.1 - 1 \text{K}$$

Clearly this result is very sensitive to the distance between nearest neighbours.

If we include the crystal anisotropy energy $K(\underline{S})$, and now go to an energy scale $\ll |K^{(n)}|$, then each spin will be described by the lowest levels only — in this case we have a very interesting system, which will be discussed in great detail when we look at glasses and at spin qubits.

(VII) <u>HYPERFINE & INTERNUCLEAR INTERACTIONS</u> : Let us now consider what might be called the "quantum environment" of the electronic spin system. In an insulator, the electronic spins interact with 3 outside "reservoirs" : the nuclear spins, lattice phonons, and photons. We begin with the very important interaction with nuclear spins.

Let us first consider the "intrinsic" Hamiltonian of the nuclear spins, in the absence of their interaction with the electrons. For a <u>single</u> nuclear spin one has the Hamiltonian

$$\mathcal{H}_N = -\mu_N \cdot \underline{H}_0 + Q_{\alpha\beta} I^\alpha I^\beta \quad (78)$$

where the nuclear moment

$$\mu_N = g_N \mu_N \underline{I} \left.\rule{0pt}{30pt}\right\} \quad (79)$$
$$\mu_N = e\hbar/2M_N$$

and the nuclear g-factor $g_N = e\hbar/2M_p$ lies in the range $-5 < g_N < 5$. Since μ_N is thousands of times smaller than μ_B, the nuclear Zeeman energies are in the range

$$I|\mu_N \cdot \underline{H}_0| \sim I \times mK/T \quad (80)$$

The quadrupole term

$$Q_{\alpha\beta} = = U_{\alpha\beta}^Q(\underline{r}) \left[3(I^\alpha I^\beta + I^\beta I^\alpha) - 2\delta_{\alpha\beta} I(I+1) \right] \left.\rule{0pt}{55pt}\right\}$$
$$U_{\alpha\beta}^Q(r) = \frac{eQ}{6I(2I+1)} \cdot \frac{\partial^2 V(\underline{r})}{\partial r_\alpha \partial r_\beta} \quad (81)$$

receives its name because it depends on the quadrupole form of the electric potential $V(\underline{r})$, at the site of the nucleus, generated by the surrounding electrons. Here φ is the quadrupole moment of the nuclear charge. This quadrupole moment is zero when the nuclear spin $I = \frac{1}{2}$. For larger spin nuclei it forces the spacing between nuclear Zeeman levels in a field H_0 to be non-uniform.

There are other terms (e.g., the diamagnetic contribution to the coupling of μ_N to H_0) but we will ignore these.

Now consider the interaction between the μ_N and the electronic spins. For a TM system this is written as

$$\mathcal{H}_{Hyp} = A_{\alpha\beta} S^\alpha I^\beta = \underline{S}.\underline{\underline{A}}.\underline{I} \qquad (82)$$

where $A^{\alpha\beta}$ is the hyperfine coupling. Ultimately the hyperfine coupling is quite simple - it comes from the interaction of μ_N with the field $\underline{B}(r)$ generated at the nucleus by currents from the surrounding electrons. If we divide these contributions into currents far away from the nucleus, and those nearby, we end up with two contributions.
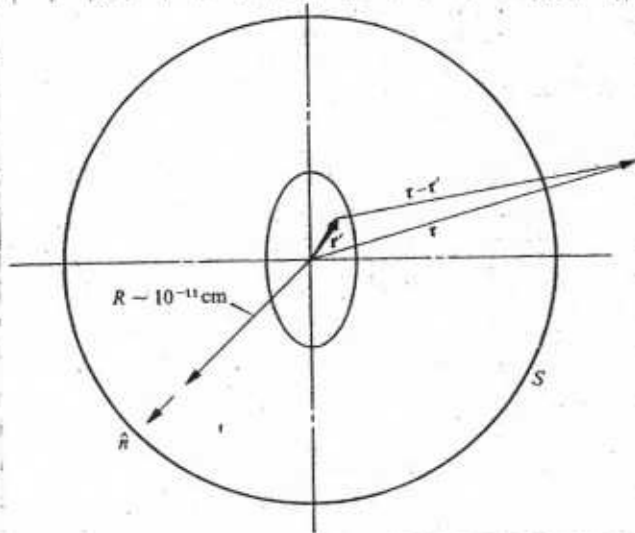
The first comes from averaging over the local "contact" interaction between electronic spin density and the field generated by the nucleus. Writing

$$\left.\begin{array}{l} \underline{B}_N = \nabla \times \underline{A}_N(r) \\[2mm] \underline{A}_N(r) = \dfrac{\mu_N \times \underline{r}}{r^3} \end{array}\right\} \qquad (83)$$

we then have an interaction

$$\mathcal{H}_{local} = -2\mu_B \underline{S}.\int d^3r \, |\psi_e(\underline{r})|^2 \underline{B}_N(\underline{r}) \qquad (84)$$

We see that this "contact hyperfine interaction" only occurs for s-electron states (otherwise $\psi_e(r \to 0) \to 0$). Writing as a surface integral on the surface S in the figure above, we get

$$\left.\begin{array}{l} \mathcal{H}_{Hyp}^{contact} = -2\mu_B \underline{S} \, |\psi_e(0)|^2 . \int d\Omega_S \, \dfrac{\underline{R} \times \underline{A}_N(\underline{R})}{|R|} \\[4mm] \qquad \longrightarrow -\dfrac{8\pi}{3} |\psi_e(0)|^2 \, \mu_N \cdot \underline{m}_S \end{array}\right\} \qquad (85)$$

where $\underline{m}_S$ is the electronic moment in (75). The interaction of μ_N with the electronic currents far from the nucleus is handled by a multipole expansion, to give finally

$$\hat{\mathcal{H}}_{Hyp} = -\dfrac{8\pi}{3} |\psi_e(0)|^2 \, \mu_N \cdot \underline{m}_S - \sum_j \left[\dfrac{2}{r_j^3} \underline{m}_j^L \cdot \mu_N - \dfrac{1}{r_j^3}\left(\underline{m}_j^S \cdot \mu_N - 3 \dfrac{(\mu_N \cdot \underline{r}_j)(\underline{m}_j^S \cdot \underline{r}_j)}{r_j^2} \right) \right] \qquad (86)$$

where in the dipolar terms we sum over all the electrons in the ion that have either an orbital moment $\underline{m}_j^L$ or a spin moment $\underline{m}_j^S$.

These interactions are all very messy, and as you can imagine when we rewrite them in the basis set of crystal field/spin-orbit states, we get something even messier. Just for the record I give the result, which you can think of as an addition to the spin Hamiltonian in (64) & which for TM ions looks like (82), with

$$A_{\alpha\beta} = A_S - \lambda A_L \Lambda_{\alpha\beta} + A_{LS}\left[3\langle 0|L^{\alpha}L^{\beta}|0\rangle - L(L+1)\right] \tag{87}$$

where the coefficients are

$$A_S = \frac{2}{S(S+1)}\mu_B^2 g_N \mu_N \sum_j \langle LS|\frac{8}{3}\pi\, \underline{S}_j\cdot\underline{S}\,\,\delta(r_j)|LS\rangle$$

$$A_L = \frac{2}{L(L+1)}\mu_B^2 g_N \mu_N \sum_j \langle LS|\frac{L_j\cdot L}{r_j^3}|LS\rangle \tag{88}$$

$$A_{LS} = \sum_j \frac{\langle LS|\hat{T}_j|LS\rangle}{\langle L|\underline{L}|L\rangle}\langle LS|\underline{S}_j\cdot\underline{S}|LS\rangle$$

and $\hat{T}_j$ in (86) is the dipolar form in (86) (i.e., the 3rd term).

Unless you are rather interested in hyperfine interactions you will not need to know more about this, except to note that the size of hyperfine couplings varies a great deal. In TM systems, one has values like

$$|A_{\alpha\beta}| \sim 2 - 15 \text{ mK} \qquad (TM) \tag{89}$$

between the nuclear moment and its own electrons. However in any TM compound, the magnetic nucleus will also interact with the electron clouds of other atoms – and the electron clouds of the magnetic ion will interact with other nuclei. These interactions are primarily dipolar, but they will of course also have contributions coming from the polarisation of the other electronic clouds – thus the exchange interactions and other inter-atomic interactions will be involved. These interactions are called "transfer hyperfine interactions", and they are often quite important. We can write them as

$$\mathcal{H}_{Hyp}^{Tran} = \frac{1}{2}\sum_{i\neq j} A_{ij}^{\alpha\beta} S_i^{\alpha} I_j^{\beta} \tag{90}$$

and sometimes $|A_{ij}^{\alpha\beta}|$ is as high as 1 mK.

Finally, one has the interaction between different nuclear spins. This of course is very small but is quite crucial in the understanding of NMR. We write

$$\mathcal{H}_{NN} = \frac{1}{2}\sum_{kk'} V_{kk'}^{\alpha\beta} I_k^{\alpha} I_{k'}^{\beta} \tag{91}$$

and the most obvious contribution to $V_{kk'}^{\alpha\beta}$ is dipolar:

$$V_{kk'}^{\alpha\beta}(dip) = \frac{1}{r_{kk'}^3}\left[\mu_N^k\cdot\mu_N^{k'} - 3\frac{(\mu_N^k\cdot r_{kk'})(\mu_N^{k'}\cdot r_{kk'})}{r_{kk'}^2}\right] \tag{92}$$

but there are also interactions mediated through the electron clouds (i.e., a nucleus I_k has hyperfine interactions with its local electrons, which then interact via exchange with other ions, which then interact with the nuclei of these ions). Obviously an analysis of these terms will be rather complex.

In any case, one typically has

$$|V_{kk'}| < 10^{-7} K \qquad (nn) \qquad (93)$$

even for quite close nuclei. This is very small - it is down by 10^6 from the dipole interaction between electron spins in (77).

The reason H_{NN} is important is because in the absence of any electronic spin dynamics, the nuclear dynamics is driven by $V_{kk'}$. This will be a slow dynamics, but it is crucial for NMR.

At extremely low T, the internuclear interactions can lead to nuclear ordering. This is tough to look at experimentally, but the phase diagram of some nuclear spin systems has been examined in some detail at nK temperatures.

The understanding of internuclear interactions is very important in ultra-low T physics, since thermal equilibration & cooling depend on it.

(viii) <u>PHONONS & SPIN-PHONON INTERACTIONS</u> : The second "quantum environment" that spins can interact with is the phonon bath. The description of phonons as quantized lattice vibrations is well known. We define a "displacement field" $u(r)$ (here treated in a long-wavelength "continuum approximation") for the lattice, and introduce the fields

$$\left.\begin{array}{ll} \epsilon_{\alpha\beta}(r) = \frac{1}{2}\left(\partial_\alpha u_\beta(r) + \partial_\beta u_\alpha(r)\right) & \text{symmetric strain} \\[2mm] \omega_{\alpha\beta}(r) = \frac{1}{2}\left(\partial_\alpha u_\beta(r) - \partial_\beta u_\alpha(r)\right) & \text{antisymmetric "twist"} \end{array}\right\} \quad (94)$$

The quantization of $u(r)$ gives phonons:

$$\hat{u}_\alpha(r) = \sum_{q\lambda}\left(\frac{\hbar}{2NM\omega_q^\lambda}\right)^{1/2} \epsilon_\alpha^\lambda\left[\hat{a}_{q\lambda} + \hat{a}_{-q\lambda}^\dagger\right] e^{iq\cdot r} \qquad (95)$$

where ϵ_q^λ is a polarization vector, and N and M are the number and mass of the ions involved. A spin will interact most obviously with a phonon if the lattice locally rotates — because the anisotropy interaction $K(\underline{S})$ in (65) is not invariant under rotations, the transverse phonons will interact with the spin.

The bare phonon Hamiltonian is of course just

$$H_{ph} = \hbar\sum_{q\lambda}\omega_q^\lambda\left(a_{q\lambda}^\dagger a_{q\lambda} + \frac{1}{2}\right) \qquad (96)$$

where for acoustic phonons the characteristic energy scale is θ_D, the Debye energy (or else the energy of some sharp van Hove singularity in the phonon density of states). One typically has

$$\theta_D \sim 100\text{-}400\,K \qquad (97)$$

in electronic solids, with

$$\hbar\omega_q^\lambda \sim \frac{qa_0}{\pi}\theta_D \sim c_s q \qquad (98)$$

44

where sound velocities $C_s \sim 1-80$ km/sec in solids.

The mechanism is easily understood formally. Consider an infinitesimal rotation of S_z, and its effect on the anisotropy term $K(\underline{S})$. Choose, e.g., a rotation by a small angle $\delta\theta$, and then consider the effect on the operator $\hat{S}_z$ in the new rotated frame. We have

$$\hat{S}_z \rightarrow \hat{S}_z + \delta\theta \left(\hat{S}_x \cos\phi + \hat{S}_y \sin\phi \right) \qquad (99)$$

so that a simple anisotropy term like $D\hat{S}_z^2$ (cf (67)) transforms like

$$D\hat{S}_z^2 \rightarrow D\left\{ \hat{S}_z^2 + \left[(\hat{S}_z\hat{S}_x + \hat{S}_x\hat{S}_z)\cos\phi + (\hat{S}_z\hat{S}_y + \hat{S}_y\hat{S}_z)\sin\phi \right]\delta\theta \right\} \qquad (100)$$

In the crystal such rotations are generated by a combination of symmetric & antisymmetric strains, and one ends up therefore with terms of form

$$\mathcal{H}_{ph}^{S} \sim iq\, D\left\{ (\epsilon_{xz} + \omega_{xz})(\hat{S}_x\hat{S}_z + \hat{S}_z\hat{S}_x) + (\epsilon_{yz} + \omega_{yz})(\hat{S}_y\hat{S}_z + \hat{S}_z\hat{S}_y) \right\} \qquad (101)$$

More generally one ends up with a general interaction between phonons and spins of the form

$$\mathcal{H}_{ph}^{S} = i\sum_{q\lambda} \underline{q}\cdot\left[g(\underline{S})\,\hat{a}_{q\lambda} - g^*(\underline{S})\,\hat{a}_{q\lambda}^\dagger \right] \qquad (102)$$

where the couplings $g(\underline{S})$ are functions of the anisotropy parameters $K_{\alpha\beta}^{(2)}$ in (66). One can of course go to higher orders in the spin anisotropy in making the rotation, and this leads to coupling between phonon multiplets and the spins — we do not look at this non-linear coupling any further.

Note that phonons will also affect the interaction between spins. We can imagine a process involving a spin pair flip, mediated by the exchange of phonons; and by the same arguments as above, the phonon which is exchanged between the spins will couple at each vertex by the coupling $g(\underline{S})$. Usually this coupling is much weaker than the exchange or superexchange interaction.

Finally, notice that phonons can modulate the exchange interaction itself. This happens because J depends on the distance between the ions, typically decreasing with increasing distance. This process, like the other three (see Fig. at left) is important because it provides a way of relaxing the atomic spin dynamics. We come to this later on.
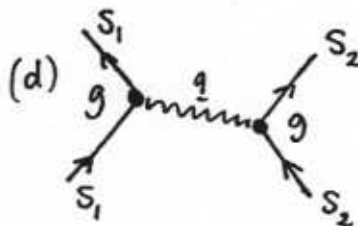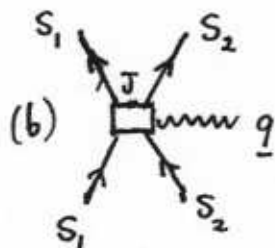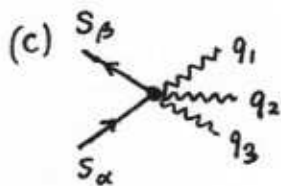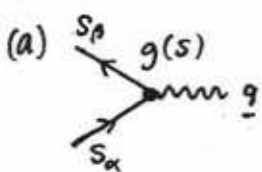
SPIN-PHONON INTERACTIONS. (a) THE BASIC COUPLING $\mathcal{H}_{ph}^{S}$.
(b) COUPLING BETWEEN AN EXCHANGE FLIP AND A PHONON
(c) NON-LINEAR SPIN-PHONON COUPLING. (d) SPIN-SPIN
MAGNETOACOUSTIC COUPLING BETWEEN $\underline{S}_1$ & $\underline{S}_2$

B.2.   SPINS in CONDUCTING SYSTEMS

The delocalisation of electrons in conductors leads to a rather different picture of the low-energy physics from that obtaining in insulators, in which one concentrates on the delocalised energy bands near the Fermi energy. Traditionally the teaching of this topic has started from the free-electron limit, ie., from the simple hopping Hamiltonian in (3). This is why traditional solid-state texts spend so much time on band theory, Brillouin zones, Bravais lattices, & so on. There is a very serious flaw in such an approach, which we have already seen - in most solids, $U > t$ or even $U \gg t$. As we will discuss in more detail later, this is why most solids are insulating.

Nevertheless a band approach is very useful for conductors if done properly. The best way found so far uses Landau Fermi liquid theory (FLT), and in high fields, adapts this to include Landau levels. However there is a big surprise waiting in 2 dimensions, as we will see.

B.2.1.   BAND STRUCTURE & FERMI LIQUID THEORY

As we already saw, the band structure for a simple band is defined by the simple Hamiltonian in (3), which for multiple bands is written, to zero-th approximation:

$$\mathcal{H}_0 = -\sum_{i \neq j} \sum_{n6} \left(t_{ij}^{(n)} c_{in,6}^+ c_{jn,6} + H.c \right)$$

$$\equiv \sum_{n6} \epsilon_{kn}^0 \left(c_{kn,6}^+ c_{kn,6} \right) \qquad \qquad (103)$$

where the "dispersion relation" for the n-th band is

$$\epsilon_{kn}^0 = -\sum_{i \neq j} t_{ij}^{(n)} e^{ik \cdot (R_i - R_j)} \xrightarrow[\substack{\text{tight-binding} \\ \text{limit}}]{\langle ij \rangle} -\sum_{\langle ij \rangle} t_{ij}^{(n)} e^{ik \cdot (R_i - R_j)} \qquad (104)$$

For a band when $t^{(n)} \ll U$ this approach is almost meaningless. If however we can ignore interactions for the moment, then we see from the Anderson model that a better "zero-th" approximation would be to include hybridisation between the bands where they approach each other, ie., write

$$\mathcal{H}_0 = -\sum_{i \neq j} \sum_{n} \sum_{m} \sum_{6} \left(t_{ij}^{nm} c_{in,6}^+ c_{jm,6} + H.c. \right)$$

$$\equiv \sum_{kn6} \epsilon_{kn}^0 c_{kn,6}^+ c_{kn,6} + \sum_{n \neq m} \sum_{k6} \left(V_{nm}(k) c_{kn,6}^+ c_{km,6} + H.c. \right). \qquad (105)$$

where now

$$\epsilon_{kn}^0 = -\sum_{i \neq j} t_{ij}^{nm} e^{ik \cdot (R_i - R_j)} \qquad (106)$$

$$V_{nm}(k) = -\sum_{i \neq j} t_{ij}^{nm} e^{ik \cdot (R_i - R_j)} \qquad (107)$$

(compare eqn. (12), without the local repulsion term U_0). The elementary texts in

solid-state physics are full of the results of calculations of such band structures for "simple metals". In reality these texts describe results that are only useful the most delocalized electron states, where $U < t$. However if the Fermi energy happens to be located in one of these broad bands, then such a picture is very useful indeed.

The most obvious examples are provided by the alkali metals, in which a complete atomic shell has been filled, leaving behind only a single electron in the higher s-shell. This electron very easily delocalizes, and its energy dispersion, even near the bottom of the resulting s-band, is very nearly parabolic. This "free-electron picture works so well for the alkali metals, and also for the so-called "Noble" metals, that one can actually treat the lattice potential itself as a weak perturbation on the conduction electron dynamics. The atomic potential is so effectively screened by the filled "Noble gas" shells that one is left with only a very weak periodic potential acting on the conduction electrons.

As a consequence the Fermi surfaces of the alkali metals are almost exactly spherical, as we see in the Figure at left.

LEFT: FERMI SURFACE of Na


Sodium   Potassium

Rubidium   Cesium
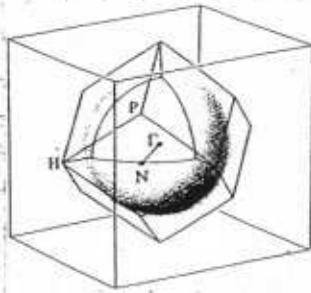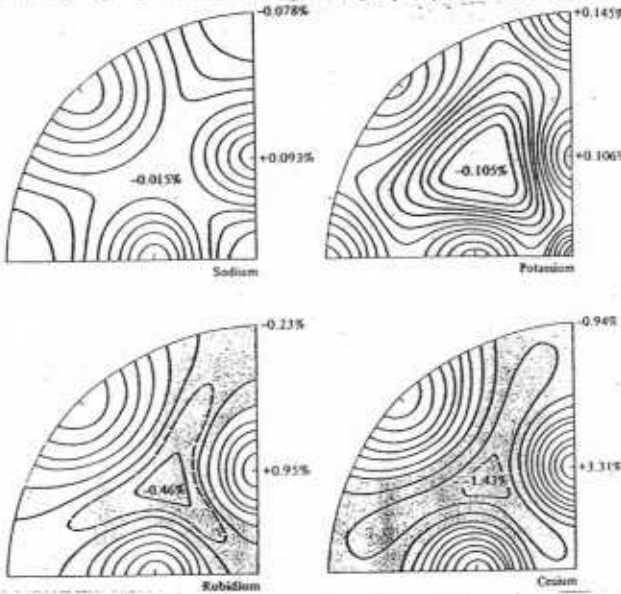
The measured Fermi surfaces of the alkali metals. Contours of constant distance from the origin are shown for that portion of the surface lying in the first octant. The numbers indicate percent deviation of k/k_0 from unity at maximum and minimum deviation, where k_0 is the radius of the free electron sphere. Contours for Na and K are at intervals of 0.02 percent, for Rb at intervals of 0.2 percent, with an extra dashed one at -0.3 percent, and for Cs at intervals of 0.5 percent, with an extra dashed one at -1.25 percent. (From D. Shoenberg, *The Physics of Metals*, vol. 1, J. M. Ziman, ed., Cambridge, 1969.)

Incredibly, this is even almost true for the Fermi surfaces of some transition metals; we see here the examples of Cu and Ag, which are almost indistinguishable.
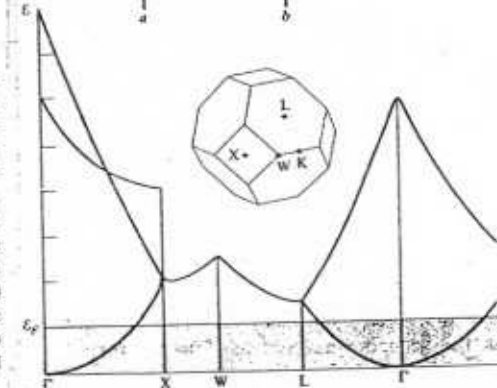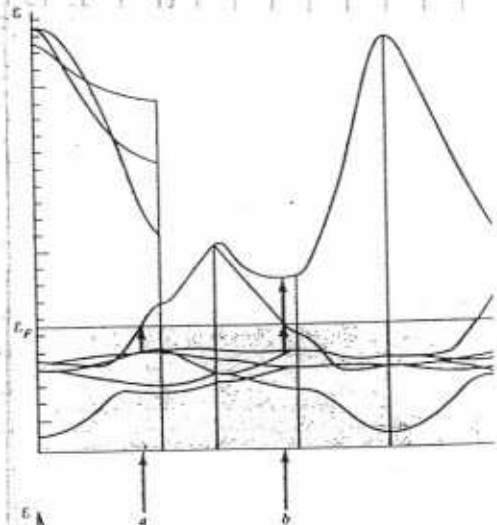

Burdick's calculated bands for copper, illustrating that the absorption threshold for transitions up from the conduction band is about 4 eV, while the threshold for transitions from the d-band to the conduction band is only about 2 eV. (The energy scale is in tenths of a rydberg (0.1 Ry = 1.36 eV).) Note the resemblance of the bands other than the d-bands to the free electron bands plotted below.

LEFT: FERMI SURFACE of Ag
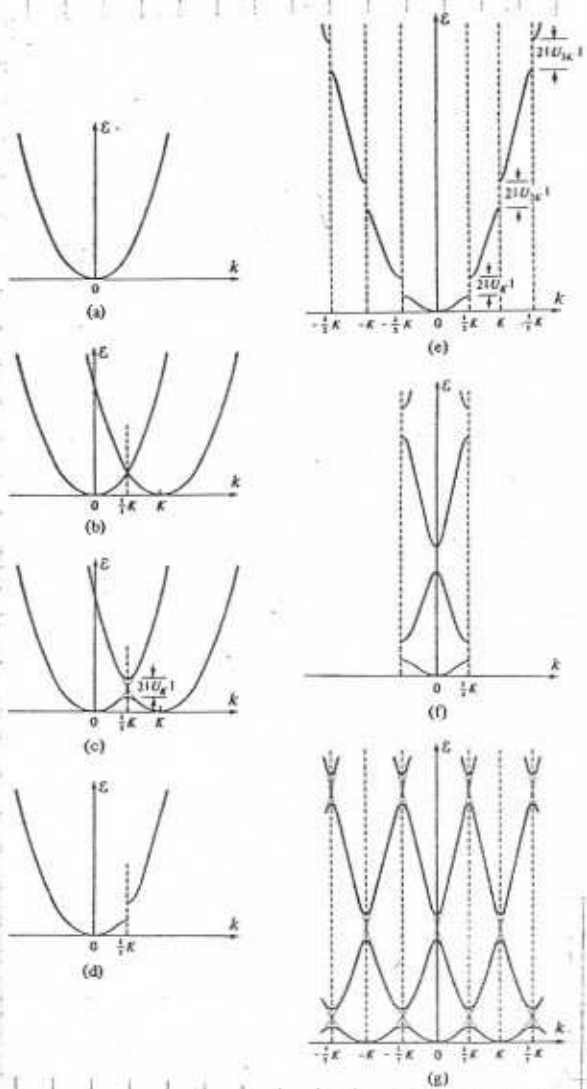
(a) The free electron ε vs. k parabola in one dimension. (b) Step 1 in the construction to determine the distortion in the free electron parabola in the neighborhood of a Bragg "plane," due to a weak periodic potential. If the Bragg "plane" is that determined by K, a second free electron parabola is drawn, centered on K. (c) Step 2 in the construction to determine the distortion in the free electron parabola in the neighborhood of a Bragg "plane." The degeneracy of the two parabolas at $K/2$ is split. (d) Those portions of part (c) corresponding to the original free electron parabola given in (a). (e) Effect of all additional Bragg "planes" on the free electron parabola. This particular way of displaying the electronic levels in a periodic potential is known as the *extended-zone scheme*. (f) The levels of (e), displayed in a *reduced-zone scheme*. (g) Free electron levels of (e) or (f) in a *repeated-zone scheme*.

The way this works is easily understood by looking at the simple constructions shown. At left we see how the parabolic dispersion in 1 dimension is distorted by weak coupling to a periodic potential, at wave vectors given by the "Bragg planes" (which in a 1-d system are just points).
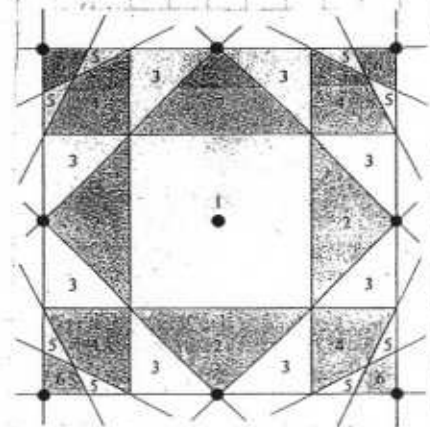
DEFINITION of BRAGG POINTS, PLANES, & REDUCED ZONES
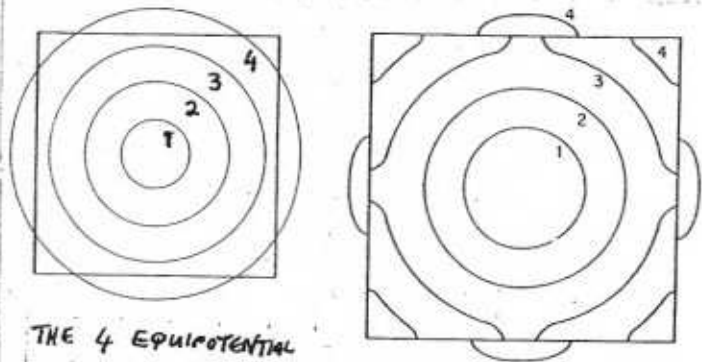
THE 4 EQUIPOTENTIAL LINES ARE DISTORTED AS SHOWN BY A WEAK LATTICE POTENTIAL

We recall from elementary crystal lattice theory the definition of reciprocal lattice vectors $\underline{G}$, such that

$$e^{i\underline{G}\cdot\underline{R}_n} = e^{i\underline{G}\cdot(n_1\underline{a}_1 + n_2\underline{a}_2 + n_3\underline{a}_3)} = 1 \qquad (108)$$

where $\underline{R}_n$ defines all points on the real-space lattice, and $\underline{G}$ all points on the reciprocal lattice; the Bragg planes bisect the lines between the $\underline{k}$-space origin and any reciprocal lattice point $\underline{G}$. The weak potential interacts resonantly with an electron near these planes.
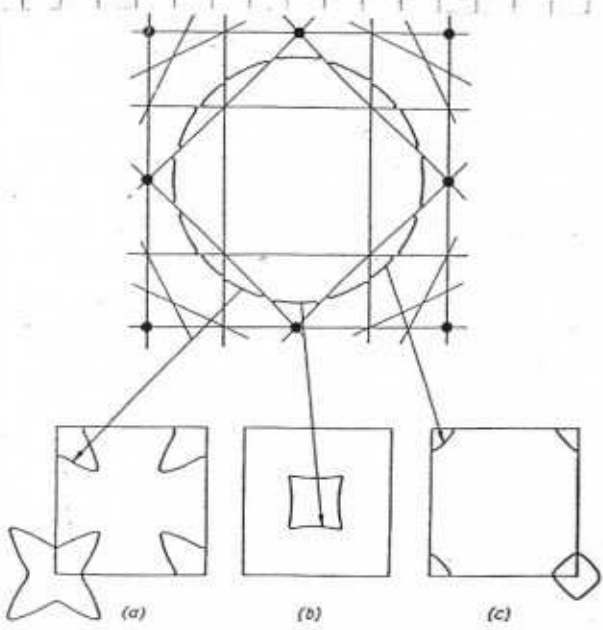
"FOLDING BACK" THE WEAKLY PERTURBED FERMI SURFACE TO THE REDUCED ZONES

48

We see from the pictures on the last pages that the effect of a lattice potential is very weak in metals like Na, K, etc., or Cu, Ag, and Au. In the case of the Noble metals one does not have quite the simple picture of

THE MONOVALENT METALS

ALKALI METALS (BODY-CENTERED CUBIC)[a]	NOBLE METALS (FACE-CENTERED CUBIC)
Li: $1s^2 2s^1$	—
Na: $[Ne]3s^1$	—
K: $[Ar]4s^1$	Cu: $[Ar]3d^{10}4s^1$
Rb: $[Kr]5s^1$	Ag: $[Kr]4d^{10}5s^1$
Cs: $[Xe]6s^1$	Au: $[Xe]4f^{14}5d^{10}6s^1$

the alkali metals, but they are both monovalent, with in both cases a set of s-electrons high above the deeper quasi-bound electrons, and a very small effective lattice potential acting on the conduction band. In fact the main difference between the 2 cases, as we see in the table at left, is the crystal structure, which brings the Noble metal conduction electron Fermi sphere much closer to the 1st Brags plane.

It is actually quite amazing how well this picture works even for some of the
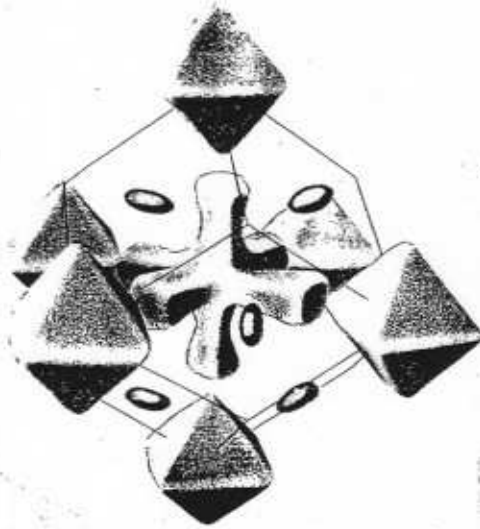
Proposed Fermi surface for bcc tungsten. The six octahedron-shaped pockets at the zone corners contain holes. They are all equivalent; i.e., any one can be taken into any other by a translation through a reciprocal lattice vector, so that all physically distinct levels in the group are contained in any one of them. The twelve smaller pockets in the centers of the zone faces (only five are visible) are also hole pockets. They are equivalent in pairs (from opposite faces). The structure in the center is an electron pocket. Tungsten has an even number of electrons, and is therefore a compensated metal. It therefore follows that the volume of a large hole pocket plus six times the volume of a small hole pocket is equal to the volume of the electron pocket at the center of the zone. Consistent with a Fermi surface composed entirely of closed pockets, the magnetoresistance has been ob-served to increase quadratically with H for all field directions, as predicted for a compensated metal without open orbits. Note that the surface, unlike those considered earlier, is not a distortion of the free electron surface. This is a consequence of the Fermi level lying within the d-band, and is characteristic of transition metals. (After A. V. Gold, as quoted in D. Shoenberg, *The Physics of Metals*—1. *Electrons*, J. M. Ziman, ed., Cambridge, 1969, p. 112.)

transition metals. In these cases one needs to include significant electron-electron interaction effects to understand the actual band structure (this will already be clear from our previous look at the d-bands of Cu, back on page 25). Nevertheless, in cases where the Fermi energy finds itself in the middle of a hybridised d-band, one gets conduction in this band, and a well-defined Fermi surface (as we see above for BCC W).

<u>Fermi Liquid Theory</u> : So what about the effect of interactions? A quite remarkable theory designed to handle these was given by Landau in the late 1950's. It was originally designed to describe ^{3}He liquid (where there is no crystal lattice), but gives a very good description of metals so well, once suitably adapted to incorporate the crystal lattice, other non-conducting bands, and electron-phonon interactions.

In its original form the theory had 3 components. The first was a "phenomenological" theory of the equilibrium properties. For an isotropic Fermi liquid like ^{3}He, one starts from an energy functional

$$E\{n_{p6}\} = E_0 + \sum_{k6} \epsilon_{k6}^0 \, \delta n_{k6} + \frac{1}{2} \sum_{kk'} \sum_{66'} f_{kk'}^{66'} \, \delta n_{k6} \, \delta n_{k'6'} \qquad (109)$$

for a set of "quasiparticles", which are elementary excitations of the system labelled by quantum numbers $\underline{k}$ and 6 (these being the "good quantum numbers", ie the conserved quantities of the system. The distribution (a classical distribution function) and the deviation δn_{p6} are probability distributions for the

quasiparticles, which we assumed to be fermions.: In this equilibrium theory we have

$$n_{p\sigma} = \left[e^{\beta(\epsilon_{p\sigma} - \mu)} + 1 \right]^{-1}$$

$$\delta n_{p\sigma} = n_{p\sigma} - n_{p\sigma}^{(0)} \qquad\qquad n_{p\sigma}^{(0)} = n_{p\sigma}(T) = \theta(\mu - \epsilon_{p\sigma}) \qquad\Big\} \quad (110)$$

An immediate consequence of (109) is that we can assign an energy to a given quasiparticle state $|p\sigma\rangle$, given by

$$\epsilon_{p\sigma} = \delta E / \delta n_{p\sigma}$$

$$= \epsilon_{p\sigma}^{(0)} + \sum_{p'\sigma'} f_{pp'}^{\sigma\sigma'} \delta n_{p'\sigma'} \qquad\qquad\Big\} \quad (111)$$

so that by definition

$$\epsilon_{p\sigma}^{(0)} = \epsilon_{p\sigma}(T=0)$$

$$f_{pp'}^{\sigma\sigma'} = \delta \epsilon_{p\sigma} / \delta n_{p'\sigma'} \qquad\qquad\Big\} \quad (112)$$

Note that $\epsilon_{p\sigma}^{(0)}$ as defined here is **not** usually the quantity which is calculated in most band-structure calculations. I shall say more about this below.

The interaction function $f_{pp'}^{\sigma\sigma'}$ describes the way in which the appearance of a quasiparticle state $|p'\sigma'\rangle$ affects the energy of a state $|p\sigma\rangle$ (or vice-versa). As we shall see these interactions can be **strong** - the condition for validity of Landau's FLT is not that the interactions be weak, but rather that

$$\sum_{p\sigma} \delta n_{p\sigma} = \delta n \ll 1. \qquad\qquad (113)$$

i.e., that the density of quasiparticles be low.

The 2nd part of Fermi liquid theory extends this phenomenological picture to non-equilibrium phenomena. One defines a spatially inhomogeneous distribution $\delta n_{p\sigma}(r,t)$, so that now

$$\epsilon_{p\sigma}(r,t) = \epsilon_{p\sigma}^0 + \int d^3r' \sum_{p'\sigma'} f_{pp'}^{\sigma\sigma'}(r-r') \, \delta n_{p'\sigma'}(r',t) \qquad (114)$$

where $f_{pp'}^{\sigma\sigma'}(r-r')$ is still considered to act instantaneously, but can now also act over long distances.

The remarkable insight of Landau was to realise that the $\delta n_{p\sigma}(r,t)$ would satisfy a modified Boltzmann eqn. for their dynamics, called the Landau-Boltzmann eqn:

$$\partial_t n_p^\sigma(r,t) + \left(\nabla_p \epsilon_p^\sigma(r,t) \cdot \nabla_r n_p^\sigma(r,t) - \nabla_r \epsilon_p^\sigma(r,t) \cdot \nabla_p n_p^\sigma(r,t) \right) = I\{n_p^\sigma\} \qquad (115)$$

In the first phenomenological derivation of this equation, Landau simply appealed to a continuity equation for the distribution function:

$$D_t \, n_p^\sigma(r,t) = I\{n_p^\sigma\} \qquad\qquad (116)$$

where

$$D_t \equiv \left[\partial_t + \underline{v} \cdot \nabla_r + \dot{p} \cdot \partial_p \right] \qquad\qquad (117)$$

is the total time derivative, and $I[n_p^\sigma]$ is the "collision integral", which describes the scattering of quasi-particles off each other; and $v = dr/dt$. This equation describes incompressible flow in phase space. Now (116) is just the standard Boltzmann eqn for a dilute/low-density gas if $n_{p\sigma}(r,t)$ is the distribution function for _particles_; the big difference here is that for a particle, $\epsilon_{p\sigma}$ is quite independent of $n_{p\sigma}(r,t)$, whereas for Landau quasiparticles we have (114).

In most cases one uses the linearized Landau-Boltzmann eqn., produced by expanding $n_{p\sigma}(rt)$ to lowest order in δn_p^σ; we then get:

$$\left(\partial_t + v_{p\sigma}\cdot\nabla_r\right)\delta n_p^\sigma(r,t) - \nabla_p n_{p\sigma}^{(0)}\cdot\sum_{p'\sigma'}\int d^3r'\, \nabla_r f_{pp'}^{\sigma\sigma'}(r,r')\,\delta n_{p'\sigma'}(r',t) = I \tag{118}$$

and actually this eqn. can be simplified even more by noting that

$$\nabla_p n_{p\sigma}^{(0)} = \underline{v}_{p\sigma}\cdot\frac{\partial n_{p\sigma}^{(0)}}{\partial \epsilon_{p\sigma}} \qquad\longrightarrow\qquad -\underline{v}_{p\sigma}\,\delta(\epsilon_p^\sigma - \mu) \tag{119}$$

from the def^n of $n_{p\sigma}^{(0)}$ in (110); thus we have a velocity term concentrated around the Fermi surface.

It is common to separate $f_{pp'}^{\sigma\sigma'}(r-r')$ into short-range & long-range parts. In this case we write

$$f_{pp'}^{\sigma\sigma'}(\underline{r}-\underline{r}') \approx f_{pp'}^{\sigma\sigma'}\,\delta(r-r') + V_{pp'}^{\sigma\sigma'}(r-r') \tag{120}$$

and in this case, if we drop the long-range part, the linearized L-B eqn becomes

$$\left(\partial_t + \underline{v}_p^\sigma\cdot\underline{\nabla}_r\right)\delta n_{p\sigma}(r,t) + v_{p\sigma}\,\delta(\epsilon_p^\sigma - \mu)\cdot\sum_{p'\sigma'} f_{pp'}^{\sigma\sigma'}\,\underline{\nabla}_r\,\delta n_{p'}^{\sigma'}(r,t) = I\{\delta n_p\} $$

i.e.

$$\left(\omega - \underline{q}\cdot\underline{v}_p^\sigma\right)\delta n_p^\sigma(\underline{q},\omega) - \delta(\epsilon_p^\sigma - \mu)\,\underline{q}\cdot\underline{v}_p^\sigma\sum_{p'\sigma'} f_{pp'}^{\sigma\sigma'}\cdot\delta n_{p'}^{\sigma'}(\underline{q},\omega) = I\{\delta n_p\} \tag{121}$$

where in the 2nd eqn we use the Fourier transform

$$\delta n_p^\sigma(\underline{q},\omega) = \int d^3r\int dt\, e^{i(\underline{q}\cdot\underline{r} - \omega t)}\,\delta n_p^\sigma(\underline{r},t) \tag{122}$$

The crucial term of interest in (121), which makes it different from a weakly-interacting system, is the 3rd term on the LHS; without it we would just have the Boltzmann eqn:

$$\left(\partial_t + v_{p\sigma}\cdot\underline{\nabla}_r\right)\delta n_{p\sigma}(\underline{r},t) = I\{n_p^\sigma\} \qquad [\text{BOLTZMANN}] \tag{123}$$
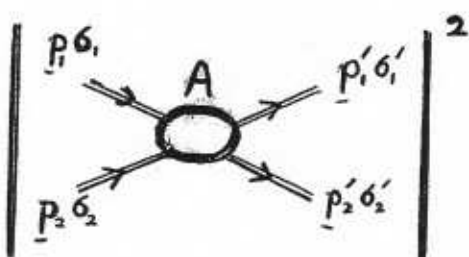
The 3rd term is usually called the "molecular field" term, and it describes an extra non-dissipative field acting on the quasiparticles $|p\sigma\rangle$ coming from all the other quasiparticles. The existence of this field leads to some remarkable properties for a Fermi liquid - for example, in the low-T limit, the collision integral $I[n_{p\sigma}]$ becomes negligible, but the system can still support collective

modes which are almost undamped - the most famous of these is "zero-th" sound, which is a density oscillation in the absence of collisions (this makes it quite different from ordinary sound!).

The collision integral can be treated both phenomenologically and using the 3rd part of FLT, which is the microscopic part. In phenomenological theory one writes

$$I\{\delta n_{p\sigma}\} = \sum_{p_2 \sigma_2} \sum_{\substack{p_1' \sigma_1' \\ p_2' \sigma_2'}} W^{p_1' p_2' \sigma_1' \sigma_2'}_{p_1 p_2, \sigma_1 \sigma_2} \delta(\epsilon_{p_1} + \epsilon_{p_2} - \epsilon_{p_1'} - \epsilon_{p_2'}) \delta(p_1 + p_2 - p_1' - p_2')$$

$$\times \left[n_{p_2}^{\sigma_2}(1 - n_{p_1'}^{\sigma_1'})(1 - n_{p_2'}^{\sigma_2'}) - (1 - n_{p_2}^{\sigma_2}) n_{p_1'}^{\sigma_1'} n_{p_2'}^{\sigma_2'} \right] \qquad (124)$$

$$W^{\sigma_1 \sigma_2 \sigma_1' \sigma_2'}_{p_1 p_2, p_1' p_2'} =$$

The scattering probability W is, as is usual in any quantum system, given by an amplitude squared:

$$W^{p_1' p_2' \sigma_1' \sigma_2'}_{p_1 p_2 \sigma_1 \sigma_2} = \left| A^{p_1' p_2' \sigma_1' \sigma_2'}_{p_1 p_2 \sigma_1 \sigma_2} \right|^2 \qquad (125)$$

To calculate the scattering amplitudes, we need a more microscopic underpinning to the Landau FLT. I will not go into this in any detail at all, since it is not central to the main themes we want to discuss here. The useful points that I just note here in passing are

(a) The quasiparticles in a Fermi liquid do have a finite overlap with the underlying fermions - this overlap $z_k^\sigma = |\langle p\sigma_{GAS} | p\sigma_{FLT} \rangle|$ is however typically _smaller_ near the Fermi surface, where interesting many-body effects tend to come into play. If one looks at the probability that the non-interacting states will be occupied in the ground state $|0\rangle_{FLT}$ of the interacting system, we still see a jump in this probability at the Fermi energy.
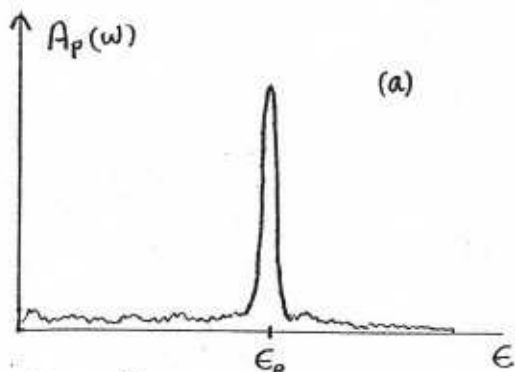
(a) THE "SPECTRAL WEIGHT" IN ENERGY, FOR AN EXCITATION WITH MOMENTUM $\underline{p}$.
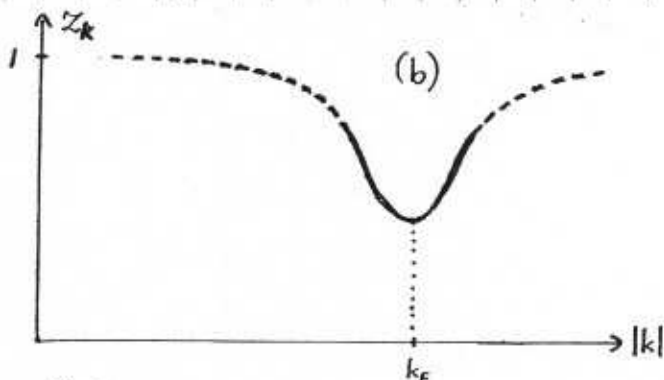
(b) THE OVERLAP BETWEEN THE "QUASIPARTICLE STATE" $|p\rangle$, AND A NON-INTERACTING STATE WITH THE SAME MOMENTUM
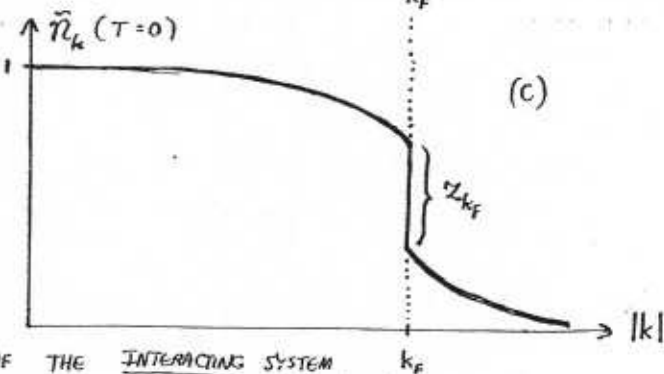
(c) THE PROBABILITY THAT STATES $|k\rangle_0$ OF THE NON-INTERACTING SYSTEM WILL STILL BE OCCUPIED IN THE GROUND STATE OF THE _INTERACTING_ SYSTEM

(b) All of the preceding results can be quantified if we can calculate the 1-particle Green function $G_{p\sigma}(\epsilon)$ of the system, defined by

$$G_{p\sigma}(\epsilon) = \int dt \int d^3r \, e^{i(p\cdot r - \epsilon t)} G_\sigma(r,t)$$

$$G_\sigma(r,t) = \langle 0_{RT} | \hat{T} \{ \psi_\sigma(r,t) \psi_\sigma^\dagger(0,0) \} | 0_{FLS} \rangle$$
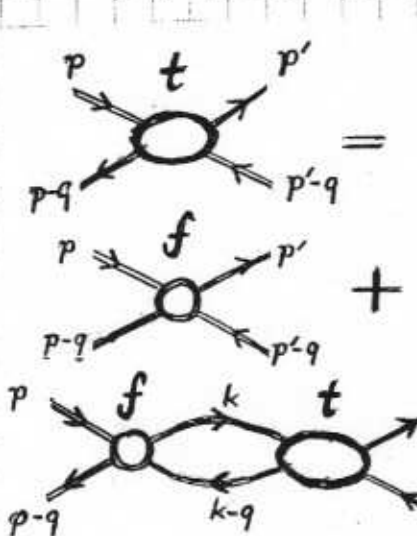
(126)

In fact the spectral function has the form

$$A_{p\sigma}(\epsilon) = \frac{1}{2\pi} \operatorname{Im} G_{p\sigma}(\epsilon) \sim Z_p^\sigma f_\sigma(\epsilon - \epsilon_{p\sigma}) + \phi_{p\sigma}(\epsilon) \tag{127}$$

which was shown on the last page, where $\phi_{p\sigma}(\epsilon)$ is spread very broadly over energy space, and represents the "incoherent" part of the quasiparticle propagator, whereas $f_p(x)$ is sharply peaked around $x=0$, with a half-width

$$\Gamma_p \sim (\epsilon_p - \mu)^2 / \epsilon_F \qquad \text{for } |\epsilon_p - \mu| \ll \epsilon_F \tag{128}$$

and we define $\int dx \, f(x) = 1$. Thus a fraction $Z_{p\sigma} < 1$ of the quasiparticle Green function is propagating coherently.

(c) Both the scattering amplitude $A_{pp_2^{\sigma,\sigma_2,\sigma',\sigma_2'}}^{\sigma,\sigma_2,\sigma',\sigma_2'}$ and the "f-function" $f_{pp'}^{\sigma\sigma'}$ can be understood field-theoretically by starting from the same quantity, viz., the 4-point vertex $\Gamma(P,P';Q)$, where $P \equiv (p,\epsilon)$, $P' \equiv (p',\epsilon')$, and $Q \equiv (q,w)$ are 4-momenta for a 3-d system. The actual relations are

$$f_{pp'}^{\sigma\sigma'} = Z_p^\sigma Z_{p'}^{\sigma'} \Gamma_w(p,\epsilon_p; p'\epsilon_{p'})$$

$$a_{pp'}^{\sigma\sigma'} = Z_p^\sigma Z_{p'}^{\sigma'} \Gamma_q(p,\epsilon_p; p'\epsilon_{p'})$$

(129)

where Γ_w and Γ_q are special limits of the general 4-point vertex:

$$\Gamma_w(P,P') = \lim_{q/w \to 0} \lim_{Q \to 0} \Gamma(PP'; Q)$$

$$\Gamma_q(P,P') = \lim_{w/q \to 0} \lim_{Q \to 0} \Gamma(PP'; Q)$$

(130)

We will not go into any detail here about this microscopic formulation, except to note one of its important consequences, viz., a microscopic derivation of the Landau-Boltzmann equation. This is derived from the field-theoretic result shown in the graphs in the Figure; if you wish to read more about this you should go to the references. A key result may be written in the following form

$$t_{pp'}^{\sigma\sigma'}(q,w) = f_{pp'}^{\sigma\sigma'} + \sum_{k,\sigma''} f_{pk}^{\sigma\sigma''} \frac{n_k^{\sigma''} - n_{k+q}^\sigma}{w - (\epsilon_{k+q} - \epsilon_k) + i\eta_k} t_{kp'}^{\sigma''\sigma'}(q,w) \tag{131}$$

which is an equation for the <u>quasiparticle</u> T-matrix, which gives a general

description of the scattering of 2 quasiparticles – it is defined by

$$t_{pp'}^{\sigma\sigma'}(q,\omega) = \lim_{q \to 0} z_p^{\sigma} z_{p'}^{\sigma'} \Gamma(P,P';Q) \tag{132}$$

and $t_{pp'}^{\sigma\sigma'}(q,\omega)$ interpolates between $f_{pp'}^{\sigma\sigma'}$ (when $q/\omega \to 0$) and $A_{pp'}^{\sigma\sigma'}$ (when $q/\omega \to \infty$).

This eqn. (131) for the T-matrix actually has the same structure as the linearised L-B eqn, in the low-T limit. To see this it is very helpful to define a set of dimensionless interaction parameters, in the present case of an isotropic system with a spherical Fermi surface (here $\mu_{pp'} = \cos\theta_{pp'} = \hat{p}\cdot\hat{p}'$):

$$
\left.
\begin{aligned}
F_{pp'}^{\sigma\sigma'} &= N(0) f_{pp'}^{\sigma\sigma'} = \sum_\ell F_\ell^{\sigma\sigma'} P_\ell(\mu_{pp'}) \\
A_{pp'}^{\sigma\sigma'} &= N(0) a_{pp'}^{\sigma\sigma'} = \sum_\ell A_\ell^{\sigma\sigma'} P_\ell(\mu_{pp'})
\end{aligned}
\right\} \tag{133}
$$

where $N(0)$ is the Fermi surface density of states, which in 3d is

$$
\left.
\begin{aligned}
N(0) &= \sum_{p\sigma} \delta(\epsilon_p - \mu) = -\sum_{p\sigma} \frac{\partial n_{p\sigma}^{(0)}}{\partial \epsilon_{p\sigma}} \qquad (T=0) \\
&= \frac{P_F^2}{\pi^2 \hbar^3 V_F}
\end{aligned}
\right\} \tag{134}
$$

In an isotropic Fermi liquid without spin-orbit coupling, it is also the case that

$$f_{pp'}^{\sigma\sigma'} = f_{pp'}^S + f_{pp'}^A \, \underline{\sigma}\cdot\underline{\sigma}' \tag{135}$$

where

$$f_{pp'}^S = \tfrac{1}{2}\left(f_{pp'}^{\sigma\sigma} + f_{pp'}^{\sigma,-\sigma}\right) \qquad f_{pp'}^A = \tfrac{1}{2}\left(f_{pp'}^{\sigma\sigma} - f_{pp'}^{\sigma,-\sigma}\right) \tag{136}$$

Note that the inverse transformation to (133) is

$$F_\ell^\lambda = \frac{2\ell+1}{2} \int_{-1}^{1} d\mu \, f_{pp'}^\lambda P_\ell(\mu) \tag{137}$$

To solve (131), we note that as $|q| \to 0$, $(\epsilon_{k+q} - \epsilon_k) \to q\cdot v_k$, and also that

$$n_k - n_{k+q} \to -\frac{\partial n_k^0}{\partial \epsilon_k} q\cdot v_k = q\cdot v_k \, \delta(\epsilon_k - \mu) \tag{138}$$

so that (131) becomes (here $\lambda = S,A$, following the def^n in (135)):

$$t_{pp'}^\lambda = f_{pp'}^\lambda + \sum_k f_{pk}^\lambda \, \delta(\epsilon_k - \mu) \frac{q\cdot v_k}{\omega - q\cdot v_k + i\eta_k} t_{kp'}^\lambda(q,\omega) \tag{139}$$

This is an integral equation for $t_{pp'}^\lambda$, and if you look at (121) you will see that the L-B equation has the same structure. Both can be solved by transforming

to angular representations like (133), (137). Thus, to solve the T-matrix equation (139) we write

$$t^{\lambda}_{pp'} = \sum_{\ell} t^{\lambda}_{\ell} P_{\ell}(\mu_{pp'}) \tag{140}$$

and to solve the L-B eqn we write

$$\delta n^{\lambda}_p(q,\omega) = -\delta(\epsilon_p - \mu)\, \phi^{\lambda}_p(q,\omega) \quad\Bigg\} \tag{141}$$
$$\phi^{\lambda}_p(q,\omega) = \sum_{\ell} \phi^{\lambda}_{\ell} P_{\ell}(\mu_{pq})$$

so that the LB eqn (121) reads now, in the collisionless limit $I\{\delta n\} = 0$:

$$\phi_{\ell} + \sum_{\ell'} \frac{2\ell+1}{2\ell'+1}\, \Omega_{\ell\ell'}(s)\, F^{\lambda}_{\ell'}\, \phi^{\lambda}_{\ell'} = 0 \tag{142}$$

where we have used the addition theorem for Legendre polynomials, and defined $s = \omega/qv_F$, where v_F is the Fermi velocity.

If we look at the def^n of the ϕ_{ℓ}, we see that the components ϕ_{ℓ} tell us the angular components of distortions of the Fermi sphere. Thus ϕ_0 corresponds to an infinitesimal distortion of the radius of the Fermi sphere. In effect the L-B eqn is describing a set of oscillations of the Fermi surface shape, driven by the interquasiparticle interactions. The angular components

$$\Omega_{\ell\ell'}(s) = \frac{1}{2}\int_{-1}^{1} d\mu\, P_{\ell}(\mu)\, \frac{\mu}{\mu-s}\, P_{\ell'}(\mu) \tag{143}$$

couple these oscillations together.

A similar eqn can be derived for the T-matrix, in terms of the F-function. In the limit where $s \to 0$, we recover the very simple equation

$$A^{\lambda}_{\ell} = F^{\lambda}_{\ell}\Big/\left[1 + F^{\lambda}_{\ell}\Big/2\ell+1\right] \tag{144}$$

It is interesting to ask about the physical significance of the 2 sets of dimensionless interaction parameters $\{F^{\lambda}_{\ell}\}$ and $\{A^{\lambda}_{\ell}\}$:

<u>Landau interaction parameters F^{λ}_{ℓ}</u>: These dimensionless numbers tell us the strength of the interaction energy between 2 quasiparticles, in the sense that the energy of 2 quasiparticles is, from (109) or (111), just

$$E_{12} = \epsilon^{(0)}_{p_1} + \epsilon^{(0)}_{p_2} + f^{\sigma_1\sigma_2}_{p_1 p_2} \tag{145}$$

If the dimensionless parameters are large then these interactions are strong. Thus, in a low-density Fermi gas, one finds that

$$|F^{A}_0| \sim (ak_F)^2 \ll 1 \tag{146}$$

where a_0 is the "scattering length" (the typical range of the potential) and k_F the Fermi wave-vector. On the other hand for a dense Fermi liquid like ^{3}He liquid, the Landau interaction parameters are not small, although $F_{\rho\rho'}^{\lambda}$ is still fairly isotropic, so that only the $\ell=0$ and $\ell=1$ parameters have appreciable size. Note that for a dense Fermi liquid, we cannot calculate the FLT parameters. In fact we measure them. In order to do this we need to calculate experimental properties in terms of the $\{F_\ell^{\lambda}\}$. Then the measurements allow us to fix the $\{F_\ell^{\lambda}\}$. Thus

P (bar)	V (cm³)	m^*/m	F_1^s	F_0^s	F_0^a
0	36.84	2.80	5.39	9.30	−0.695
3	33.95	3.16	6.49	15.99	−0.723
6	32.03	3.48	7.45	22.49	−0.733
9	30.71	3.77	8.31	29.00	−0.742
12	29.71	4.03	9.09	35.42	−0.747
15	28.89	4.28	9.85	41.73	−0.753
18	28.18	4.53	10.60	48.46	−0.757
21	27.55	4.78	11.34	55.20	−0.755
24	27.01	5.02	12.07	62.16	−0.756
27	26.56	5.26	12.79	69.43	−0.755
30	26.17	5.50	13.50	77.02	−0.754
33	25.75	5.74	14.21	84.79	−0.755
34.39	25.50	5.85	14.56	88.47	−0.753

for example, the effective mass of a quasiparticle m^* enters into transport properties and directly into the specific heat; but FLT yields

$$\frac{m^*}{m} = 1 + \tfrac{1}{3} F_1^s$$

(147)

where m is the "bare" mass of the free particles.

<u>Landau scattering parameters A_ℓ^{λ}</u> : These dimensionless numbers tell us the real scattering rates of quasiparticles - any real transition process, involving quasiparticle collisions, will involve them. In particular, the collision integral can be written in terms of the $\{A_\ell^{\lambda}\}$, and transport quantities like viscosity, decay of spin dynamics, etc.

Note that we can set up a Landau FLT even when the $\{F_\ell^{\lambda}\}$ and/or the $\{A_\ell^{\lambda}\}$ are not small. If $\delta n \ll 1$, then the effect of collisions is small because there are very few quasiparticles; and we can calculate both the change in system energy and all scattering processes by doing an expansion up to 2nd-order only in the quasiparticle density. This was precisely our starting point in (109).

FERMI LIQUID THEORY for METALS: QUASICLASSICAL APPROX.

* The metal is no longer isotropic or translationally invariant - and we also have spin-orbit coupling. Thus the quantum numbers are no longer just p, σ; states are now to be labelled by appropriate band indices, and the interaction function $F_{nn'}(p,p'; \sigma,\sigma')$ must transform under rotations in orbital and spin space according to the correct crystal field / spin orbit group (the "double-point group).

* There are now interactions between electrons and phonons, and these mean that not only is the Fermi liquid coupled to another "bath", but also we must incorporate phonon-mediated interactions into the FLT parameters.

In spite of all these complications, FLT has proved useful for the understanding of conducting metals (although not in such a decisive way as it did for the understanding of ^{3}He). In its most useful form for metals, FLT takes on a "quasiclassical" form, which has been used for many decades now to analyse the experimental properties of metals.

The quasiclassical theory is very similar to FLT, except that it now starts in

a band representation, and it incorporates explicitly the longer-range part of the electron-electron interactions, as well as the coupling to phonons. We therefore now have a free-energy functional

$$E = E_0 + \sum_{\substack{p\delta \\ \mu}} \epsilon_\mu^\delta(\underline{p}) \, \delta n_\mu^\delta(\underline{p}) + \frac{1}{2} \sum_{\mu\nu} \sum_{\substack{pp' \\ \delta\delta'}} f_{\mu\nu}^{\delta\delta'}(pp') \, \delta n_{\mu\delta}(\underline{p}) \, \delta n_{\nu\delta'}(\underline{p}')$$

$$+ \mathcal{H}_{el-ph} + \mathcal{H}_{ph}. \tag{148}$$

where the μ,ν label band indices, and $f_{pp'}$ now includes the long-range Coulomb interaction in (120).

By specifying the form of the electron-phonon interaction, and taking into account screening, one can derive a modified L-B equation for metals. The relevant energy scales that emerge from this are as follows:

$$
\left.
\begin{array}{lll}
\text{Fermi energy} \quad \epsilon_F & \sim & 2-5 \text{ eV} \\[6pt]
\text{Plasmon energy} \quad \omega_p & \sim & 3-8 \text{ eV} \\[6pt]
\text{Fluctuation energies} \quad \Omega_f^{(j)}(q) & \sim & \epsilon_F/A^{(j)} \\[6pt]
\text{Phonon energy} \quad \theta_D & \sim & 100-500\text{ K}.
\end{array}
\right\} \text{ simple metals} \tag{149}
$$

These energies are given for simple metals like the alkali metals and the Noble metals. I have ignored other relevant energies like the crystal field and spin-orbit energies. In a metal the effect of the crystal fields is of course simply to modify the band structure, as we saw above. The spin-orbit couplings, when properly incorporated, modify the band structure as well, making the character of the spinor wave-functions more complicated. The effect of spin-orbit coupling can be very interesting (in, e.g., the discussion of the spin Hall effect) but we shall ignore it for the present. In a non-magnetic conductor, the effect of dipolar interactions and spin anisotropy is very small (we discuss itinerant ferromagnets below).

A brief word on the new energy scales here. The plasmon is a collective mode which arises because of the long-range part of the electron-electron interaction. Both it and the other collective excitations, having energies $\Omega_f^{(j)}$, are the result of interactions. Their energies are just given by eigenvalues of the L-B equation (142) (or the more complicated metallic version), and there is one such mode corresponding to each interaction channel. Thus for an isotropic system like ^{3}He liquid, we have the following collective modes from the isotropic parts of $f_{pp'}^{\delta\delta'}$:

$$
\left.
\begin{array}{lll}
A_0^s: & \text{zero-th sound} & \Omega_0^s \sim \epsilon_F/A_0^s \equiv \epsilon_F \Big/ \dfrac{F_0^s}{1+F_0^s} \\[14pt]
A_0^A: & \text{spin fluctuations/spin waves} & \Omega_0^A \sim \epsilon_F \Big/ \dfrac{F_0^A}{1+F_0^A}
\end{array}
\right\} \; {}^3\text{He} \tag{150}
$$

plus a succession of higher modes. In a metal the zero-th sound is converted into a plasmon, but one can also get spin fluctuations or spin waves in a metal. Note

that in a metal we must label the fluctuations by an index j, which represents the irreducible representations of the relevant double point group of the system.

To give you some feeling for these energy scales, I give some of the results that have been found for the alkali metals (note that in the metallic literature the symbols used are a little different: ones use A_ℓ instead of F_ℓ^S, and B_ℓ instead of F_ℓ^A).

From these results one sees immediately that the Landau parameters in are really quite small. Thus interaction effects can, to a crude approximation, be ignored in them.

Note however that there is one parameter that is predicted quite badly by a free electron theory. This is the effective mass m^* of the electrons at the Fermi surface, which is significantly enhanced over in the alkalis. The reason for this is the electron-phonon interaction. This enhancement extends over an energy scale $\sim \Theta_D$ away from the Fermi surface — at higher energies it largely disappears.

A large number of the experimental properties of metals can be understood using this kind of theory; this includes both static and dynamic

THE EXPERIMENTAL VALUES AND THEORETICAL ESTIMATES FOR THE LANDAU PARAMETERS IN Na

	Experiment (Na)	Theory[a]
A_0		−0.64
A_1		+0.11
A_2	−0.05 ± 0.01	−0.04
A_3	0.0 + 0.005	+0.005
B_0	−0.21 ± 0.05	−0.17
B_1	−0.005 ± 0.04	−0.005
B_2	0.0 ± 0.03	−0.02
B_3		+0.001
m^*/m_0	1.24 + 0.02	1.21

[a] Electron–electron using Hubbard approximation, electron–phonon in one plane-wave and Ashcroft pseudopotential.

THE EXPERIMENTAL VALUES AND THEORETICAL ESTIMATES FOR THE LANDAU PARAMETERS IN K

	Experiment	Theory I[a]	Theory II[b]
A_0			−0.58
A_1			+0.04
A_2	−0.03 ± 0.005	−0.21	−0.02
B_0	−0.285 ± 0.02	−0.21	−0.24
B_1	−.06 ± 0.03		−0.04
B_2	0.0 ± 0.05		+0.003
m^*/m_0	1.2 ± 0.001	1.23	1.11

[a] Theory I: Electron–electron calculated using Hubbard and electron–phonon using Lee–Falicov potential.
[b] Theory II: Electron–electron from Hedin and same electron–phonon.

ALKALI METAL PARAMETERS

METAL	a_0 (Å)	$N \times 10^{-22}$ (cm^{-3})	m_c/m_0	m/m_0 (SPECIFIC HEAT)	ω_p(CALC) eV	v_F (cm/s)	k_F cm^{-1}	r_s	g VALUE	E_F FREE ELECTRON	$\rho \times 10^{-6} \Omega$ cm (20° C)
Li	3.491 (4.2°K)	4.69		2.17	7.8	1.31×10^8	1.1×10^8	3.22	2.0023	4.72	8.55
Na	4.225 (4.2°K)	2.65	1.24	1.23	5.9	0.86×10^8	0.93×10^8	3.96	2.0015	3.12	4.3
K	5.225 (4.2°K)	1.40	1.21	1.23	4.25	0.71×10^8	0.746×10^8	4.87	1.9997	2.14	6.1
Rb	5.585 (4.2°K)	1.15	1.20	1.31	3.76			5.18	1.9984	1.82	11.6
Cs	6.045 (4.2°K)	0.905	1.44	1.58	3.46	$\approx .521 \times 10^8$	0.65×10^8	5.57	2.005	1.53	19.0

IN THE ABOVE TABLE, m_c IS THE "CYCLOTRON MASS", AND m^* THE LOW-ENERGY RENORMALISED MASS CONTAINING MANY-BODY EFFECTS.

phenomena, as well as transport. When the interactions are weak one can even ignore them to first approximation. Whether or not one does this, the L-B equation

58

provides us with a very simple intuitive "quasiclassical picture" for the dynamics of the quasiparticles. In this picture one imagines the quasiparticles following <u>trajectories</u> governed by the quasiclassical equations of motion:

$$\dot{r}_\mu^\sigma(p,\sigma;t) = v_\mu^\sigma(p;t) = \frac{\partial \epsilon_\mu^\sigma(p,r)}{\partial p}$$

$$\dot{p}_\mu^\sigma(\sigma;t) = f_\mu^\sigma(p,t) = -\nabla_r \epsilon_\mu^\sigma(p,r) \qquad\qquad \Bigg\} \qquad (151)$$

where in general the quasiparticle energy takes the form

$$\epsilon_\mu^\sigma(p,r) = \epsilon_\mu^{(0)}(p) + \frac{1}{2}\sum_{\nu\sigma'\ p'} f_{\mu\nu}^{\sigma\sigma'}(p,p')\,\delta n^{\sigma'}(p') + U(r) \qquad (152)$$

where we add in (151) any applied potential field $U(r)$ that might be applied to the system (representing, e.g., an applied electric field $eE = -\nabla U(r)$).

In many applications the trajectories emerging from (151) are taken very seriously; in fact one also writes

$$\ddot{r}_\mu = \frac{d}{dt}\frac{\partial \epsilon_\mu}{\partial p} \equiv \frac{\partial^2 \epsilon_\mu}{\partial p_\alpha \partial p_\beta}\frac{dp_\alpha}{dt} \qquad (153)$$

which allows to define an effective mass

$$m_{\alpha\beta}^*(\mu;p,\sigma) = \left(\frac{\partial^2 \epsilon_{\mu\sigma}(p)}{\partial p_\alpha \partial p_\beta}\right)^{-1} \qquad (154)$$

Then eqtn. (153) is nothing but "Newton's 2nd law" for the quasiparticle trajectories. The literature on this topic is huge, but not terribly relevant to our topic - see the references.

B.2.2. METALS IN MAGNETIC FIELDS

The effect of a magnetic field on a conductor is profound, as first realised by Landau (for 3 dimensional systems). In 2 dimensions it is even more extraordinary, since it leads to the Quantum Hall liquids.

In this section I give a brief discussion of magnetic fields and their effect on 3-dimensional metals, where they can be discussed using a modified quasiclassical theory. The emphasis will be on the new energy scales, with a brief word on the quasiclassical dynamics. The topic of Quantum Hall liquids is covered later, when we come to discuss Topological Quantum fluids and Topological spin states.

(i) <u>QUASICLASSICAL THEORY IN A MAGNETIC FIELD.</u> : The way to modify Landau FLT in the quasiclassical form, with or without the effect of interactions, was first discussed by Peierls in the 1950's, and the manoeuvre he devised has since become known as the "Peierls substitution". The way this works is as follows

<u>Peierls substitution in tight-binding limit</u> : Suppose we are able to approximate our system by a single band, so that the effective Hamiltonian in zero field is just the Hopping Hamiltonian in (3). Now if we are allowed to assume nearest neighbour coupling only, the Peierls substitution goes like

$$\mathcal{H}_0(\underline{A}) = -t \sum_{<ij>} \left(e^{i\phi_{ij}} c_i^\dagger c_j + H.c \right)$$

$$\phi_{ij} = \frac{e}{\hbar} \int_{R_i}^{R_j} d\underline{\ell} \cdot A(\underline{\ell})$$

$$\quad (155)$$

where the integration is done along the path between the 2 lattice sites – this means that there is some constant flux threading each plaquette, given by

$$\Phi = \phi \Phi_0 \qquad\qquad \phi = \frac{e}{\hbar} a_0^2 B_0$$

$$\Phi_0 = \frac{h}{e}$$

$$\quad (156)$$

in the case of square lattice, where we assume a lattice constant a_0; here Φ_0 is the flux quantum and ϕ is the dimensionless flux per plaquette.

Clearly this can be transformed to a band Hamiltonian, and this is done as follows. Suppose, in line with our discussion at the beginning of B.2.1, that we have a band energy $\epsilon_{n\underline{k}}^\circ$, for the n-th band, which is the solution of the Schrödinger eqtn for the Hamiltonian (103) for the n-th band :

$$\mathcal{H}_0^{(n)} |n\underline{k}\rangle = \epsilon_{n\underline{k}}^\circ |n\underline{k}\rangle$$

$$\epsilon_{n\underline{k}}^\circ = -\sum_{<ij>} t_{ij}^{(n)} e^{i k \cdot (R_i - R_j)}$$

$$\quad (157)$$

Then the Peierls substitution says that we have to resolve Schrödinger's equation for this band, but with

$$\epsilon_{n\underline{k}}^\circ \to \epsilon_{n\underline{k}}^\circ (A_0) = -\sum_{<ij>} t_{ij}^{(n)} e^{i(\underline{k} + e\underline{A}_0/\hbar) \cdot (\underline{R}_i - \underline{R}_j)} \qquad (158)$$

<u>Peierls substitution in weak-binding</u> : Suppose instead we have some free-electron band which is shaped by coupling to some periodic lattice potential, so that the Schrödinger eqtn is :

$$\mathcal{H}_0(-i\nabla) \psi_{n\underline{k}}(\underline{r}) = \epsilon_{n\underline{k}}^\circ$$

$$\mathcal{H}_0(i\nabla) = -\frac{\hbar^2 \nabla^2}{2m} + V(\underline{r})$$

$$\quad (159)$$

Now in a finite field, we need to solve

$$\mathcal{H}_0(-i\nabla + e\underline{A}(\underline{r})) \psi_{n\underline{k}}(\underline{r}) = \epsilon_{n\underline{k}}(\underline{A}) \psi_{n\underline{k}}(\underline{r})$$

$$\mathcal{H}_0(-i\nabla + e\underline{A}) = \frac{1}{2m}(-i\hbar\nabla_r + eA(\underline{r}))^2 + V(\underline{r})$$

$$\quad (160)$$

The problem is that a solution of (160) may be very difficult, so instead we use the substitution

$$\mathcal{H}_0(-e\nabla + eA(r)) \longrightarrow \tilde{\mathcal{H}}_{nk}(A) \equiv \epsilon_n^0(\hat{k} + e\hat{A}(r)) \tag{161}$$

in other words, instead of solving (160) directly, we take the argumed band dispersion ϵ_{nk}^0 (an ordinary function), and turn it into an OPERATOR with the substitution $k \to k + eA$.

If we are only dealing with a single band then the tight-binding & weak-binding approaches are the same. An example will help us see how this works. Suppose we have a 2-d tight-binding spectrum

$$\epsilon_k^0 = -t(\cos k_x a_0 + \cos k_y a_0) \tag{162}$$

which applies to the 2-d square lattice with Hamiltonian (3). We choose the Landau gauge

$$A(r) = (-B_0 y, 0) \qquad [\text{LANDAU}] \tag{163}$$

so that the Peierls substitution then gives a new Hamiltonian

$$\tilde{\mathcal{H}}_{nk}(A) = -t\left\{ \cos\left[(\hat{k}_x a_0 + e\hat{A}_x) + \cos(\hat{k}_y a_0 + e\hat{A}_y)\right] \right\}$$

$$\equiv -t\left\{ \cos\left[-i a_0 \hbar \partial_x - eB_0 y\right] + \cos\left[-i a_0 \hbar \partial_y\right] \right\} \tag{164}$$

where we substitute (163), and use the operator substitution $k_\alpha \to -i\hbar\nabla_\alpha$. The problem then reduces to solving the Schrödinger eqtn:

$$\tilde{\mathcal{H}}_{nk}(A)\phi_{nk}(r) = \tilde{\epsilon}_{nk}\phi_{nk}(r) \tag{165}$$

This equation, with $\tilde{\mathcal{H}}_{nk}(A)$ given by (164), is known as Harper's eqtn. We will be looking at it again in much more detail, and also at deviations from the Peierls substitution.

Now, suppose we can make a semiclassical approximation to all of this — what does this mean? In the absence of Fermi liquid interactions, it means we replace (151) and (152) by
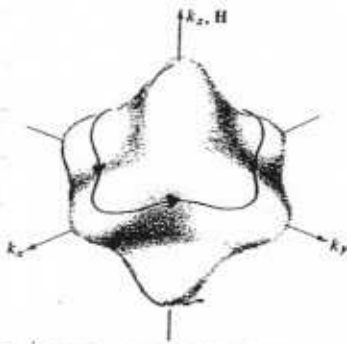
$$\dot{r}_n(p,\sigma) \equiv v_n(p\sigma) = \frac{\partial\epsilon_{np\sigma}^{(0)}}{\partial p} \left.\begin{array}{l} \\ \\ \end{array}\right\} \begin{array}{l}\text{No}\\ \text{interactions}\end{array} \tag{166}$$

$$\dot{p}_n^\sigma(r) = f_n^\sigma(r) = e(v_n^\sigma(p) \times B_0)$$

One could also add the effects of interactions but will not do so here, since the are already interesting enough without them. Note first that from the 2nd eqtn in (166) we have

$$\dot{p}\cdot v_p = p\cdot B_0 = 0. \implies \dot{p}\cdot\frac{\partial\epsilon_p}{\partial p} = 0 \tag{167}$$

from which we deduce $\begin{array}{l} p\cdot B_0 = \text{const} \\ \epsilon_p = \text{const} \end{array} \Big\} \tag{168}$

In the figure we see what these constraints lead to for a set of electrons in a crystalline solid. Any surface of constant energy (including the Fermi surface) will be distorted by the coupling to the crystal lattice, and so it will follow the path shown in k-space. By integrating up (166) this will also correspond to a "quasiclassical trajectory" in real space. From the 2nd eqn in (166) we notice that

$$\dot{\underline{P}}_n \times \frac{\underline{B_0}}{|\underline{B_0}|} = e(\dot{\underline{r}}_n \times \underline{B_0}) \times \frac{\underline{B_0}}{|\underline{B_0}|} = eB_0\dot{\underline{r}}_n$$

from which we have, for $\underline{k}_n = \underline{P}_n/\hbar$, that

$$\dot{\underline{k}}_n \times \hat{z} = \frac{eB_0}{\hbar}\dot{\underline{r}}_n \qquad (169)$$

where we assume here that $\underline{B_0} = \hat{z}B_0$. Eqn (169) shows that the real space orbit has the same shape as the k-space orbit, but multiplied by a scale factor $(eB_0/\hbar)^{-1}$.

Intersection of a surface of constant energy with a plane perpendicular to the magnetic field. The arrow indicates the direction of motion along the orbit if the levels enclosed by the surface have lower energy than those outside.

(ii) <u>LANDAU LEVEL QUANTIZATION IN A FIELD</u> : Let us first consider the well-known problem of a Fermi gas in a magnetic field. We ignore the spin for the moment; the Hamiltonian is

$$\mathcal{H}_0 = \frac{1}{2m}(\hat{\underline{p}} + e\hat{\underline{A}}(\underline{r}))^2$$
$$\underline{\nabla} \times \underline{A}(\underline{r}) = \underline{B_0} \qquad \qquad \Big\} \qquad (170)$$

The eigenvalues are of course independent of the gauge choice for $\underline{A}(\underline{r})$, but not the eigenfunctions. We choose the Landau gauge :

$$\underline{A}(\underline{r}) = (-yB_0, 0, 0) \qquad (171)$$

with $\underline{B_0} = \hat{z}B_0$, so that

$$\mathcal{H}_0 = \frac{1}{2m}(\hat{p}_x - eB_0\hat{y})^2 + \frac{1}{2m}(\hat{p}_y^2 + \hat{p}_z^2) \qquad (172)$$

Since $\mathcal{H}_0$ commutes here with both $\hat{p}_x$ and $\hat{p}_z$, the eigenfunctions can be written in the form

$$\psi(\underline{r}) = e^{i(k_x x + k_z z)}\phi(y) \qquad (173)$$

so that

$$\phi''(y) - \frac{2m}{\hbar^2}\left[\frac{p_z^2}{2m} + \frac{1}{2}m\omega_c^2(y-y_0)^2 - E\right]\phi(y) = 0 \qquad (174)$$

where

$$\omega_c = |eB_0|/m \qquad (175)$$

and the coordinate y_0 is related to p_x :

$$y_0 = -p_x/eB_0 \qquad (176)$$

We see from the form of (174) that we are dealing with a simple harmonic

62

oscillator problem, with eigenvalues

$$E_n(p_z) = \epsilon_n + \frac{p_z^2}{2m}$$

$$\epsilon_n = \hbar\omega_c(n+\tfrac{1}{2})$$

(177)

and eigenfunctions

$$\psi_{np_z}(\underline{r}) = e^{i(k_x x + k_z z)}\left[e^{-\frac{1}{2}m\omega_c(y-y_0)^2}\chi_n\left(m\omega_c\sqrt{y-y_0}\right)\right]$$

(178)

$$\chi_n(x) = (-1)^n e^{x^2}\frac{d^n}{dx^n}e^{-x^2}$$

where the $\chi_n(x)$ are Hermite polynomials. The eigenvalues in another gauge, defined by the transformation

$$\underline{A}(\underline{r}) \to \underline{A}'(\underline{r}) = \underline{A}(r) + \nabla f(\underline{r})$$

(179)

are given by

$$\psi(\underline{r}) \to \psi'(r) = \psi(\underline{r})\,e^{-\frac{i}{\hbar}ef(\underline{r})}$$

Consider first what all of this looks like for a set of N electrons in 2 dimensions, in the xy-plane perpendicular to B_0. We then drop the $p_z^2/2m$ term from (177), and end up with a "Landau quantization of fermionic states onto a set of "Landau levels" with energies $\epsilon_n = \hbar\omega_c(n+\tfrac{1}{2})$. The resulting density of states can be determined in various ways. The simplest is to note that in a 2-d Fermi system, the density of states for a system of surface area A is

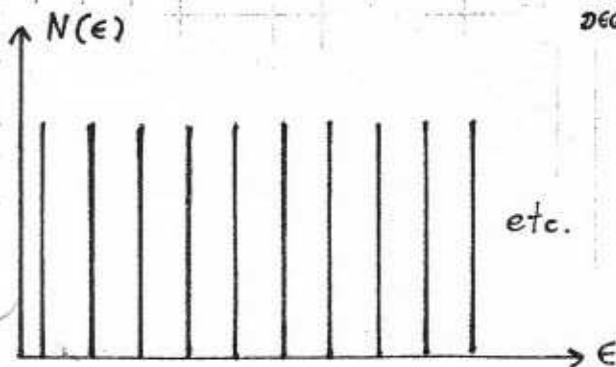$$N(\epsilon) = A\int\frac{d^2k}{(2\pi)^2} = A\frac{m}{2\pi\hbar^2} \qquad [2D] \qquad (180)$$

so that if the Landau condensation shown at left occurs,

$$N(\epsilon) \to AB_0\frac{e}{h}\sum_{n=0}\delta(\epsilon-\epsilon_n) \qquad [2D] \qquad (181)$$
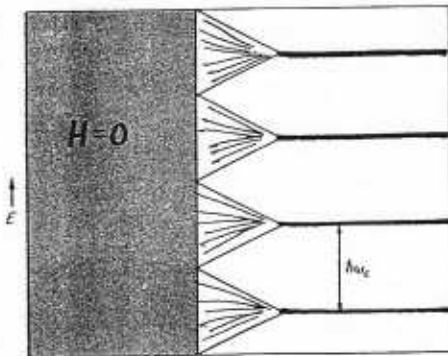
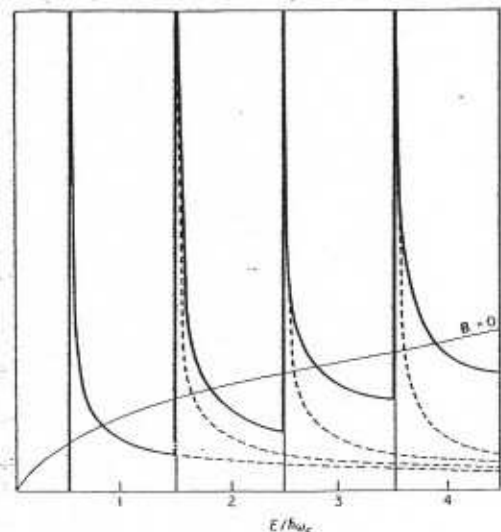ABOVE: THE "LANDAU CONDENSATION" OF THE FREE ELECTRONS, IN 2-D, ONTO THE LANDAU LEVELS.
BELOW: THE CORRESPONDING DENSITY OF STATES, A SET OF δ-FUNCTIONS.

RIGHT: THE DENSITY OF STATES FOR 3-D FREE ELECTRONS, BOTH IN ZERO FIELD (B=0), AND AT FINITE FIELD - THE δ-FNS ARE SPREAD BY THE p_z DEGREE OF FREEDOM

etc.

We can also write this as

$$N(\epsilon) \to \Phi^{tot}/\Phi_0\sum_n\delta(\epsilon-\epsilon_n) \qquad [2D] \qquad (182)$$

where $\Phi^{Tot} = AB_0$ is the total flux through the system, and $\Phi_0 = h/e$ is the flux quantum. Thus we have a flux quantum associated with each Landau state in a given level. There is a corresponding length scale associated with the Landau states, which is

$$l_0 = \sqrt{\hbar/eB_0} \qquad \text{(Landau length)} \qquad (183)$$

so that $2\pi l_0^2 = \Phi_0$ (note that this length is seen directly in the wave-function in eqtn (178)).

The density of states in 3-d is the obvious generalisation of (181) or (182), given by

$$N(\epsilon) \xrightarrow[\text{3D GAS}]{} \frac{L_z}{\pi} \frac{\Phi^{tot}}{\Phi_0} \left(\frac{2m}{\hbar^2}\right)^{\frac{1}{2}} \sum_n \frac{\theta(\epsilon - \epsilon_n)}{(\epsilon - \epsilon_n)^{1/2}} \qquad (184)$$

once the sums have been done, assuming a length L_z of the sample along $\hat{z}$. This structure is shown on the last page.

Suppose we now have a finite number N electrons per unit area (unit volume) in the system. Then the states fill up to a Fermi energy determined by N, and clearly $\mu(B_0)$ must oscillate, as will the free energy $F(B_0)$. Alternatively one can fix $\mu = \text{const}$ by connecting the system to an external reservoir, so that $N(B_0)$ oscillates.
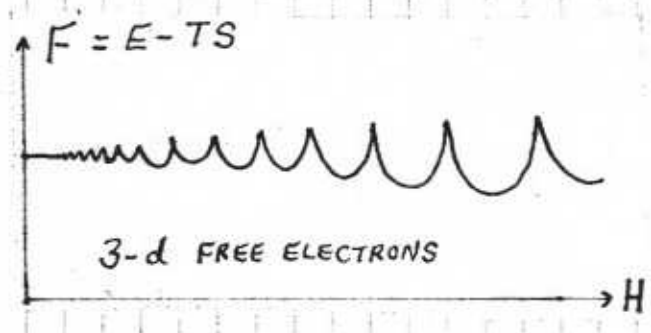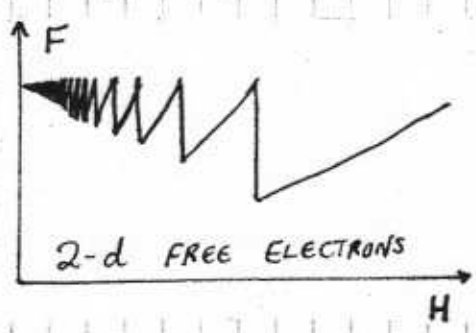
LEFT: FREE ENERGY OF FREE ELECTRONS IN 2d and 3-d FERMI GASES AS A FUNCTION OF APPLIED FIELD (WITH μ HELD CONSTANT).

What now of band electrons? Even without electron-electron interactions, the problem of a set of electrons in a periodic potential and an applied field is very difficult. If we can make the Peierls substitution, we get the Hamiltonian given in (160), and we will look at the solution of this in a moment. Let us first however ask what we can get by making a quasiclassical / Fermi liquid approximation, in which Landau quantization has been incorporated. This gives us the following ansatz:

Ansatz: Suppose the area in k-space of the n-th Landau level is given by A_n, and that in the absence of the field one has a quasiclassical spectrum $\epsilon^0(\underline{k})$. Then we assume that

$$A_n = \int dk_x \, dk_y \, \theta(\epsilon_n(\underline{k}) - \epsilon^0(\underline{k}))$$

$$= 2\pi(n+\gamma) \frac{eB_0}{\hbar} \equiv \frac{2\pi m}{\hbar} \omega_c(n+\gamma) \qquad \Big\} \quad (185)$$

where $0 < \gamma < 1$ (and $\gamma = \frac{1}{2}$ for a free gas).

This ansatz defines implicitly a set of energy surfaces $\epsilon_n(\underline{k})$ in k-space. The value of γ is complicated to determine. Notice that this ansatz is exactly what we might expect using a Bohr-Sommerfeld "correspondence principle" argument, in which allowed quantum states are specified by a quantization of the action of the system, for

64

periodic orbits of the classical system. Recall that for a particle in ordinary mechanics, one has the Bohr-Sommerfeld condition

$$S = \int_{t_1}^{t_2} dt\, L(x,\dot{x};t) \equiv \int_{x_1}^{x_2} \frac{dx}{2\pi} p(x) \xrightarrow[\text{periodic orbits}]{} \oint \frac{dx}{2\pi} p_x = S_n \\ = \hbar(n+\gamma) \qquad (186)$$

and in the case of quasiclassical orbits around the Fermi surface it is easy to verify that we have

$$S_n = \oint d\underline{r}\cdot(\underline{p}+e\underline{A}(\underline{r})) \equiv \oint dy\,(p_x + eA_x(y)) \qquad (187)$$

and that this leads to the same result as (185).

Actually this semiclassical result works extraordinarily well in real systems, and has given us some extraordinarily powerful experimental and diagnostic tools in experimental physics (notably the de Haas-van Alphen and Shubnikov-de Haas effects). To see how all of this works, consider first the 2-d case, shown below:
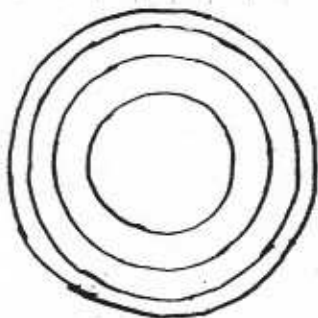

ORBITS IN k-SPACE OF AREA A_n, FOR A GIVEN FIELD. ABOVE IS SHOWN THE CASE OF FREE ELECTRONS; AND AT RIGHT FOR THE SPECTRUM IN EQTN (162).
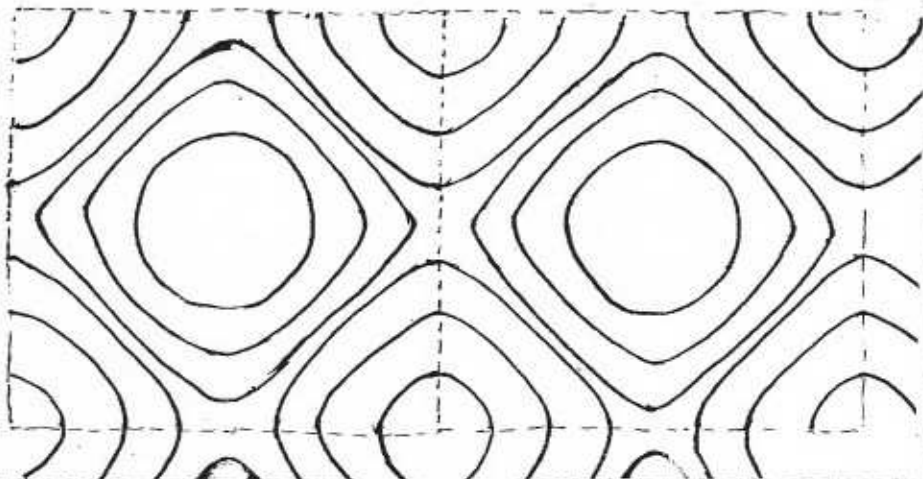
The figure, by showing surfaces of constant energy, is also showing the Fermi surfaces for different filling factors, ie., for different electron densities. However at low T the only electrons that are free to move are those at or very near to the Fermi surface $S_F(\underline{k})$ (within kT in energy of E_F). These electrons then move in k-space, in accordance with (166) or (169)., ie., they move around closed paths in k-space.
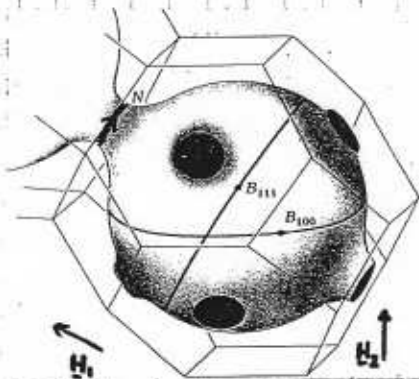
In 3-d things are a little more subtle. An intuitive discussion proceeds by first noting that the singular behaviour of the free energy F (sharp jumps in 2-d, cusps in 3-d) occurs each time a Landau level passes through the Fermi energy. It must then "dump" all its fermions down to the levels below, which lowers the total energy. This happens instantly in 2-d (at T=0), but in 3-d many Landau levels pass through the Fermi surface at any field. However one set of electrons plays a crucial role - these are the electrons on "extremal orbits", as shown on the next page. Intuitively one can see that as an extremal orbit passes through S_F, a large number of electrons are dumped to the levels below. A more correct argument notes that the contribution of individual electrons to the action and related quantities is going like a phase integral around these orbits, and that when sum over orbits we get a form

$$F_{tot} \sim \sum_{orbits} e^{i\phi_{orbit}}$$

EXTREMAL ORBIT

$\underline{H}$
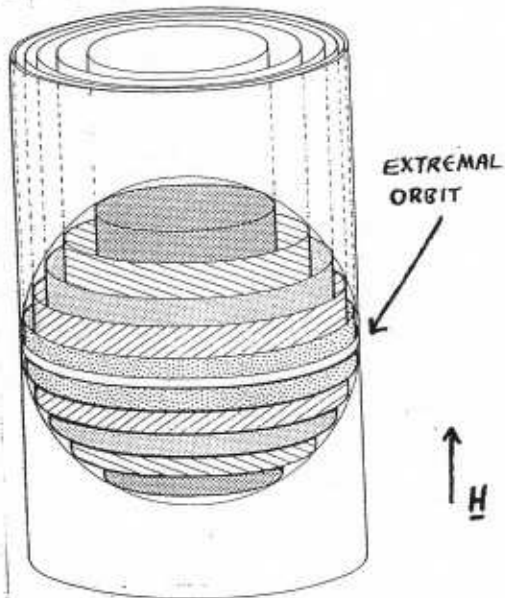
GENERALISATION TO 3 DIMENSIONS FOR FREE ELECTRONS. THE ALLOWED ORBITS NOW GENERALIZE TO CYLINDERS. THESE ARE OCCUPIED UP TO THE FERMI SPHERE.
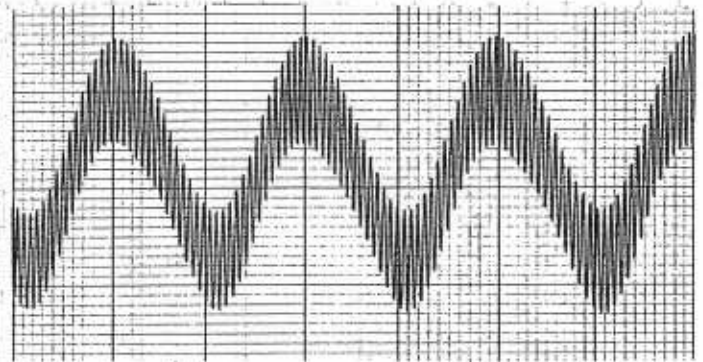
and that if we treat this sum over orbits as an integral (which it is in 3-d), we get a standard form (the variable x parametrises orbits):

$$\int dx \, e^{i\phi(x)} \sim \sum_{\alpha}^{orbits} C_{\alpha} e^{i\phi_{\alpha}} \qquad (\alpha = extremal \; orbit)$$

where extremal values of ϕ are picked out by the steepest descent evaluation.

The oscillations in $F(B_0)$ are reflected in all response functions; for example, the magnetisation

$$M(B_0) = -\partial F/\partial B_0$$

shows very pronounced oscillations, as we see in the figures here for dHVA oscillations in Au metal.


31.7 kG   31.8 kG

ABOVE: dHVA OSCILLATIONS IN THE MAGNETISATION OF A GOLD CRYSTAL, FOR H IN THE [111] DIRECTION. THE RAPID OSCILLATIONS COME FROM THE BELLY ORBIT B_{111}, THE SLOW ONES FROM THE NECK ORBIT N (SEE FIGURE BELOW LEFT).

H_1 H_2

AT LEFT: THE FERMI SURFACE OF Au IS SHOWN ALONG WITH EXTREMAL ORBITS IN 2 DIFFERENT FIELD ORIENTATIONS. FOR FIELD $\underline{H} = \underline{H}_1$, ALONG THE [111] DIRECTION, WE HAVE THE BELLY ORBIT B_{111} AND THE NECK ORBIT N. FOR $\underline{H} = \underline{H}_2$ ALONG [100], WE HAVE THE BELLY ORBIT B_{100}.

From eqn (185) we see that the cusps occur at fields B_n, where

$$B_n = \frac{2\pi e}{\hbar A_F} (n+\gamma)$$
$$= \frac{(2\pi)^2}{\Phi_0 A_F} (n+\gamma) \qquad \left.\right\} (188)$$

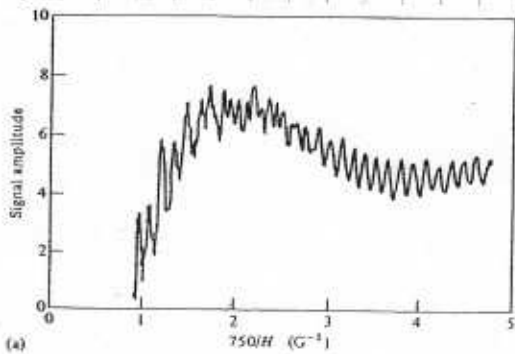where A_F is the Fermi surface area.
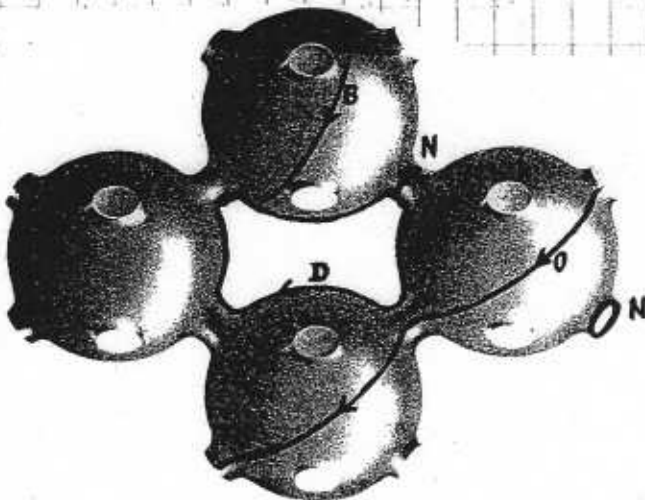
SOME EXTREMAL ORBITS IN Cu, FOR DIFFERENT FIELD ORIENTATIONS PERPENDICULAR TO THE ORBITS.

O: OPEN ORBIT
D: DOG'S BONE
N: NECK
B: BELLY.

NOTICE THAT THE OPEN ORBIT NEVER CLOSES, AND THAT THE DOG'S BONE IS TRAVERSED IN THE OPPOSITE SENSE (WITH RESPECT TO $\underline{H}$) TO THE OTHER ORBITS. ALL OF THESE ORBITS ARE FOR $\underline{H}$ ALONG A SYMMETRY AXIS, EXCEPT B.

(a)

$T = 0.4 K$

(b)

(c)
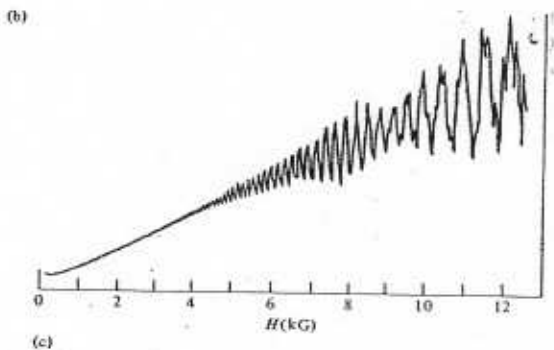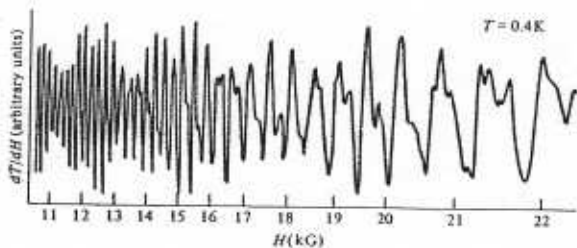
The ubiquity of the oscillations, of which the de Haas–van Alphen effect is the most celebrated example. (a) Sound attenuation in tungsten. (C. K. Jones and J. A. Rayne.) (b) dT/dH vs. field in antimony. (B. D. McCombe and G. Seidel.) (c) Magnetoresistance of gallium vs. field at 1.3 K.

This result shows that the oscillations are periodic in INVERSE FIELD, with period

$$\Delta(1/B_0) = \frac{(2\pi)^2}{\Phi_0 A_F} \qquad (189)$$

so that large extremal orbits have short periods, and small extremal orbits have large period. The example of Au metal on the last page shows this very clearly. In even simple metals like Cu or Au, one can have complicated behaviour as a function of the field orientation, and this allows experimentalists to map out the Fermi surface of metals with quite exquisite accuracy. Usually the magnetisation is looked at in experiments, because it can be measured with great sensitivity using SQUID magnetometers. However any equilibrium response will oscillate - another quite popular technique is to look at oscillations in the torque on a sample in a tilted field.

The transport properties of the sample will also oscillate. This is because the Landau condensation completely changes the density of states, giving it very marked structure (see page 63, and since the collisional scattering rate in any transport process is proportional to the quasiparticle density of states near the Fermi surface, we will see strong oscillations in conductivity (the Shubnikov-de Haas, or SdH oscillations), and other quantities like sound attenuation, etc. Three examples are shown at left.

It is actually quite easy to appreciate the general expressions used to analyse such experiments. Thus the general result for a 3-d conductor takes the form
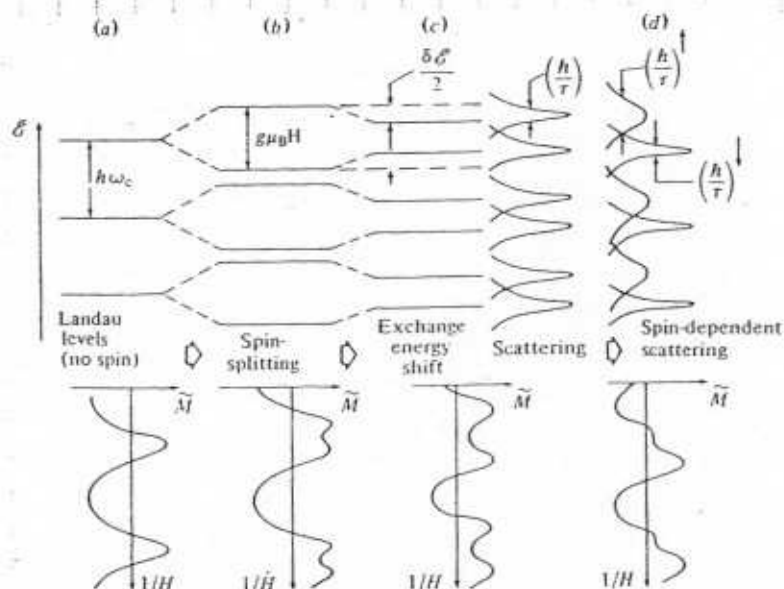
$$F(B_0, T) = F_0(B_0, T) + F_{osc}(B_0, T) \qquad (190)$$

where $F_0(B_0, T)$ has no oscillations in $1/B_0$, and

$$F_{osc}(B_0, T) = \sum_\alpha \sum_{r=1}^\infty (-1)^r C_{r\alpha} T_{r\alpha} D_{r\alpha} S_{r\alpha} \cos\left\{2\pi r\left[\left(\frac{\hbar A_F}{2\pi e B_0}\right) - \gamma\right] \pm \frac{\pi}{4}\right\} \qquad (191)$$

where we sum over Fourier components r of the periodic function, for different extremal orbits α. The constants $C_{r\alpha} \sim 1/(r A_{F\alpha}'')^{1/2}$, where $A_{F\alpha}''$ is the second derivative of the extremal orbit area $A_{F\alpha}$ around the extremum, and we have:

$$\text{Temperature factor}: \quad T_{r\alpha} = \frac{\lambda_{r\alpha}}{\sinh \lambda_{r\alpha}} \qquad \qquad (192)$$

$$\text{with} \quad \lambda_{r\alpha} = \pi^2 r \frac{m_\alpha}{m}\left(kT/\hbar\omega_c\right)$$

Modification of (a) electronic orbital Landau levels due to (b) spin-splitting (Zeeman effect), (c) exchange interaction with a local magnetic moment (antiferromagnetic case shown) and (d) unequal (↑, ↓)-spin level broadening ($\Gamma^{\uparrow} > \Gamma^{\downarrow}$ shown). The corresponding qualitative changes in the waveshape of the oscillatory magnetization are shown below.

Dingle factor (from scattering):

$$D_{r\alpha} = \exp\left[-\pi^2 r \frac{m_\alpha}{m}\left(\tau_\alpha^{-1}/\omega_c\right)\right] \quad (193)$$

where τ_α^{-1} is the scattering rate of quasiparticles on the α-th external orbit;

Spin factor:

$$S_{r\alpha} = \cos\left(\pi r \frac{g_\alpha}{2}\frac{m_\alpha}{m}\right) \quad (194)$$

coming from the contributions of the 2 separate spin-↑ and spin-↓ Fermi surfaces (split by the Zeeman coupling).

How these terms affect the oscillations is shown schematically in the Figure at left. We see that to see significant oscillations,

We require

$$\frac{m}{m_\alpha}\hbar\omega_c \gg \left\{\begin{array}{c} kT \\ \tau_\alpha^{-1} \end{array}\right\} \quad (195)$$

ie, we need high fields, low T, and pure samples with small impurity scattering. Some numbers are useful here. We have

$$\hbar\omega_c \sim 0.7 K/T \qquad \text{(free electrons)} \quad (196)$$

$$\frac{\hbar\tau^{-1}}{\varepsilon_F} \sim a_0/l_0 \quad (197)$$

where a_0 is the lattice spacing and l_0 the mean free path of the Fermi surface electrons - thus to get $\hbar\tau^{-1}$ down to $\sim 1K$, we need $l_0 \sim \mu m$, ie very good samples (we talk here of simple metals); and we need fields of several Tesla at least.

It is possible to extend this quasiclassical picture to incorporate Fermi liquid interactions explicitly. In FLT language, one writes

$$E = E_0(B_0) + \sum_{\nu k_z \sigma} \varepsilon_{\nu\sigma}^0(k_z)\,\delta n_\nu^\sigma(k_z) + \frac{1}{2}\sum_{\substack{\nu\nu' \\ \sigma\sigma'}}\sum_{\substack{k_z \\ k_z'}} f_{\nu\nu'}^{\sigma\sigma'}(k_z,k_z')\,\delta n_\nu^\sigma(k_z)\delta n_{\nu'}^{\sigma'}(k_z') \quad (198)$$

where now ν labels Landau levels, and $f_{\nu\nu'}^{\sigma\sigma'}(k_z,k_z')$ is the new interaction function. Such a programme has never been carried out in full, but it leads to rather interesting results, which are discussed in the literature.

How good is this quasiclassical approximation? In the 1980's, with the intense studies made of both the Harper eqtn (eqtns (164) & (165)) and the Fractional

68

Quantum Hall effect (FQHE), the value of quasiclassical calculations was dismissed for fundamental studies. However in experiments it is found to work with quite amazing accuracy.

We will come back to this question again when we come to look at topological quantum states, specifically the FQHE and WAH (Wannier-Azbel-Hofstadter) problem (of which the Harper equation is an example).

REFERENCES TO (B)

(1) GENERAL REFERENCES ON MAGNETIC INTERACTIONS, etc.

P. Fazekas : "Electron Correlation & Magnetism" (World Sc., 1999)

HJ Zeiger & G Pratt : "Magnetic Interactions in Solids" (Clarendon Press, 1973)

NW Ashcroft ND Mermin : "Solid State Physics" (Holt, Rinehart, & Winston, 1976)

NF. Mott : Proc. Roy. Soc. $\underline{A62}$, 416 (1949)
"Metal-Insulator Transitions" (Taylor & Francis, 1974).

J. Hubbard, Proc Roy Soc. $\underline{A276}$, 238 (1963); ibid $\underline{A277}$, 237 (1964); ibid $\underline{A281}$, 401 (1965); ibid $\underline{A285}$, 542 (1965); ibid $\underline{A296}$, 82 (1967); ibid A296, 100 (1967).

PW Anderson : Phys. Rev. $\underline{86}$, 694 (1952)   (AFM state).
Phys. Rev. $\underline{79}$, 350 (1950); Phys. Rev. 115, 2 (1959)   (superexchange).
"Basic Notions of Condensed Matter Physics" (Benjamin, 1984).

H. A. Kramers : Physica $\underline{1}$, 182 (1934)   (superexchange)

The books are general reviews of metals physics; Fazekas & Ashcroft & Mermin are fairly introductory, whereas Zeiger & Pratt is an extended & detailed tome. Anderson's book is v. stimulating. The original papers of Kramers, Mott, & Anderson are well-known. The original papers of Hubbard are less often read but merit close study.

(2) FERMI LIQUID THEORY for ^3He and METALS

L.D. Landau : Sov. Phys. JETP $\underline{3}$, 920 (1957); ibid $\underline{5}$, 101 (1957); ibid $\underline{8}$, 70 (1959)

D. Pines, P. Nozières : "Theory of Quantum Liquids, vol I " (Benjamin, 1966)

P. Nozières : " Theory of Interacting Fermi systems "

A.A. Abrikosov : "Fundamentals of the Theory of Metals", (North-Holland, 1988)

A.A. Abrikosov, I.M. Khalatnikov. Rep. Prog. Phys. $\underline{22}$, 329 (1961)

G. Baym, C.J. Pethick, " Landau Fermi liquid theory : concepts & applications (Wiley, 1991).

M. Ya. Azbel, I.M. Lifshitz, Kaganov,

P. Platzman, P.A. Wolff, "Waves & Interactions in Solid State Plasmas" (Academic, 1973)

A.B. Pippard : "Dynamics of Conduction Electrons"

M. Springford (ed.) : "Electrons at the Fermi surface"

D. Shoenberg : "Magnetic Oscillations in Metals " (CUP, 1984)

S. Schultz, G. Dunifer : PRL 18, 283 (1967)
G.L. Dunifer, D. Pinkel, S. Schultz, PR $\underline{B10}$, 3159 (1974)
A. Wilson, D.R. Fredkin Phys. Rev. $\underline{B2}$, 4656 (1970)

The books of Abrikosov, Pines & Nozières, Baym & Pethick, Pippard, Springford, Shoenberg, and Azbel et al cover various aspects of the theory of charged & neutral Fermi liquids (^{3}He, metals, etc). The book of Nozières is a more advanced treatise. The book of Platzman & Wolff, & the papers of Schultz, Dunifer, & Wilson & Fredkin give an interesting picture of collective modes in metals.

The celebrated papers of Landau, and the review of Abrikosov & Khalatnikov, are well worth reading..

(3)

(3) WANNIER – AZ'BEL – HOFSTADTER MODEL

P.G. Harper :   Proc Roy Soc. $A\underline{68}$, 874 (1955)

M.Ya. Azbel :   JETP $\underline{19}$, 634 (1964)

D. Hofstadter : Phys. Rev B$\underline{14}$, 2239 (1976)

G.H. Wannier : Rev. Mod Phys. $\underline{34}$, 645 (1962)

The early papers on the WAH problem (at least some of them!).

© | MAGNETIC BEHAVIOUR OF THE HUBBARD-ANDERSON MODEL |

In this section we take a closer look at the Anderson-Hubbard model, and at the physics of its magnetic phases. We first look at the underlying microscopic physics again in a little more detail, making sure we understand how the model relates to real systems- the role of orbital degeneracy and its lifting by various perturbations, of hybridisation, and of the various Hubbard terms, is clarified. We then take a first look at the Mott transition, and at some of the physical systems that show it. The Mott transition is just one of the interesting transitions in this system - we move on to look at how Ferromagnetic (FM) and Antiferromagnetic (AFM) order arise, and at the low-energy behaviour of systems with such order. In doing this we acquire some understanding of the phase diagram of the system.

No discussion of this topic would be complete without a study of the dynamics of holes in the ordered magnetic phases, i.e., of magnetic polarons. We shall look at this topic in an introductory way.

Some topics will not be dealt with here, but later on in this course, because they are connected with the strongly-correlated nature of the system and with the topological properties of spin phase. These include 1-d systems, and also the more complex physics of some of the TM compounds and the "Heavy Fermion" RE systems. This latter physics includes high-Tc superconductivity, and the discussion of the underlying nature of the Mott transition.

Finally, we will very briefly describe how the Anderson-Hubbard model works for a set of dilute spins, and under what circumstances it reduces to a Kondo model. This allows us to understand how spins interact in such systems, depending on whether they are conducting or insulating. This is a necessary preliminary to the study of glasses, & Kondo lattices.

C.1. <u>THE ANDERSON-HUBBARD MODEL</u>

We have already had a very quick look at this model in section B.1. Let us consider it again more carefully. We will assume that we are interested in energy scales down to roughly 0.5 eV or so, and so write the Anderson lattice model as

$$\mathcal{H}_{And} = \sum_{k6} \epsilon_k c^+_{k6} c_{k6} + \sum_{k6} \sum_{jm} V_{km} \left(c^+_{k6} d_{jm6} + H.c. \right) + \sum_{jm6} E_m d^+_{jm6} d_{jm6}$$

$$+ \frac{1}{2} \sum_{j} \sum_{m,6} \sum_{m',6'} \left[U_0 \delta_{mm'} \delta_{6,-6'} + U^{66'}_{mm'} \right] n_{jm6} n_{jm'6'} \qquad (1)$$

$$(1-\delta_{mm'})$$

Thus we have included different d sub-orbitals on each site, allowing for crystal-field splitting of the different sub-orbitals, with resultant energies E_m; and we allow Coulomb terms U_0 and $U_{mm'}$ for these orbitals. Only one extended band is assumed - the Hamiltonian is easily modified (at the increase of indices) to include several of these.

Note what we have dropped from (1). The most serious omissions are the Hund's rule exchange J_H, which is at the lower end of the energy scale we are interested in; we will look briefly at its effects later on. The spin-orbit coupling is negligible for TM systems, and for these we can also neglect intersite exchange & super-exchange.

For RE systems we can certainly start from an Anderson lattice model, but the scale of energies changes radically - we can drop crystal field energies, but we must include the spin-orbit interactions and the on-site Hund's exchange. We shall see that this leads to a rather different kind of physics, in which the Kondo effect plays an important role.

How does one determine the size of the various parameters in (1) for a real system? This is a complicated problem, touched upon only briefly in section B.1; we now go into more details, and also take a look at some of the symmetries of the system.

C.1.1 : TERMS IN THE ANDERSON-HUBBARD MODEL :

What we wish to know here is how these terms are determined, both theoretically & experimentally. We will save the discussion of experiments for later on, and first look at how theory can be brought to bear.

(i) Light (s/p) Band Dispersion : We have already looked this in section B; the light-band dispersion ϵ_k is generally the most straightforward of the terms in $\mathcal{H}_{AHO}$ to understand, because we are dealing with small perturbations of the free-electron band, coming both from the periodic lattice potential and weak electron-electron interactions. Whether one starts with a free-particle dispersion and adds the lattice potential, or from a set of Wannier functions and then add tunneling terms, the calculations are straightforward. The main subtlety is in the determination of the correct screened form for the potential coming from the ion and the other electrons, which depends on getting the physics of the d-shells right.

(ii) Hybridisation terms : Hybridisation between the extended s/p-states and the quasi-localised d- or f-states arises naturally because the un-hybridized bands are not orthogonal - they overlap with each other in the region of space occupied by the unhybridized localised states.

It follows that a good estimate of the size of the hybridisation integral must be given by comparing the real space volume occupied by the localised states up to the total Wigner-Seitz volume occupied by the relevant ion in the lattice.* This is easily shown to give

$$V_{k,\ell m} = 2\epsilon_k^0 \left(\frac{r_\ell}{R_{WS}}\right)^{3/2} Y_{\ell m}(\hat{k}) \tag{2}$$

for the matrix elements, where $\ell = 2$ (d-electrons) or 3 (f-electrons), and r_ℓ is the calculated RMS radius for the states (calculated using, e.g., Hartree-Fock wave-functions); R_{WS}^3 is the Wigner-Seitz volume, and $\epsilon_k^0 \neq \hbar^2 k^2/2m$. This leads to a "bandwidth"

Hybridization widths Δ of the valence d and f shells of the transition metals using Eqs. (2) and (3)

3d elements	W/2 (eV)	4d elements	W/2 (eV)	5d elements	W/2 (eV)	4f elements	W/2 (eV)	5f elements	W/2 (eV)
Sc	0.71	Y	1.52	Lu	1.78	La	0.142	Ac	
Ti	0.65	Zr	1.35	Hf	1.56	Ce	0.077	Th	0.231
V	0.62	Nb	1.25	Ta	1.49	Pr	0.055	Pa	0.166
Cv	0.51	Mo	1.14	W	1.38	Nd	0.045	U	0.145
Mn	0.43	Tc	0.99	Re	1.22	Pm		Np	0.127
Fe	0.39	Ru	0.88	Os	1.13	Sm	0.031	Pu	0.102
Co	0.36	Rh	0.74	Ir	0.97	Eu	0.018	Am	0.071
Ni	0.31	Pd	0.59	Pt	0.89	Gd	0.023	Cm	0.070
Cu	0.25	Ag	0.44	Au	0.86	Tb	0.022	Bk	0.068
						Dy	0.019	Cf	0.066
						Ho	0.017		
						Er	0.016		
						Tm	0.014		
						Yb	0.009		
						Lu	0.009		

* Recall that the Wigner-Seitz cell is the region of space around a given lattice point which is closer to it than to any other lattice point.

for the renormalised d- or f-band, which we define as

$$W_{\ell m} = 2\pi \, \Im m \sum_k |V_{k\ell m}|^2 \, \delta(\epsilon - E_{\ell m}) \qquad (3)$$

which is just the broadening of a single level which hybridizes with a set of delocalised band states. In the table we actually calculate the quantity W_ℓ, given by summing over ℓ with $E_{\ell m}$ assumed near the Fermi energy. One then finds the sort of results one might expect from our earlier discussions - it is startling to see just how small a volume the 4f electrons occupy.

(iii) **Hubbard interaction terms** : In a single ion, one calculates U_0 and $U_{mm'}$ starting from the atomic wave-functions, and it is common to estimate the numbers by starting with Hartree-Fock wave functions for the electrons. The results can then be written in terms of matrix elements of the Coulomb interaction between these states - we already saw an example of this in our discussion of direct exchange, in section B, eqtns (34). It is common to specify parameters

$$F_0(\ell) = \frac{1}{2\ell+1} \sum_m \sum_{m'} \int d^3 r_1 \int d^3 r_2 \, |\psi_{\ell m}(r_1)|^2 \frac{e^2}{|r_1 - r_2|} |\psi_{\ell m'}(r_2)|^2 \qquad (4)$$

$$G_0(\ell) = \frac{1}{2\ell+1} \sum_m \sum_{m'} \int d^3 r_1 \int d^3 r_2 \, \psi_{\ell m}^*(r_1) \psi_{\ell m'}(r_2) \frac{e^2}{|r_1 - r_2|} \psi_{\ell m}(r_2) \psi_{\ell m'}^*(r_2) \qquad (5)$$

which are obvious generalisations of the numbers C and J_H discussed for a simple pair of orbitals in eqtns (34) of section B; here we average over all the sub-orbitals m. These parameters are the first in a series of "Slater-Condon" integrals, given by taking higher moments of the "direct" and "exchange" integrals in (4) and (5) respectively. Using these one quickly finds typical numbers for the atomic U_0 of 15-20 eV (see table). However these values take no account of screening which occurs in a real solid. Recall that a proper definition of U_0 or $U_{mm'}$ in a solid involves transferring charges between d- or f-states in widely separated ionic sites. The medium between these sites will polarize to partially screen the charges, thereby reducing the effective U in the solid. To calculate this effect requires more complex theory than we really want to get into here (the simplest way is to use the random phase approximation (RPA) for the screening, but this often has to be improved upon). The reduction of U is quite spectacular, usually by a factor $\sim O(3)$ [see table]. The $U_{mm'}$ will typically be down on the U_0 given above by a factor ~ 3-5.

Theoretical estimates of the d-d Coulomb interactions U and the charge transfer energy (Δ) for (fictitious) monoxides in the rock salt structure with a NiO lattice parameter. Also given are the atomic values including the B and C Racah parameters. The atomic values are taken from Moore's tables

	U_{at}	B_{at}	C_{at}	$E_A(x^{2+})$	U	Δ
Cu	16.3	0.15	0.58	20.3	5.1	4.0
Ni	18.0	0.13	0.60	18.2	7.3	6.0
Co	16.2	0.14	0.54	17.1	4.9	5.4
Fe	14.7	0.13	0.48	15.9	3.5	6.1
Mn	20.2	0.12	0.41	13.8	7.8	8.9
Cr	14.4	0.10	0.42	16.5	3.3	6.3
V	15.5	0.09	0.35	14.2	4.8	9.9
Ti	14.6	0.09	0.33	13.5	2.9	8.3

(iv) **Charge Transfer Terms** : The charge transfer energy gap between the 2 bands was defined in section B, eqtns. (15)-(17). Again, a naive calculation starts by considering the atomic states of the system, calculating

the ionisation potentials and electron affinities for the relevant ions. However again, as we might expect, these numbers are strongly corrected by the screening effects of other electrons in the actual solid. It is hard to give a systematic discussion here, since the details depend on how full each of the atomic shells is, and is a result of cancellation of large energies (electron affinities & Madelung potentials for the relevant ions).

C.1.2. PHASE DIAGRAM of HUBBARD MODEL - SIMPLE DISCUSSION

One can look at the Hubbard model in a very naive manner, as first done by Peierls in 1937 and then in much more detail by Mott in 1939; and we have already done the groundwork for this in looking at the 2-site model in section B (see eqns (B.38) et seq.). Recall that the system of 2 sites with 2 electrons shows strong charge fluctuations (ie., significant fluctuations to states where one site is doubly-occupied, the other unoccupied), when U/t is small; but that when $U/t \gg 1$, the ground state is almost entirely made up from singly-occupied states, with very little in the way of charge fluctuations.

One way to think about this is to say that when $U/t \ll 1$, the system lowers its energy by delocalising spins as much as possible (ie., it lowers the kinetic energy as much as possible), with very little potential energy cost. On the other hand when $U/t \gg 1$, it lowers its energy by localising electrons on sites, with no double occupancy.

Thus in this case, of a HALF-FILLED 2-site system (the maximum number of electrons that can be accommodated is actually 4), we actually see the glimmerings of an understanding of both the metal-insulator transition which may take place near ½-filling in the Hubbard model, and in many real physical systems, and of the magnetism which then immediately emerges once the system goes insulating.
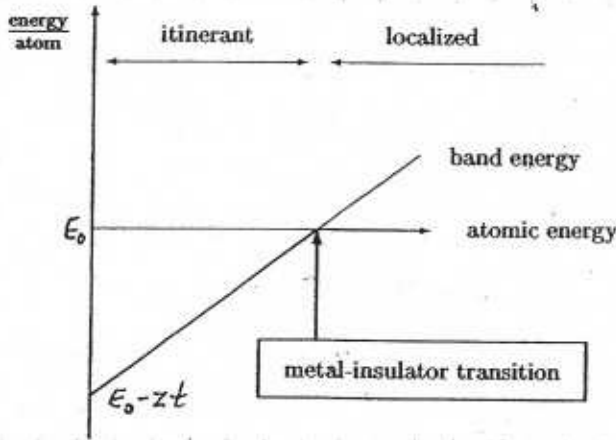

The most naive picture that one can infer from this for N-site system, where $N \gg 1$, is shown schematically at left, assuming the system is again ½-filled.

As we shall see this picture is in very many ways rather misleading, but remarkably the prediction that one can have a sharp phase transition - the famous Mott transition - is borne out by more sophisticated theory. Moreover, it is borne out by experiment, and we shall look at the comparison between theory & experiment later on.

The simplest way to get results for the Hubbard model of N sites is using a Hartree-Fock
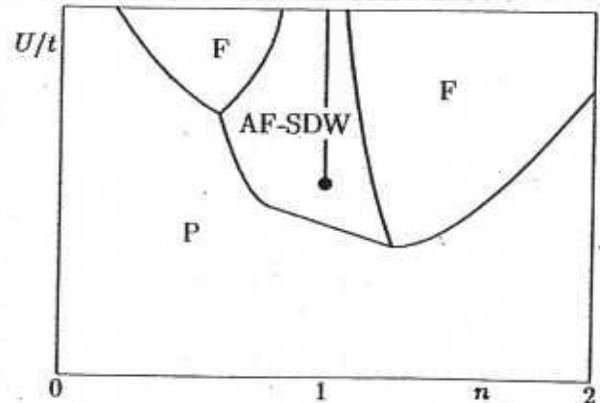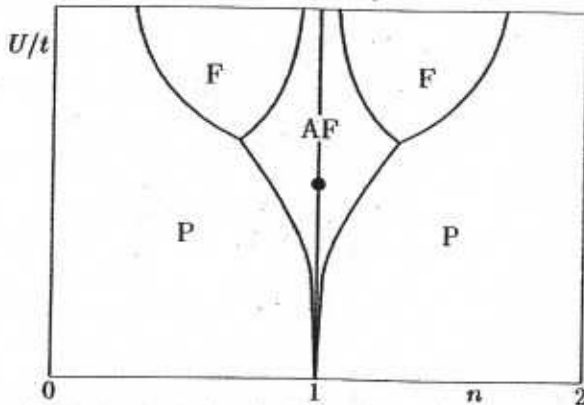
$F \equiv$ ferromagnetic
$AF \equiv$ anti ferromagnetic
$P \equiv$ paramagnetic

74

approximation for the system. The results are shown on the last page for both cubic lattices, and for a non-bipartite lattice. The results for a cubic lattice are a little special — in this case the system is unstable at half-filling to the formation of a spin-density wave state (SDW) for arbitrarily small U, because of a "nesting" property of the $U = 0$ Fermi surface. Going to a triangular lattice removes this instability and we see the Mott transition more clearly. These instabilities will be discussed in a more sophisticated way later on.
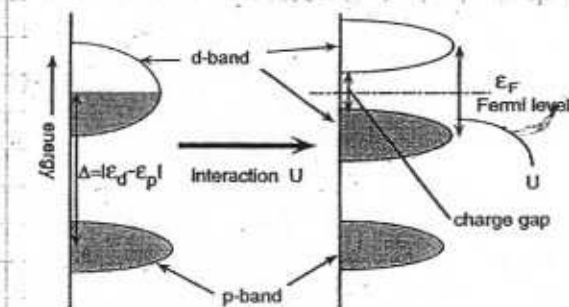
C.1.3 : PHASE DIAGRAM of ANDERSON LATTICE : SIMPLE DISCUSSION

The Anderson lattice is clearly more complicated than the Hubbard model, but a fairly interesting and simple picture has emerged here as well. As we saw in our introductory discussion in section B.1., there are really 5 energy scales of importance in the Anderson lattice, viz., U_0, Δ, W_p and W_d, and V_{kd} (ie, the on-site U_0, the charge transfer Δ, the bandwidth W_p and W_d for the sp and d-bands, and the sp-d hybridization V_{kd}).

A very illuminating picture of what kind of phases can be expected in the Anderson lattice was provided by the Zaanen-Sawatzky-Allen (ZSA) classification of states, shown at left. We can understand this by imagining that Δ is finite, and then slowly switching on U_0 (see diagram below). Two possible scenarios are shown, viz.

(a) Mott-Hubbard Insulator

(b) Charge Transfer Insulator
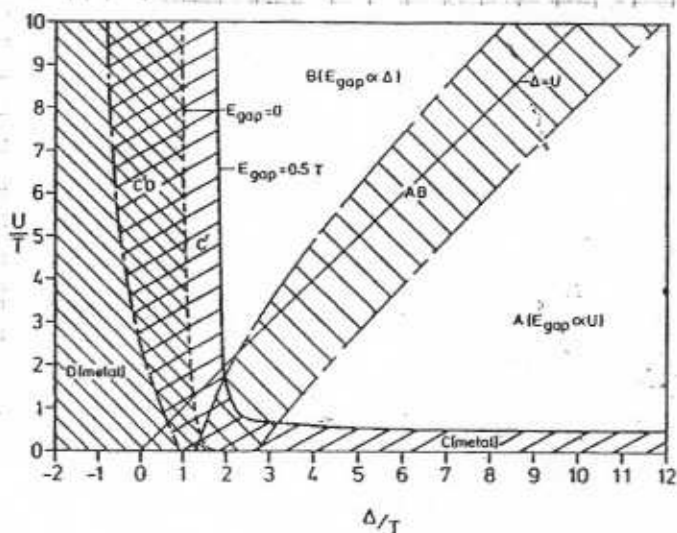
Zaanen-Sawatzky-Allen plot for classifying $3d$ transition-metal compounds. The straight line $U = \Delta$ separates the Mott-Hubbard regime (A) and the charge-transfer regime (B). Between the two regimes is located an intermediate regime (AB). The shaded areas near $U = 0$ and $\Delta = 0$ are metallic regions where a Mott-Hubbard-type or charge-transfer-type band gap is closed. From Zaanen, Sawatzky, and Allen, 1985.
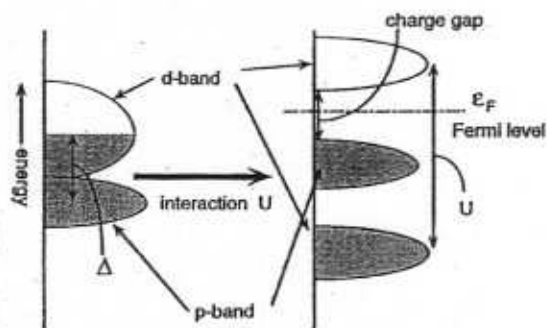
(i) We imagine a substantial charge gap exists already between d- and s-bands. Then adding U simply splits the d-band, to give an insulator. This is just the Mott instability discussed above.

(ii) The d- and s-bands start off on top of each other because Δ is now small. Then a large U again leaves an insulator, with the gap now a charge gap between the s- and d-bands. Notice that when Δ and/or U_0 are small, so small as the bandwidths W_p and/or W_d, then the system will not generally be insulating: either the s- and d-bands overlap, or the d-band has not yet split into 2 Hubbard sub-bands. Again, we will look at the comparison between theory & experiment later on.
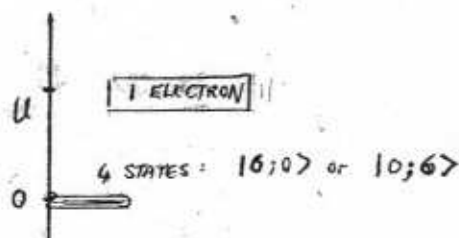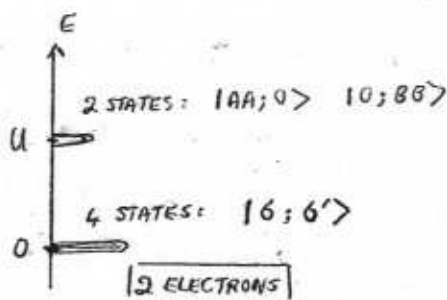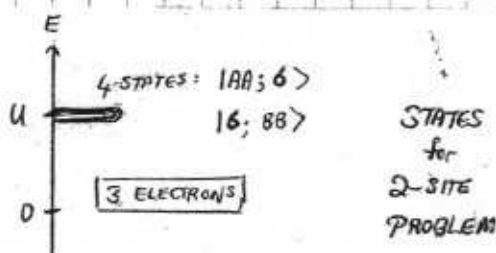
C.2. THE LARGE U LIMIT

At first glance the large U limit, with $U/t \gg 1$, seems to be the simplest region of the Hubbard/Anderson parameter space. One has intersite AFM interactions, and charge fluctuations are suppressed - the system is a simple magnetic insulator.

In certain ways this naive picture is correct, but there are some remarkable underlying subtleties, which first appear when we start to look in detail at the many-body states of this system. We begin by doing this, for the simple 1-band Hubbard model. This shows that the naive use of a $t-J$ model is justified under many circumstances, as is the use of multiple-exchange Hamiltonians in certain cases. The parameter regime at or close to $\frac{1}{2}$-filling (ie., 1 electron per site) is of particular interest.

C.2.1. COUNTING STATES IN THE LARGE-U LIMIT

In section B.1 we looked at the problem of 2 electrons on 2 sites of the Hubbard model. We now wish to generalise this to look at an N-site system, with N arbitrarily large, and containing an arbitrary number of electrons up to $2N$; but in the regime $U/t \gg 1$.

Consider first what are the available states for the 2-site problem, as we vary the number of electrons in the system. The figure below shows what we get when we do this. Consider first what happens when we have 3 electrons on the 2 sites. In the figure we show the states that one gets when $t = 0$ identically; so we saw in section B.1 the effect of t will be to split these states by amounts $\sim O(t^2/U)$, and since these splittings are $\ll U$, we show them as a small broadening of the levels - the tunneling term t will also mix the almost degenerate states.

The physics of the 3-electron, 2-site problem is simple: one of the sites is doubly-occupied, and the other is singly-occupied, and this singly-occupied site can have an electron of either spin. Thus we end up with 4 possible states, all of energy U (because there is one doubly-occupied site).
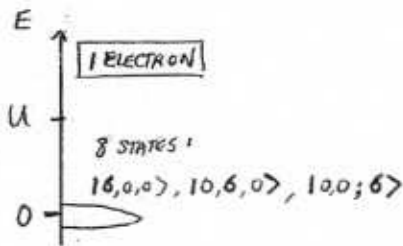
There is a particle-hole symmetry in this problem, because once a site is either doubly-occupied or unoccupied, it has no degrees of freedom left. All the spin degrees of freedom are attached to the singly-occupied sites.

We can extend this particle-hole symmetry to include even the completely full system, with $2N$ electrons on N sites, provided we allow the completely empty system to be called a "state" as well!

E

U ⊢⊟ 4-STATES: $|AA;6\rangle$

$|6;BB\rangle$

0 ⊢ ▭ 3 ELECTRONS

STATES for 2-SITE PROBLEM

E

U ⊢⊟ 2 STATES: $|AA;0\rangle$ $|0;BB\rangle$

0 ⊢⊟ 4 STATES: $|6;6'\rangle$

▭ 2 ELECTRONS

U ⊢ ▭ 1 ELECTRON

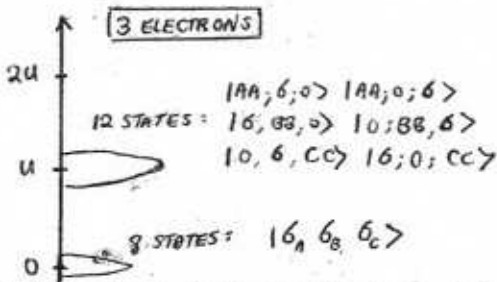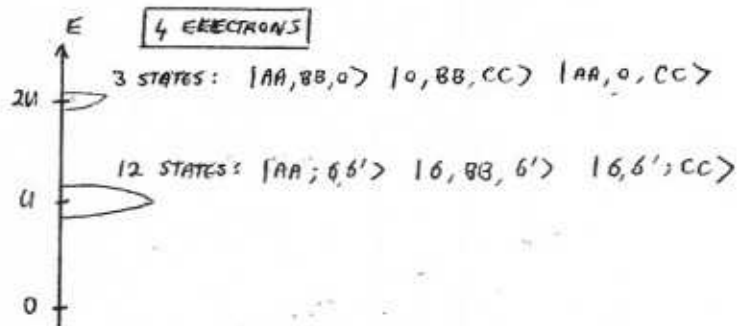0 ⊢⊟ 4 STATES: $|6;0\rangle$ or $|0;6\rangle$

Notice however that this particle-hole symmetry is not necessarily exact once we add the hopping term - it then depends on the lattice symmetry, & we return to this point later. Nor is a symmetry in energy space implied - we see this already in the $\frac{1}{2}$-filled problem of 2 electrons on 2 sites, where there are 4 states at low energy, but only 2 at higher energy U.

We can generalize all these considerations to a larger number of sites. Consider first

the example of 3 sites (an odd number), which we see immediately below:

HUBBARD STATES ON A 3-SITE SYSTEM. ($U \gg t$)

1 ELECTRON

8 STATES:
$|6,0,0\rangle, |0,6,0\rangle, |0,0;6\rangle$

2 ELECTRONS

3 STATES: $|AA;00\rangle \quad |0,BB,0\rangle \quad |0,0,CC\rangle$

12 STATES: $|6,6';0\rangle \quad |0;6,6'\rangle \quad |6,0,6'\rangle$

5 ELECTRONS

8 STATES:
$|AA,BB;6\rangle$
$|AA,6,BB\rangle$
$|6,BB,CC\rangle$

4 ELECTRONS

3 STATES: $|AA,BB,0\rangle \quad |0,BB,CC\rangle \quad |AA,0,CC\rangle$

12 STATES: $|AA;0,6'\rangle \quad |6,BB,6'\rangle \quad |6,6';CC\rangle$

3 ELECTRONS

12 STATES:
$|AA;6;0\rangle \quad |AA;0;6\rangle$
$|6,BB,0\rangle \quad |0;BB,6\rangle$
$|0,6,CC\rangle \quad |6;0;CC\rangle$

8 STATES: $|6_A, 6_B, 6_C\rangle$
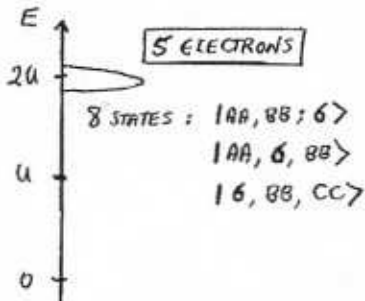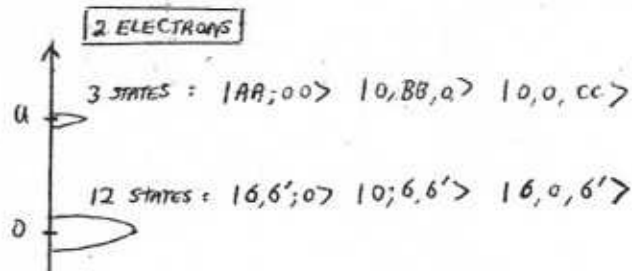
Now let us proceed to the problem of N sites, and we will assume that there are $2N-M$ particles in the system (ie., M "holes"). Thus we have

$$N \text{ sites}$$
$$2N-M \text{ particles} \qquad \text{and} \qquad$$
$$M \text{ "holes"}$$

d doubly-occupied sites
ℓ singly-occupied sites (ℓ "spins") $\qquad$ (6)
e empty sites

so that

$$2d + \ell = 2N - M$$
$$\ell + d + e = N \qquad\qquad (7)$$

From our remarks above it is clear that we can assume $M \leq N$; the case where the system is less than $\frac{1}{2}$-filled is equivalent to the corresponding problem with greater than $\frac{1}{2}$-filled, with $M \leftrightarrow 2N-M$.

Noting that a state with d doubly-occupied sites and ℓ singly-occupied sites has 2^ℓ different possible spin configurations, we see that the total number of possible states with d doubly-occupied sites and ℓ singly-occupied sites is

$$n_M^{d\ell} = 2^\ell \frac{N!}{d! \, \ell! \, (N-(d+\ell))!}$$

$$\equiv 2^\ell \frac{N!}{\ell! \, (N - \frac{M+\ell}{2})! \, (N + \frac{M-\ell}{2})!} \qquad (8)$$

where we have just used elementary combinatorics; and the energy of these same states

(which we can label the states by: M, d, ℓ or N, d, ℓ) is given by

$$E_M^{d\ell} = Ud = \left(N - \frac{M+\ell}{2}\right)U \qquad (9)$$

For a given M, we have a range of possible values of d; one has

$$d_{max} \geq d \geq d_{min} \qquad \text{with} \qquad \ell_{min} \leq \ell \leq \ell_{max} \qquad (10)$$

where

$$d_{max} = \begin{cases} N - M/2 & (2N-M \text{ even}) \\ N - \frac{M+1}{2} & (2N-M \text{ odd}) \end{cases} \qquad \ell_{min} = \begin{cases} 0 & (2N-M \text{ even}) \\ 1 & (2N-M \text{ odd}) \end{cases} \qquad (11)$$

$$d_{min} = N - M \qquad\qquad \ell_{max} = M \qquad (12)$$

To see what these results mean, we can look at a few special cases. Suppose we look first at situations where the system is almost completely full. If $M = 0$ (i.e., we have $2N$ particles), then there is only one state with energy NU. What ensues when we start taking particles out is shown below:
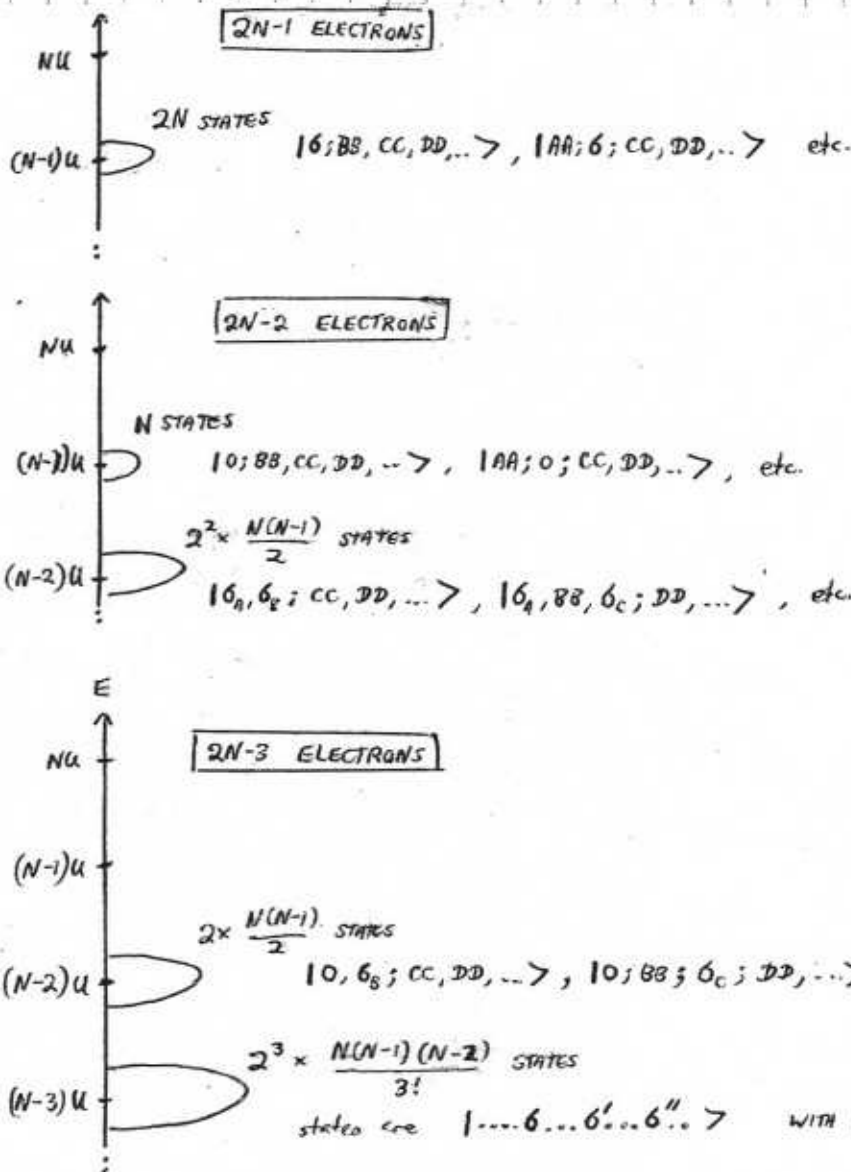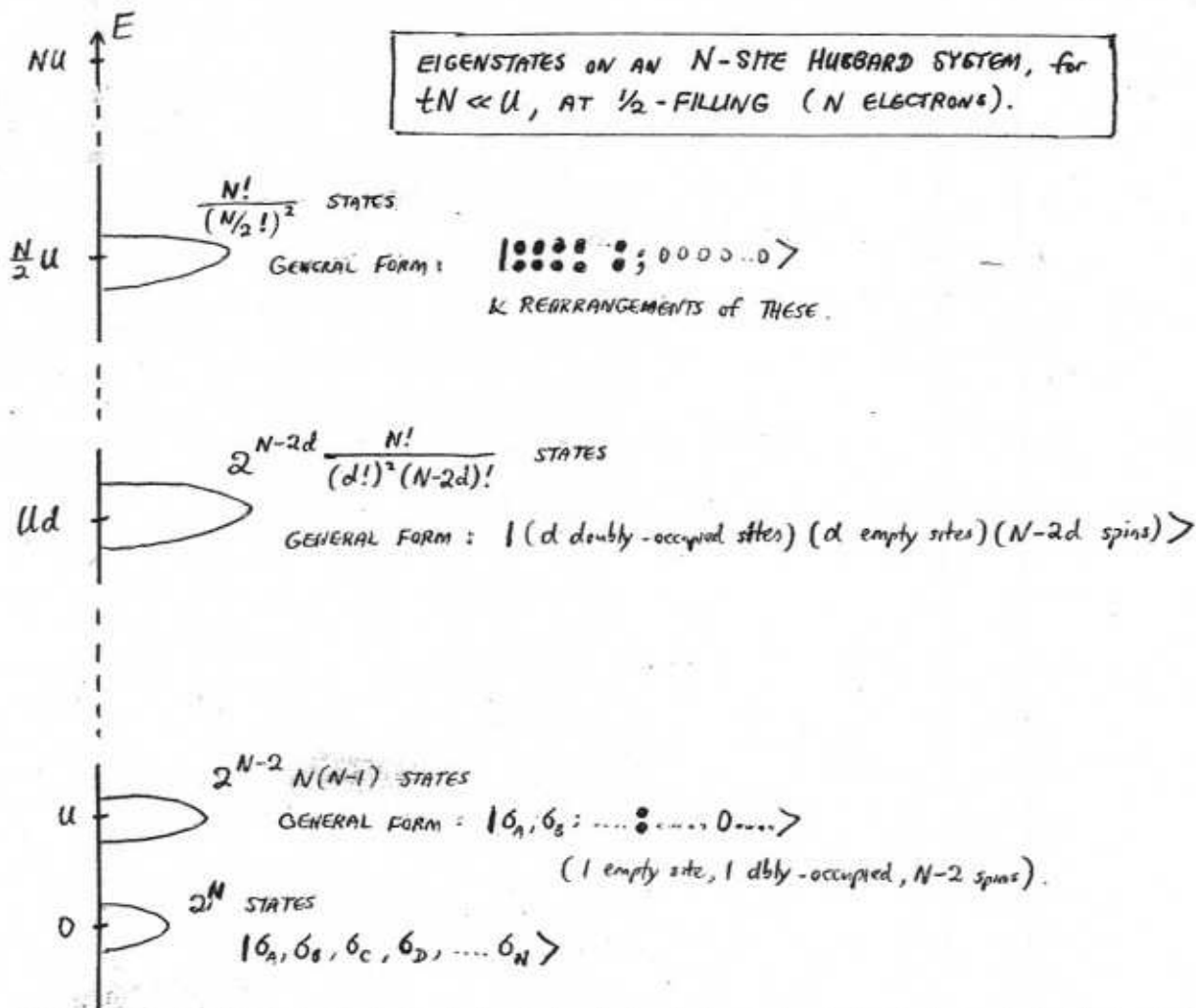

EIGENSTATES ON AN N-SITE HUBBARD SYSTEM FOR $tN \ll U$, AS A FUNCTION OF OCCUPANCY, NEAR COMPLETE FILLING

$\boxed{2N-1 \text{ ELECTRONS}}$

NU

$2N$ STATES

$(N-1)U$

$|6; BB, CC, DD, ...\rangle$, $|AA; 6; CC, DD, ..\rangle$ etc.

$\boxed{2N-2 \text{ ELECTRONS}}$

NU

N STATES

$(N-1)U$

$|0; BB, CC, DD, ..\rangle$, $|AA; 0; CC, DD, ...\rangle$, etc.

$2^2 \times \frac{N(N-1)}{2}$ STATES

$(N-2)U$

$|6_A, 6_B; CC, DD, ...\rangle$, $|6_A, BB, 6_C; DD, ...\rangle$, etc.

E

$\boxed{2N-3 \text{ ELECTRONS}}$

NU

$(N-1)U$

$2 \times \frac{N(N-1)}{2}$ STATES

$(N-2)U$

$|0, 6_B; CC, DD, ...\rangle$, $|0; BB; 6_C; DD, ...\rangle$ ... $|AA; 0; 6_C; DD... \rangle$, etc

$2^3 \times \frac{N(N-1)(N-2)}{3!}$ STATES

$(N-3)U$

states are $|....6...6'...6''..\rangle$ WITH ALL OTHER SITES DOUBLY OCCUPIED.

Notice that the lowest-energy states in this system are sets of spins, with no unoccupied states, as we might expect.

Above these lowest states one has combinations of single spin excitations and unoccupied states (where 2 holes have come to the same site).

These 2 kinds of excitation are the primitive excitations in this system.

Now suppose we go to the ½-filled band. This has states extending from energy $E_N^{N/2,0} = UN/2$, all the way down to 0; in the former case, $N/2$ sites are doubly occupied, and all the others are empty; in the latter case, all sites are singly occupied. The situation is shown below. We now have states extending over a huge energy range.

NU — E axis

EIGENSTATES ON AN N-SITE HUBBARD SYSTEM, for $tN \ll U$, AT ½-FILLING (N ELECTRONS).

At $\frac{N}{2}U$:

$\dfrac{N!}{(N/2 \,!)^2}$ STATES

GENERAL FORM: $|::::: \;\; \cdot\cdot \; ; 0000 \ldots 0\rangle$

& REARRANGEMENTS OF THESE.

At Ud:

$2^{N-2d} \dfrac{N!}{(d!)^2 (N-2d)!}$ STATES

GENERAL FORM: $|\,(d\ \text{doubly-occupied sites})\,(d\ \text{empty sites})\,(N-2d\ \text{spins})\rangle$

At U:

$2^{N-2} N(N-1)$ STATES

GENERAL FORM: $|6_A, 6_B : \ldots \overset{\bullet}{\bullet} \ldots 0 \ldots \rangle$

(1 empty site, 1 dbly-occupied, N-2 spins).

At 0:

2^N STATES

$|6_A, 6_B, 6_C, 6_D, \ldots 6_N\rangle$

Using Stirling's approximation we can easily get rough values for the size of these contributions – thus, we see that for the lowest of these "banks" of states, one has states with energy

$$E_{d\ell} = Ud \qquad \left.\begin{array}{c}\end{array}\right\} \; d \ll N \qquad (13)$$

and d number of states $\qquad n_{d\ell} \sim 2^N \left(\dfrac{N}{2d}\right)^{2d}$

whereas for an energy half-way between the top and bottom of the whole spectrum of states, when half of all the particles have combined into $N/4$ doubly-occupied sites (leaving $N/2$ single spins and $N/4$ empty sites), we have

$$E_{d=N/4} = \dfrac{N}{4} U \qquad \left.\begin{array}{c}\end{array}\right\} \; d = N/4 \qquad (14)$$

$$n_{d=N/4} \sim 2^{2N}$$

The sharp rise in density of states, for small d, is reflected in a similar rise in the number of states as one increases the number ℓ of free spins upon going down from the very top of the spectrum.

From all these details we can clearly discuss the available states for any sort of process in this atomic limit. Usually we are interested in low-energy properties, near the ground state. However at this point it becomes important to ask what is being fixed in the problem. If we fix the total number of particles in the system, then most of the states become unavailable to the system. For example, in the 2-site system, we see from the Fig. on page 45 that when there are 1 or 3 electrons in the problem, we are stuck in either the lower or upper of the 2 bands. On the other hand if there are 2 electrons per site, we have low-energy and high-energy states available.

This spectrum of available states when the number $2N-M$ of particles is kept constant is clearly relevant to, e.g., the equilibrium properties of a closed system. On the other hand one also often does experiments in which particles are added or subtracted from the system. This completely changes the available states. Suppose, e.g., that in the 3-site problem we are in the ground state of the ½-filled 3 electron system, and we want to know the possible excitations available if we either (i.) excite the system while keeping $M=3$ (ii) Excite the system while adding a particle (iii.) excite the system while kicking a particle out.

The results are obvious from the Fig. on p. 76. The details depend on whether we allow the spins to flip or not while exciting the system — if we do, then we see that the available states for excitations are

$M=3$ (no change in particle number) :   7 other states, energy ~ 0.
                                                  12 " " , energy ~ U.

$M=2$ (add one particle: "electron addition") :   12 " " , energy ~ U
                                                  3 " " , energy ~ $2U$

$M=4$ (subtract one particle : "electron removal")   11 other states, energy ~ 0
                                                  3 " " , energy ~ U.

There is a somewhat different way of thinking about this which is used, e.g., by experimentalists who are thinking about the available transitions in either "photoemission spectroscopy" (PES), where an electron is removed from the system, or "inverse photoemission spectroscopy" (IPES), where an electron is added to the system. In such experiments one is not interested in the M-particle density of states, but instead one is interested only in transitions between different "charge sectors", in which an electron is either added or removed. If we have an insulating system, at ½-filling, then we can slightly redraw the figures shown on pp. 27 and 74. for this case, showing the PES and IPES processes for a system where we assume the chemical potential is halfway between the filled and unfilled 1-particle bands. Notice the difference between these plots and those above, which are plots of the M-particle densities of states and energies.

Now consider what happens in the same system when we are no longer at ½-filling. Two crucial changes occur in this case, which we see by plotting the same kind of figures for these

Mott-Hubbard : Insulating
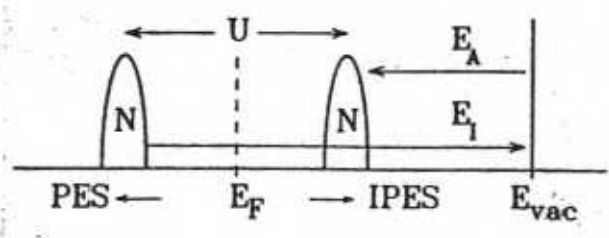
AVAILABLE 1-PARTICLE STATES FOR ELECTRON ADDITION (IPES) OR ELECTRON REMOVAL (PES) FOR THE ½-FILLED MOTT-HUBBARD SYSTEM.

2 situations. The first change is of course that the Fermi energy moves to the upper or lower Hubbard 1-particle band, depending on which situation we are dealing with. The second change is that the number of available states for PES or IPES processes changes. This change is called "spectral weight transfer", and

Mott-Hubbard

Semiconductor
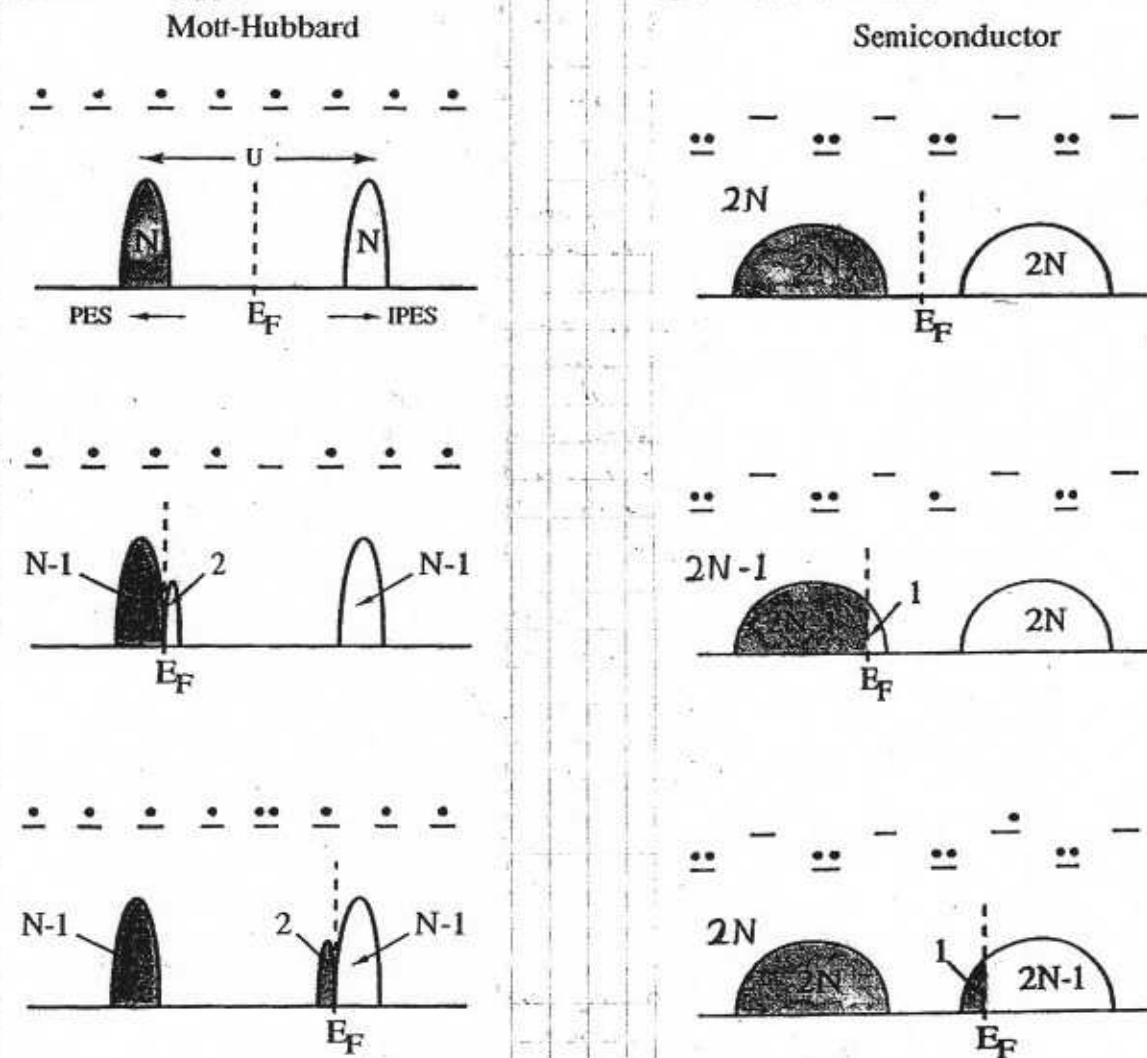
it causes a very interesting change in the "band structure" in this localized limit. We see that the 1-particle bands in this problem are not independent of their filling at all - in fact, as we fill up the system towards the upper limit of 2N particles per site, there are less and less available states in the lower Hubbard band.

This situation can be usefully contrasted with the situation in which we have no interactions at all, and just a valence and conduction band - this is the old Wilson-Sandheimer picture appropriate to a semiconductor, which is shown in the Fig. at right above, and which has been taught in solid-state texts for over 50 yrs now.

It is interesting to try and relate this picture back to the N-particle picture. Notice that we need to compare the low energy states available to the system for different numbers of particles - one thus needs to consider the Fig. shown on p. 78, and its equivalent for N-1 and N+1 particles in the system. This is left as an exercise.

C.2.2. THE t-J MODEL

In section B.1 we indicated how one might derive and effective low-energy Hamiltonian for the 2-site, ½-filled problem, and we got the form in eqn (B.52) for this Hamiltonian- the "t-J" model.

Let us now rederive this for the N-site system in a more systematic way, so that we can see what the limitations are. We assume at the outset that the system is ½-filled, with one electron per site, and we wish to derive the t-J model for this case, and see what corrections may appear at higher orders, or away from ½-filling. The crucial problem here is that we wish to do this now for finite t, and as we have just seen, there is a massive degeneracy in the ground state of the Hubbard model when $t=0$. This makes the problem more complicated, and to deal with it we need (following Hubbard) to introduce some formal measures.

<u>Hubbard operators</u>: It is useful, in the atomic limit, where $t=0$, to introduce operators which describe the different transitions that are possible. Note first that for a given site j we have 4 possible states:

$$|0\rangle_j \quad : \quad \text{empty site}$$

$$|\sigma\rangle_j \quad : \quad \text{singly-occupied w/ spin } \sigma \qquad |\sigma\rangle_j = c^+_{j\sigma}|0\rangle_j$$

$$|d\rangle_j \quad = \quad \text{doubly-occupied.} \qquad |d\rangle_j = c^+_{j\uparrow} c^+_{j\downarrow}|0\rangle_j \tag{15}$$

Note that we have had to choose a convention for the order in which we put spins into the doubly-occupied state — and this leads to a crucial sign change if we swap this order:

$$c^+_{j\downarrow} c^+_{j\uparrow}|0\rangle = -c^+_{j\uparrow}c^+_{j\downarrow} = -|d\rangle_j \tag{16}$$

Suppose we label such states by letters, so that the general states are $|p\rangle_j$, $|q\rangle_j$, etc. We define operators $\hat{X}^{pq}_j$, such that

$$X^{pq}_j = |p\rangle_j \langle q|_j \tag{17}$$

The diagonal Hubbard operators are projection operators:

$$X^{00}_j = |0\rangle_j\langle 0|_j \equiv (1-n_{j\uparrow})(1-n_{j\downarrow})$$

$$X^{\sigma\sigma}_j = |\sigma\rangle_j\langle\sigma|_j \equiv n_{j\sigma}(1-n_{j\cdot\sigma})$$

$$X^{dd}_j = |d\rangle_j\langle d|_j \equiv n_{j\uparrow}n_{j\downarrow} \equiv \tfrac{1}{2}\sum_\sigma n_{j\sigma}n_{j\cdot\sigma} \tag{18}$$

and we notice that these diagonal operators satisfy

$$\sum_{q=1}^{4} X^{qq}_j = 1 \tag{19}$$

which verifies the completeness of this basis set.

The off-diagonal operators are related to the usual Fermi operators by having a projection attached. To see this, note first that we should be able to write any operator O_j acting only on site j in the form

$$O_j = \sum_{p,q} \langle p|_j \hat{O}_j|q\rangle_j \hat{X}^{pq}_j \tag{20}$$

and this applies in particular to the fermion operators:

$$C_{j\sigma}^{+} = \sum_{pq} \langle p |_j C_{j\sigma}^{+} | q \rangle_j \; \hat{X}_j^{pq} \tag{21}$$

Let us see how this works in practise. Considering that $C_{j\sigma}^{+}$ can either create a spin σ from an empty site, or a doubly-occupied site from a state $|-\sigma\rangle$, we must have

$$C_{j\sigma}^{+} = X_j^{\sigma 0} + \sigma X_j^{d,-\sigma} \qquad (\sigma = \pm) \tag{22}$$

where we take account of the ordering of the spins. One also has interesting commutation relations for the Hubbard operators. From the def^{n} of the X_j^{pq} one has for a given site that

$$\hat{X}_j^{pq} \; \hat{X}_j^{rs} = \delta_{qr} X_j^{ps} \tag{23}$$

From this it follows that the commutation relations for a pair of sites are

$$[X_j^{pq}, X_i^{rs}] = \delta_{ij} \left(\delta_{qr} X_j^{ps} - \delta_{ps} X_j^{rq} \right) \tag{24}$$

From these results, or by inspection (the easiest way is to use the projectors in (18)):

$$\begin{matrix} X_j^{\sigma 0} & \equiv & C_{j\sigma}^{+} (1-n_{j-\sigma}) \\ X_j^{d\sigma} & \equiv & -\sigma C_{j-\sigma}^{+} \, n_{j\sigma}(1-n_{j-\sigma}) \\ X_j^{d0} & \equiv & \sigma C_{j\sigma}^{+} C_{j-\sigma}^{+} \, (1-n_{j\sigma})(1-n_{j-\sigma}) \end{matrix} \right\} \tag{25}$$

One can now represent the Hubbard Hamiltonian using the Hubbard operators, using

$$C_{j\sigma}^{+} = X_j^{\sigma 0} + \sigma X_j^{d,-\sigma}$$

The interaction term is easily written:

$$V_u = \frac{U}{2} \sum_{j\sigma} n_{j\sigma} n_{j-\sigma} \equiv U \sum_j X_j^{dd} \tag{26}$$

It is common to split up the hopping term:

$$\hat{T} \equiv -t \sum_{j\sigma} C_{j\sigma}^{+} C_{j\sigma} = \hat{T}_0 + \hat{T}_1 + \hat{T}_1 \tag{27}$$

where the terms $T_{\pm 1}$ increase/decrease the number of doubly-occupied states, and T_0 leaves their number unchanged. It will by now be clear why it is useful to make this separation - depending on what is the total number d of doubly-occupied states, one ends up in different sub-spaces of the total Hilbert space, with big changes in energy. If we write these terms explicitly, we have

$$\hat{T}_0 \equiv -t \sum_{\langle ij \rangle \sigma} \left\{ \left[(1-n_{i,-\sigma}) C_{i\sigma}^{+} C_{j\sigma} (1-n_{j,-\sigma}) + n_{i,-\sigma} C_{i\sigma}^{+} C_{j\sigma} n_{j,-\sigma} \right] + H.c \right\}$$

$$\equiv -t \sum_{\langle ij \rangle \sigma} \left\{ \left[X_i^{\sigma 0} X_j^{0\sigma} + X_i^{d,-\sigma} X_j^{-\sigma,d} \right] + H.c. \right\} \right\} \tag{28}$$

for the term involving no change in d, and

$$\hat{T}_{l} = -t \sum_{\langle ij \rangle} \sum_{\sigma} \left[n_{i,-\sigma} c_{i\sigma}^{\dagger} c_{j\sigma} (1-n_{j,-\sigma}) + (i \leftrightarrow j) \right]$$

$$\equiv -t \sum_{\langle ij \rangle} \sum_{\sigma} \sigma \left[X_{i}^{d,-\sigma} X_{j}^{0\sigma} + (i \leftrightarrow j) \right] \tag{29}$$

$$\hat{T}_{-l} = -t \sum_{\langle ij \rangle} \sum_{\sigma} \left[(1-n_{i,-\sigma}) c_{i\sigma}^{\dagger} c_{j\sigma} n_{j\sigma} + (i \leftrightarrow j) \right]$$

$$\equiv -t \sum_{\langle ij \rangle} \sum_{\sigma} \sigma \left[X_{i}^{\sigma 0} X_{j}^{-\sigma,d} + (i \leftrightarrow j) \right] \tag{30}$$

and of course we have

$$\mathcal{H}_{Hubb} = \hat{T}_{0} + \hat{T}_{l} + \hat{T}_{-l} + \hat{V}_{u} \tag{31}$$

Note the commutation relations between these various terms; we have

$$[\hat{T}_{l}, \hat{V}_{u}] = -U\hat{T}_{l} \qquad\qquad [\hat{T}_{-l}, \hat{V}_{u}] = U\hat{T}_{-l}$$

$$[\hat{T}_{l}, \hat{T}_{l}] = \sum_{\langle ij \rangle} \left[\underline{\sigma}_{i} \cdot \underline{\sigma}_{j} - n_{i} n_{j} \right] \tag{32}$$

From the last of these equations we can already see how the standard kinetic exchange term (section B, eqtns (49), (50), (52)) is going to arise in perturbation theory — from the process involving the operator sequence $T_{-l} V_{u} T_{l}$. However there is a more convenient way to get the perturbation theory out, as follows:

Canonical Transformation :

The method of canonical transformation is a well-known & occasionally useful method for solving quantum-mechanical (& classical) problems. Most commonly it is used to solve a problem by bringing it to a simpler form by a rotation in Hilbert space. For any operator function $f(\hat{O})$ which can be written as a power series in $\hat{O}$, we have

$$\tilde{f}(\hat{O}) = e^{iS} f(\hat{O}) e^{-iS}$$

$$\equiv e^{iS} \sum_{n} c_{n} \hat{O}^{n} e^{-iS} = \sum_{n} c_{n} \tilde{\hat{O}}^{n} = f(\tilde{\hat{O}}) \tag{33}$$

where

$$\tilde{\hat{O}} = e^{iS} \hat{O} e^{-iS} \tag{34}$$

Moreover, using the standard Baker-Hausdorff result

$$\tilde{O} = e^{iS} O e^{-iS} = O + i[S, O] + \frac{i^{2}}{2!} [S, [S, O]] + \cdots \tag{35}$$

we can expand the rotated operators in powers of the operator $\hat{S}$. The key to the use of this method is to find an operator $\hat{S}$ which makes $\tilde{f}(O)$ take a simpler form than the original $f(O)$.

The canonical transformation method can also be used to find a simpler form for a TRUNCATED effective Hamiltonian, in which we confine the Hilbert space to some regime of low energies. We will see now how this method can be used to generate not only the t-J model, but in principle

to generate an expansion in powers of t/U, for $t/U \ll 1$. This expansion has played a very important role in the history of quantum magnetism, simply because $t/U \ll 1$ for the majority of real systems.

We wish to generate this expansion starting from the expansion in (35), for the Hubbard model. We have therefore

$$
\begin{aligned}
\check{\mathcal{H}}_H &= e^{S} \mathcal{H}_H e^{-S} \\
&= (\hat{T} + \hat{V}_U) + i[\hat{s}, \hat{T} + \hat{V}_U] + \frac{i^2}{2!}[\hat{s}, [\hat{s}, \hat{T} + \hat{V}_U]] + \cdots
\end{aligned} \tag{36}
$$

where $\hat{T} = \hat{T}_0 + \hat{T}_1 + \hat{T}_{-1}$. Now it is fairly easy to see that a good first shot at a form for s is

$$
i\hat{S}_1 = \frac{1}{U}(\hat{T}_1 - \hat{T}_{-1}) \tag{37}
$$

because the commutator $i[\hat{S}_1, V_U] = -(\hat{T}_1 + \hat{T}_{-1})$ then cancels the terms in $\mathcal{H}_H$ that cause excitation out of the lower Hubbard band to the upper one (& vice-versa). We then find

$$
\check{\mathcal{H}}_H^{(2)} = (T_0 + V_U) + \frac{1}{U}\left([\hat{T}_1, \hat{T}_1] + [T_0, T_1] + [T_1, T_0]\right) \\
+ O(t^3/U^2) \tag{38}
$$

From this point on it is merely a question of algebra. It is left as an exercise to show that, for our usual spin-$\frac{1}{2}$ system,

(i) At $\frac{1}{2}$-filling, we get an effective Hamiltonian from this procedure of the form

$$
\mathcal{H}_H^{(2)} \equiv \mathcal{H}_{tJ} = -t \sum_{\langle ij \rangle} \sum_{\sigma} \left[(1 - n_{i,\bar{\sigma}}) c_{i\sigma}^{+} c_{j\sigma} (1 - n_{j,\bar{\sigma}}) + H.c\right] \\
+ \frac{4t^2}{U} \sum_{\langle ij \rangle} \left[S_i \cdot S_j - \frac{1}{4}\right] \tag{39}
$$
$\frac{1}{2}$-filling

(ii) For more general filling, where the initial state has a finite d and/or l, we get the form:

$$
\mathcal{H}^{(2)} \xrightarrow[\text{filling}]{\text{arbitrary}} \mathcal{H}_{tJ} + \frac{t^2}{U} \sum_{\langle ijk \rangle \sigma} \left\{ \left[X_i^{-\bar{\sigma},0} X_j^{-\bar{\sigma},0} X_j^{0\sigma} X_k^{0\sigma} + H.c.\right] \right. \\
\left. - \left[X_i^{\sigma 0} n_{j,\bar{\sigma}} X_k^{\sigma 0} + H.c.\right]\right\} \tag{40}
$$

$$
\equiv \mathcal{H}_{tJ} + \frac{t^2}{U} \sum_{\langle ijk \rangle \sigma} \left\{\left[\bar{c}_{i,\bar{\sigma}}^{+} \bar{c}_{j,\bar{\sigma}}^{+} \bar{c}_{j\sigma} \bar{c}_{k\sigma} + H.c.\right] - \left[\bar{c}_{i\sigma}^{+} n_{j,\bar{\sigma}} \bar{c}_{k\sigma} + H.c.\right]\right\}
$$

where $\langle ijk \rangle$ signifies that the sites i, j, and k are a chain of 3 nearest neighbours, in that order, and the notation

$$
\bar{c}_{j\sigma}^{+} \equiv c_{j\sigma}(1 - n_{j,\bar{\sigma}}) \tag{41}
$$

is used. The 3-site hopping terms that exist away from ½-filling are impossible at half-filling since they require at least one site to be unoccupied.

One can continue this process to higher orders by generating successively better forms for S. Thus, e.g., at the next order one finds

$$iS_2 = \frac{1}{U^2}\left([\hat{T}_1,\hat{T}_0] + [T_{-1},T_0]\right) \tag{42}$$

and so on. The net result of this is to generate an effective Hamiltonian which for ½-filling has the form up to $O(s^4)$:

$$\mathcal{H}_{eff} = \frac{1}{2}\sum_{\langle ij\rangle} J_{ij} S_i\cdot S_j + \frac{1}{4}\left\{\sum_{\langle ijk\ell\rangle} K_1^{ijk\ell}[(S_i\cdot S_j)(S_k\cdot S_\ell) + (S_j\cdot S_k)(S_i\cdot S_\ell) - (S_i\cdot S_\ell)(S_j\cdot S_k)] \right.$$
$$\left. + K_2^{ijk\ell}[(S_i\cdot S_k) + (S_j\cdot S_\ell)]\right\} + \frac{J_4}{4}\sum_{\langle ij\rangle}(S_i\cdot S_j)^2 \tag{43}$$

where $\langle ijk\ell\rangle$ signifies a set of 4 nearest-neighbor sites. The coefficients of these terms depend on the crystal structure. For a 2-d square lattice, to pick an example, one has

$$J_{ij} = J = \frac{4t^2}{U} \qquad\qquad K_1 = 20\frac{t^4}{U^3}$$
$$K_3 = \qquad\qquad\qquad\qquad K_2 = 16\frac{t^4}{U^3} \tag{44}$$

For higher orders things get much more complicated - and for systems away from ½-filling, much much more complicated. In fact the results for a 2-d Hubbard model away from ½ filling have been the source of considerable discussion in the last few years - see references.

Note also that our form in (43) only has even orders of S; but if the system lacks a simple symmetry, or if a magnetic field is applied, odd powers will also appear.

There are many applications of these effective Hamiltonians - we defer discussion of them until later. One of the most illuminating, because of its conceptual simplicity, is the application to solid ³He, where the spins involved are nuclear spins, and exchange is accomplished by the physical exchange of ³He atoms. The higher-order multiple-exchange terms then correspond to motion of "rings" of atoms in the background crystal. These higher-order terms are not small, because the large zero-point motion of the ³He atoms makes such ring exchange processes very easily done.

Finally we note that even this large U limit is not necessarily simple if we move away from ½-filling. This is in fact one of the key questions in the present theory of high-T_c superconductivity, and we shall return to it in our discussion of strongly-correlated systems.

C.3 MAGNETIC INSULATORS IN THE LARGE U LIMIT

We have seen that near or at ½-filling when $U/t \gg 1$, a set of spins on a lattice is likely to be insulating, with a set of interspin couplings generated by exchange processes. We have avoided the topic of detailed evaluation of the phase diagram for such systems, and of their statistical mechanics, in an effort to look at the underlying mechanisms for the magnetic order.

In this sub-section we will also ignore the details of how differently-ordered magnetic phases arise in magnetic insulators, and concentrate instead on how these ordered phases behave once they are already established.

There are basically 3 kinds of interesting ordered phase - ferromagnetic (FM), antiferromagnetic (FM), and Valence Bond solid (VBS). The main question we wish to understand here is - what are the low-energy "quasiparticle" excitations in these systems. We shall find out what these are, and also look at the other low-energy excitations of topological origin in the system - these are the "soliton" excitations.

C.3.1. EXCITATIONS IN THE FM INSULATOR

The simplest kind of magnetically ordered system is the FM insulator. In most texts this topic is explained in a simple pedagogical way, in which a simple isotropic Heisenberg exchange Hamiltonian is employed. Here we wish to give a more realistic discussion, which brings out the full low-energy physics of the system. We will therefore start from the following effective Hamiltonian:

$$\mathcal{H}_{eff} = \mathcal{H}_K + \mathcal{H}_J + \mathcal{H}_{dip.} + \mathcal{H}_Z \qquad (45)$$

which is a sum of anisotropy, exchange, dipolar, and Zeeman interactions:

(a) $\quad \mathcal{H}_K = \sum_j K_j^{\alpha\beta} S_j^\alpha S_j^\beta + O(S^4)$

(b) $\quad \mathcal{H}_J = \frac{1}{2} \sum_{ij} J_{ij}^{\alpha\beta} S_i^\alpha S_j^\beta$

(c) $\quad \mathcal{H}_{dip} = \frac{1}{2} \sum_{ij} V_{ij}^D \left[S_i \cdot S_j - 3 \frac{(S_i \cdot r_{ij})(S_j \cdot r_{ij})}{r_{ij}^2} \right] \qquad \left(V_{ij}^D = \frac{(g\mu_B)^2}{r_{ij}^3} \right)$

(d) $\quad \mathcal{H}_Z = -g\mu_B H_0 \cdot \sum_j S_j$

$\left. \right\} \quad (46)$

The origin of these interactions was discussed in section B.1. We are assuming here, for simplicity, that the g-factor is isotropic; and we will also choose simple forms for the other coefficients in order to do calculations.

In the absence of $\mathcal{H}_K$ or $\mathcal{H}_{dip}$, the system only possesses one branch of low-energy excitations - these are spin waves or "magnons". If $\mathcal{H}_Z = 0$ as well (zero applied field), these excitations are also gapless, i.e., $\lim_{q \to} \omega_q = 0$ for these modes, in the large wavelength limit.

This gapless limit is interesting from the point of view of general principle - it allows a discussion of spontaneously broken symmetry, Goldstone modes, and order

parameter. However the physics which results when H_k and/or H_{dp} is added contains crucial new ingredients. Either of them allows the existence of gaps in the magnon spectrum, and they also allow a new set of low-energy topological excitations to appear. These are solitonic excitations, and they have considerable fundamental interest.

Before looking these 2 kinds of excitation in detail, it is useful to also note the continuum form of the effective Hamiltonian in (45). The terms in (46) become:

$$(a) \quad \mathcal{H}_k = \frac{1}{2} \int \frac{d^3 r}{a_o^3} K_{\alpha\beta} S^\alpha(r) S^\beta(r) \equiv \frac{1}{2(g\mu_B)^2} \int \frac{d^3 r}{a_o^3} K_{\alpha\beta} M^\alpha(r) M^\beta(r) + O(M^4).$$

$$(b) \quad \mathcal{H}_J = \frac{1}{2} \int \frac{d^3 r}{a_o^3} J (\nabla S(r)) \cdot (\nabla S(r)) = \frac{1}{2(g\mu_B)^2} \int \frac{d^3 r}{a_o^3} (\nabla M(r)) \cdot (\nabla M(r)). \qquad (47)$$

$$(c) \quad \mathcal{H}_{d\rho} = \frac{1}{2} \int d^3 r \, \underline{M}(r,t) \cdot \nabla_r \int d^3 r' \, \underline{M}(r',t) \cdot \nabla_{r'} \frac{1}{|r-r'|}$$

$$(d) \quad \mathcal{H}_Z = - \int d^3 r \, \underline{H}_0 \cdot \underline{M}(r,t)$$

where we have assumed a cubic lattice for simplicity, with lattice constant a_0, and the magnetisation density is

$$M(r,t) = g\mu_B \frac{1}{V_0} \sum_j^{j \in V_0(r)} S_j$$

Note that it is quite common to lump together the dipolar and Zeeman terms together into a single term

$$\delta \mathcal{H} = - \int d^3 r \, (\underline{H}_0 + \underline{H}_{dm}(r,t)) \cdot \underline{M}(r,t) \qquad (48)$$

where

$$\underline{H}_{dm}(r,t) = - \nabla_r \int d^3 r' \, \underline{M}(r',t) \cdot \nabla_{r'} \frac{1}{|r-r'|}$$

$$\equiv - \nabla_r \Phi_{dm}(r,t) \qquad (49)$$

where we can then write the demagnetisation potential as

$$\Phi_{dm}(r,t) = \oint_S d^2 s' \frac{\sigma_m(r')}{|r-r'|} + \oint_V d^3 r' \frac{\rho_m(r')}{|r-r'|} \qquad (50)$$

where the surface integral $\oint d\underline{s}$ is over the sample surface, and the volume integral is over the sample volume; $\sigma_m(r)$ and $\rho_m(r)$ are the surface and volume densities of "magnetic charge" (ie, magnetic poles) respectively. This continuum limit allows us to make the connection to the macroscopic magnetisation dynamics and the "magnetostatics". However we note that we can only go to this continuum limit if the relevant excitations are long-wavelength, and if the dynamics is slow - otherwise we must go back to the lattice model. Thus the continuum Hamiltonian can be viewed as an even lower energy effective Hamiltonian - we shall see what its limits of validity are below.

Ferro Magnetic

FM Spin Waves / Magnons

: Suppose we consider the problem first with no anisotropy or dipolar interactions. This is a standard problem, which easily solved using either Holstein-Primakoff bosons or Schwinger bosons. Suppose we choose $\hat{z}$ to be along the field (the problem is isotropic otherwise), so that the state with all spins polarised along $\hat{z}$ is actually the ground state:

$$\mathcal{H}_0 |0\rangle = E_0 |0\rangle \tag{51}$$

where

$$\mathcal{H}_0 = -g\mu_B H_0 \sum_j S_j^z - \tfrac{1}{2} \sum_{ij} J_{ij} \underline{S}_i \cdot \underline{S}_j \tag{52}$$

$$E_0 = g\mu_B SNH_0 - \tfrac{S^2}{2} \sum_{ij} J_{ij} \tag{53}$$

and

$$|0\rangle \equiv \prod_{j=1}^{N} c_{j\uparrow}^{+} |vac\rangle \tag{54}$$

Most of you will know that one can easily find the lowest branch of magnon excitations for this problem by just introducing the ansatz of a single "reversed spin" (ie., going to the sector of states where $S_z^{TOT} = NS-1$), ie., a state

$$|\psi_i\rangle = \sum_j c_j |\phi_j^{(1)}\rangle \qquad\qquad |\phi_j^{(1)}\rangle = \frac{S_j^-}{\sqrt{2S}} |0\rangle \tag{55}$$

which satisfies the eigenvalue eqtn $\mathcal{H}_0 |\psi_i\rangle = E_1 |\psi_i\rangle$ in the form

$$\left[E_1 - E_0 + g\mu_B H_0 - 2S \sum_j^{j\neq i} J_{ij} \right] c_i = -2S \sum_j^{j\neq i} J_{ij} c_j \tag{56}$$

which is solved by assuming $c_j = \frac{1}{\sqrt{N}} e^{i\underline{q}\cdot\underline{r}_j}$, to give $E_1 = E_0 + \omega_q$, where

$$\omega_q = g\mu_B H_0 + 2S\gamma_q \tag{57}$$

$$\gamma_q = J(q=0) - J(\underline{q})$$

where

$$J(\underline{q}) = \sum_j^{j\neq i} J_{ij} e^{i\underline{q}\cdot(\underline{r}_i-\underline{r}_j)} \tag{58}$$

However we want to understand the spectrum in a more complete way, and for this we rewrite the Hamiltonian $\mathcal{H}_0$ in terms of Holstein-Primakoff bosons. Recalling the expansion in eqtn (A.79) for the HP operators in terms of HP bosons, we immediately get

$$\mathcal{H}_0 = E_0 + g\mu_B H_0 \sum_j b_j^\dagger b_j - S \sum_{ij} J_{ij} (b_i^\dagger b_j - b_j^\dagger b_j) + O(b_j^4) \tag{59}$$

The crucial term in this eqtn is the off-diagonal term, coming from the term $\tfrac{1}{2} \sum_{ij} J_{ij} (S_i^+ S_j^- + S_j^+ S_i^-)$; we notice that the $\sum_{ij} J_{ij} S_i^z S_j^z$ term does not contribute, because it gives a term $\sum_{ij} J_{ij} b_i^\dagger b_i b_j^\dagger b_j$ which is 4th-order in b.

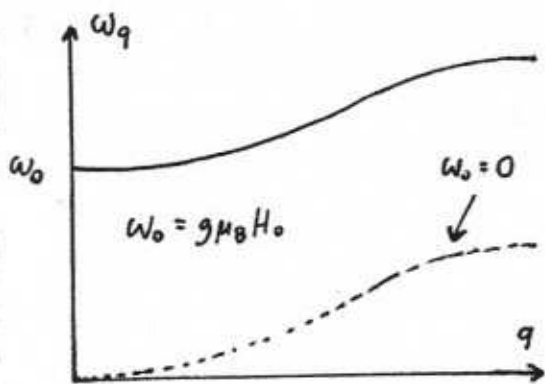We again go to a momentum representation, writing

$$b_j = \frac{1}{\sqrt{N}} \sum_q b_q e^{i\underline{q}\cdot\underline{r}_j} \qquad\qquad [b_q, b_{q'}^\dagger] = \delta_{qq'} \tag{60}$$
$$[b_q, b_{q'}] = 0$$

and then we quickly find that in this quadratic approximation in b we have the effective Hamiltonian

$$\mathcal{H}_{eff} = E_0 + \sum_q \omega_q b_q^\dagger b_q + O(b_q^4) \qquad (61)$$

For reference you may care to note the form of ω_q for a simple cubic lattice:

$$\omega_q = g\mu_B H_0 + J[6 - 2(\cos k_x a_0 + \cos k_y a_0 + \cos k_z a_0)] \qquad (62)$$

Thus the simple "flat" dispersion we would get for the spectrum of reversed spins when $J=0$ is broadened into a band of magnons, as shown at left. Note that for $qa_0 \ll 1$ (i.e., long wavelength magnon) we get

$$\omega_q \sim g\mu_B H_0 + 2JS(qa_0)^2 \qquad (63$$

This is the same result we would get by taking the purely classical long-wavelength continuum theory, and doing for the oscillatory modes of this theory, for small amplitude deviations from $\underline{M} = \hat{z}M$.

Now there is nothing to stop us continuing this expansion beyond the lowest order in the b_j. At this point things get quite interesting. If we continue to 4th-order in the $\{b_j\}$, we get

$$\mathcal{H}_{eff} = E_0 + \sum_q \omega_q b_q^\dagger b_q + \frac{1}{2N} \sum_{\substack{q_1 q_2 \\ \underline{k}}} \Gamma^{(4)}_{q_1 q_2}(\underline{k}) b_{q_1+\underline{k}}^\dagger b_{q_2-\underline{k}}^\dagger b_{q_1} b_{q_2} + O(b_q^6)$$

with

$$\Gamma^{(4)}_{q_1 q_2}(\underline{k}) = (\gamma_k + \gamma_{k+q_1-q_2} - \gamma_{k-q_2} - \gamma_{k+q_1})$$

$$= (J(\underline{k}) + J(k+q_1-q_2) - J(\underline{k}-q_2) - J(\underline{k}+q_1))$$

or, written as a lattice sum

$$\Gamma^{(4)}_{q_1 q_2}(\underline{k}) = J \sum_j^{j \neq i} e^{i\underline{k}\cdot(\underline{r}_i-\underline{r}_j)} (1 - e^{-iq_1\cdot(\underline{r}_i-\underline{r}_j)})(1 - e^{-iq_2\cdot(\underline{r}_i-\underline{r}_j)})$$

In the long-wavelength limit (where $q_1 a_0$, $q_2 a_0 \ll 1$, and $ka_0 \ll 1$), this 4-magnon scattering amplitude goes to zero. We now have an interacting field theory of magnons, and some of the relevant processes are shown at left, for the case where we truncate the theory at 4-magnon couplings. One can extend this to higher order, and under some circumstances this turns out to be quite useful.

All of this has been done for the simple exchange Hamiltonian. Notice that if
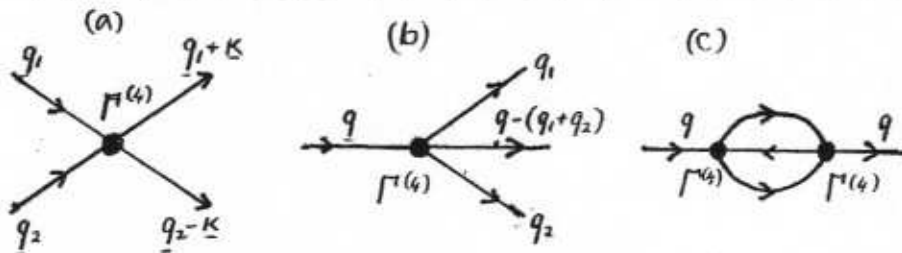
SOME PROCESSES INVOLVING 4-MAGNON INTERACTIONS: (A) 4-MAGNON SCATTERING; (B) MAGNON-DECAY (C) SELF-ENERGY CORRECTION.

we let the external field go to zero, there is no gap in the $q \to 0$ limit. The magnon has become a "Goldstone mode", with the gaplessness reflecting the rotational invariance of the system. Strictly speaking, the ground state when $H_0 = 0$ cannot choose any direction, but any small field H_0 will lift the degeneracy between the different directions. Notice that the ground state in the case where we simultaneously take the limits $N \to \infty$ (the thermodynamic limit) and $H_0 \to 0$ depends on which order we take these limits. If we take $N \to \infty$ first, then the system will end up aligned along $\hat{z}$. We return to this question of "spontaneously broken symmetry" below.

Now suppose we add the dipolar interactions. Actually this was the problem originally studied by Holstein & Primakoff. One now gets the bilinear form

$$\mathcal{H}_{eff} = C_0(H_0) + \sum_q \left[A_q b_q^\dagger b_q + \tfrac{1}{2}\left(B_q b_q b_{-q} + B_q^* b_q^\dagger b_{-q}^\dagger \right) \right] \tag{67}$$

with

$$A_q = g\mu_B H_0 + 2S\gamma_q - \frac{S}{2} \sum_j^{j \neq i} V_{ij}^D \left(1 - 3\frac{(\hat{z}\cdot(\vec{r_i}-\vec{r_j}))^2}{|\vec{r_i}-\vec{r_j}|^2}\right)\left(e^{iq\cdot(\vec{r_i}-\vec{r_j})} + 2\right)$$

$$B_q = -\tfrac{3}{2} S \sum_j^{j \neq i} V_{ij}^D \frac{((\hat{x}-i\hat{y})\cdot(\vec{r_i}-\vec{r_j}))^2}{|\vec{r_i}-\vec{r_j}|^2} e^{iq\cdot(\vec{r_i}-\vec{r_j})} \tag{68}$$

$$C_0(H_0) = -J_{(q=0)} S^2 N - g\mu_B SNH_0 + \frac{S^2}{2} \sum_j^{j \neq i} V_{ij}^D \left(1 - \frac{(\hat{z}\cdot(\vec{r_i}-\vec{r_j}))^2}{|\vec{r_i}-\vec{r_j}|^2}\right)$$

in which $\hat{x}, \hat{y},$ and $\hat{z}$ are unit vectors. The problem now is to find a canonical transformation which reduces $\mathcal{H}_{eff}$ to diagonal form. Such "Holstein-Primakoff" transformations are very useful in problems like this (in the theory of superfluidity & superconductivity they are called "Bogoliubov transformations"). The form of this transformation is

$$\begin{pmatrix} b_q \\ b_q^\dagger \\ b_{-q} \\ b_{-q}^\dagger \end{pmatrix} = \begin{pmatrix} \cosh\psi_q & 0 & 0 & -e^{2i\phi_q}\sinh\psi_q \\ 0 & \cosh\psi_q & -e^{-2i\phi_q}\sinh\psi_q & 0 \\ 0 & -e^{2i\phi_q}\sinh\psi_q & \cosh\psi_q & 0 \\ -e^{-2i\phi_q}\sinh\psi_q & 0 & 0 & \cosh\psi_q \end{pmatrix} \begin{pmatrix} \beta_q \\ \beta_q^\dagger \\ \beta_{-q} \\ \beta_{-q}^\dagger \end{pmatrix} \tag{69}$$

which can be written in more compact form as

$$\underline{b}_q = \mathbf{U}_q \underline{\beta}_q \tag{70}$$

where

$$\mathbf{U}_q = \begin{pmatrix} u_q & v_q \\ v_q & u_q \end{pmatrix} \qquad u_q = \begin{pmatrix} \cosh\psi_q & 0 \\ 0 & \cosh\psi_q \end{pmatrix}$$

$$v_q = \begin{pmatrix} 0 & e^{2i\phi_q}\sinh\psi_q \\ e^{-2i\phi_q}\sinh\psi_q & 0 \end{pmatrix} \tag{71}$$

and

$$\underline{b}_q = \begin{pmatrix} b_q \\ b_q^\dagger \\ b_{-q} \\ b_{-q}^\dagger \end{pmatrix} \tag{72}$$

and the angles are defined by

$$\tanh 2\psi_q = |B_q|/A_q$$
$$\tan \phi_q = q_y/q_x$$
$$\tag{73}$$

I have written these transformations in a way which brings out their similarity to the Bogoliubov transformations employed in BCS theory. The key point here is that the HP transformation simultaneously mixes spin-flip ($b_q \leftrightarrow b_q^+$) and momentum-flip ($q \to -q$) transformations, to produce a new set of quasiparticles $|\tilde{q}\rangle = \beta_q^+|0\rangle$, with the superposition

$$\begin{pmatrix} \beta_q \\ \beta_{-q}^+ \end{pmatrix} = \begin{pmatrix} \cosh \psi_q & e^{2i\phi_q} \sinh \psi_q \\ e^{-2i\phi_q} \sinh \psi_q & \cosh \psi_q \end{pmatrix} \begin{pmatrix} b_q \\ b_{-q}^+ \end{pmatrix} \tag{74}$$

i.e., the new quasiparticles $|\tilde{q}\rangle$ are superpositions of original magnons (down-flip) with momentum q, and "anti-magnons" (up-flip) with momentum $-q$. This is essentially the mixing of time-reversed pairs of the original magnons.

The new quasiparticles now diagonalise the problem:

$$\mathcal{H}_{\text{eff}} = E_0 + \sum_q \omega_q \beta_q^+ \beta_q \tag{75}$$

where

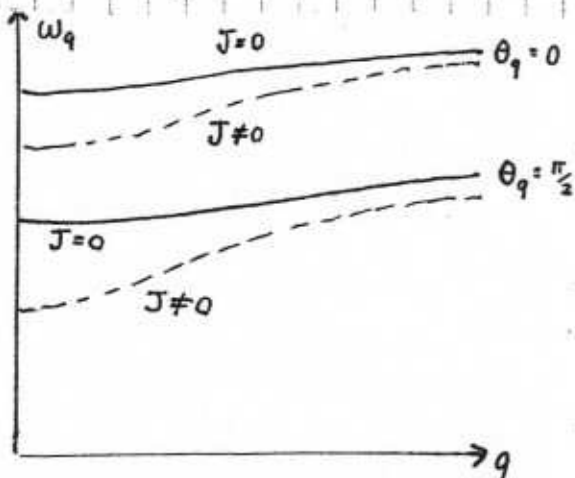$$\omega_q = (A_q^2 - |B_q|^2)^{1/2} \tag{76}$$

$$E_0 = C_0(H_0) + \frac{1}{2} \sum_q \left[A_q - (A_q^2 - |B_q|^2)^{1/2} \right] \tag{77}$$

To see what this looks like one takes the long wavelength limit of these expressions. One then finds that

$$(q a_0) \ll 1: \quad A_q \to g\mu_B(H_0 - 4\pi N_z M_0) + 2JS(q a_0)^2 + 2\pi g\mu_B M_0 \frac{q_x^2 + q_y^2}{q^2}$$
$$B_q \to 2\pi g\mu_B M_0 \frac{(q_x - iq_y)^2}{q^2} \tag{78}$$

where $M_0 = g\mu_B SN$, and where the demagnetisation factor

$$N_z = \frac{1}{3} + \frac{1}{4\pi N} \sum_j^{j \neq i} \frac{1}{|r_i - r_j|^3} \left(1 - 3 \frac{(\hat{z} \cdot (r_i - r_j))^2}{|r_i - r_j|^2} \right) \tag{79}$$

MAGNON SPECTRUM FOR SYSTEM IN 2 DIFFERENT DIRECTIONS; THE EXCHANGE $J \sim \frac{1}{3}$ THE DEMAGNETISATION FIELD.

The resulting dispersion relation then has the long-wavelength expansion, for $q a_0 \ll 1$:

$$\omega_q = \left[(\omega_0 + \alpha_1 q^2)\left(\omega_0 + \alpha_1 q^2 + \alpha_2\left(\frac{q_x^2 + q_y^2}{q^2} \right) \right) \right]^{1/2} \tag{80}$$

where

$$\omega_0 = g\mu_B(H_0 - 4\pi N_z M_0)$$
$$\alpha_1 = 2JS a_0^2$$
$$\alpha_2 = 4\pi g\mu_B M_0 \tag{81}$$

The complete dispersion is shown at left for a typical example. The magnons have now acquired an anisotropic energy, with a gap produced by both the external and "internal demagnetisation" fields.

Again, we could have derived the long-wavelength behaviour, by looking at the purely classical continuum theory. Then we would have seen the role of the demagnetisation field from the beginning. It is interesting to then notice that the symmetry-breaking field which generates a unique direction for the ferromagnetism no longer has to be applied externally - it is generated by the dipolar interaction itself.

We see from these considerations that the dipolar interaction is somewhat peculiar. In the original magnon basis we see that it is capable of creating (or destroying) pairs of magnons with opposite momenta - this is simply because the dipolar interaction itself breaks spin conservation, as is evident from its form:

$$\mathcal{H}_{dip} = \frac{1}{2} \sum_{ij} \hat{S}_i^\mu \, \mathcal{V}_{ij}^{\mu\nu} \, S_j^\nu \tag{82}$$

where we define the components

$$\hat{S}_i^\mu = \begin{pmatrix} S_i^z \\ S_i^+ \\ S_i^- \end{pmatrix} \tag{83}$$

and where

$$\mathcal{V}_{ij}^{\mu\nu} = V_{ij}^D \begin{pmatrix} D_{zz} & D_{+z} & D_{-z} \\ D_{z+} & D_{++} & D_{-+} \\ D_{z-} & D_{+-} & D_{--} \end{pmatrix} \tag{84}$$

with $V_{ij}^D = (g\mu_B)^2 / r_{ij}^2$ as before, and with matrix elements

$$
\begin{aligned}
D_{zz} &= (1 - 3\cos^2\theta_{ij}) & D_{z-} &= D_{z+} = -\frac{3}{2}\sin\theta_{ij}\cos\theta_{ij}\, e^{i\phi_{ij}} \\[2mm]
D_{++} &= -\frac{3}{4}\sin^2\theta_{ij}\, e^{-2i\phi_{ij}} & D_{+-} &= D_{-+} = -\frac{1}{4}(1 - 3\cos^2\theta_{ij}) \\[2mm]
D_{--} &= D_{++}^*
\end{aligned}
\tag{85}
$$

where we define the angles θ_{ij} and ϕ_{ij} for the interspin vector $\vec{r}_{ij} = \vec{r}_i - \vec{r}_j$, with respect to the reference axis $\hat{z}$. Implicit already in the dipolar interaction is thus an external source of spin angular momentum, and in a macroscopic system, this means an effective coupling between the shape of the system (and the magnetic poles at the surface) and the spins in the system, via the long-range demagnetisation field. This means that in the absence of either a magnetic field or any internal spin anisotropy field, the direction of $\underline{M}(r)$ will be determined by the shape of the sample - this phenomenon is known as "shape anisotropy".

One can also add the anisotropy term into the discussion, and calculate the resulting magnon dispersion. This is left as an exercise. The results are intuitively obvious - the magnon dispersion becomes anisotropic, and 2nd-order terms in S_j^α induce a gap in the spectrum. Again this gap lifts the $q=0$ gaplessness, and again one can understand this in terms of a rotational symmetry-breaking, in which the order parameter is now induced to lie along certain axes.

However the combination of dipole fields, exchange interactions, and anisotropy also leads to something qualitatively new, as we now see.

<u>Solitons in FM Insulators</u> : Suppose we start by considering the magnetisation $M(r,t)$ as a continuous field. Then it is a question of topology whether or not there can exist local configurations of $M(r,t)$ which are stable under continuous local deformations of $M(r,t)$. In a typical ferromagnet the energy cost incurred by <u>bending</u> $M(r)$ is far less then that incurred by suppressing it altogether, so we will assume that unless something drastic happens in a local region, that $|M(r,t)| \sim \underline{M}_0$ is roughly constant.

One can then find a whole variety of stable solitons, whose exact shape & energetics depends on the details of the Hamiltonian. They may be classified into point-like, line-like, & wall-like excitations. Here we shall look in a little detail at a simple wall, and then just say a few words about points & lines.

As a warm-up exercise, consider the following simple 1-d classical field problem, in which a field $\theta(x)$ has the Hamiltonian

$$\mathcal{H}_0 = \int dx \left[\tfrac{1}{2} c_0^2 \frac{d\theta}{dx} \quad \omega_0^2 \cos\theta(x) \right] \qquad (86)$$

and associated Lagrangian

$$L_0 = \int dx \ \tfrac{1}{2} \left(\frac{d}{dt} \right)^2 - \mathcal{H}_0 \qquad (87)$$

From the Euler-Lagrange eqtns for this system one recovers the eqtn of motion for $\theta(x,t)$:

$$\left(\partial_t^2 - c_0^2 \partial_x^2 \right) \theta(x,t) + \omega_0^2 \sin\theta(x,t) = 0 \qquad (88)$$

which is the classical 1-d Sine-Gordon eqtn of motion; when the amplitude of $\theta(x,t)$ is restricted to be small, ie $|\theta(x,t)| \ll 1$, it reduces to

$$\left(\partial_t^2 - c_0^2 \partial_x^2 \right) \theta(x,t) + \omega_0^2 \theta(x,t) = 0 \qquad |\theta(x,t)| \ll 1 \qquad (89)$$

This system has 2 kinds of excitation. The first, recovered immediately from the small oscillation eqtn (89), is a set of "quasiparticle" wave excitations :

$$\theta_q^{qp}(x,t) \sim \theta_0 \, e^{i(qx - \omega_q t)} \qquad \theta_0 \ll 1 \left.\begin{array}{c}\\[2em]\end{array}\right\} \qquad (90)$$

$$\omega_q^2 = \omega_0^2 + c_0^2 q^2$$

This model is well-known as the continuum analogue of a line of pendula hung from a spring, and it also possesses "kink" excitations, having the form

$$\theta_{\pm}^S(v;x,t) = 4 \tan^{-1} \left[\exp\left(\pm \frac{\omega_0}{c_0} \frac{x - vt}{(1 - v^2/c_0^2)^{1/2}} \right) \right] \qquad v \ll c_0 \qquad (91)$$

in which the field $\theta(x,t)$ "rotates" from 0 as $x \to -\infty$ to $\pm 2\pi$ as $x \to \infty$. This kink is the simplest kind of solitonic solution to a field theory — Its form is shown on the next page.

The important point I want to bring out is the way in which Sine-Gordon solitons interact with their quasiparticles. This is easily seen by choosing a solution

$$\theta_{\pm}(x,t) = \theta_{\pm}^S(x,t) + \bar\theta(x,t) \qquad |\bar\theta(x,t)| \ll 1 \qquad (92)$$

(b) **Solitons in FM Insulators** : Suppose we start by considering the magnetisation $M(r,t)$ as a continuous field. Then it is a question of topology whether or not there can exist local configurations of $M(r,t)$ which are stable under continuous local deformations of $M(r,t)$. In a typical ferromagnet the energy cost incurred by bending $M(r)$ is far less than that incurred by suppressing it altogether, so we will assume that unless something drastic happens in a local region, that $|M(r,t)| \sim M_0$ is roughly constant.

One can then find a whole variety of stable solitons, whose exact shape & energetics depends on the details of the Hamiltonian. They may be classified into point-like, line-like, & wall-like excitations. Here we shall look in a little detail at a simple wall, and then just say a few words about points & lines.

As a warm-up exercise, consider the following simple 1-d classical field problem, in which a field $\theta(x)$ has the Hamiltonian

$$\mathcal{H}_0 = \int dx \left[\frac{1}{2} c_0^2 \left(\frac{d\theta}{dx} \right)^2 - \omega_0^2 \cos\theta(x) \right] \tag{86}$$

and associated Lagrangian

$$L_0 = \int dx \, \frac{1}{2} \left(\frac{d\theta}{dt} \right)^2 - \mathcal{H}_0 \tag{87}$$

From the Euler-Lagrange eqtns for this system one recovers the eqtn of motion for $\theta(x,t)$:

$$\left(\partial_t^2 - c_0^2 \partial_x^2 \right) \theta(x,t) + \omega_0^2 \sin\theta(x,t) = 0 \tag{88}$$

which is the classical 1-d Sine-Gordon eqtn of motion; when the amplitude of $\theta(x,t)$ is restricted to be small, ie $|\theta(x,t)| \ll 1$, it reduces to

$$\left(\partial_t^2 - c_0^2 \partial_x^2 \right) \theta(x,t) + \omega_0^2 \theta(x,t) = 0 \qquad |\theta(x,t)| \ll 1 \tag{89}$$

This system has 2 kinds of excitation. The first, recovered immediately from the small oscillation eqtn (89), is a set of "quasiparticle" wave excitations:

$$\left. \begin{aligned} \theta_q^{QP}(x,t) &\sim \theta_0 \, e^{i(qx - \omega_q t)} \qquad \theta_0 \ll 1 \\ \omega_q^2 &= \omega_0^2 + c_0^2 q^2 \end{aligned} \right\} \tag{90}$$

This model is well-known as the continuum analogue of a line of pendula hung from a spring, and it also possesses "kink" excitations, having the form

$$\theta_\pm^S(v; x,t) = 4 \tan^{-1} \left[\exp \left(\pm \frac{\omega_0}{c_0} \frac{x - vt}{(1 - v^2/c_0^2)^{1/2}} \right) \right] \qquad v < c_0 \tag{91}$$

in which the field $\theta(x,t)$ "rotates" from 0 as $x \to -\infty$ to $\pm 2\pi$ as $x \to \infty$. This kink is the simplest kind of solitonic solution to a field theory. Its form is shown on the next page.

The important point I want to bring out is the way in which Sine-Gordon solitons interact with their quasiparticles. This is easily seen by choosing a solution

$$\theta_\pm(x,t) = \theta_\pm^S(x,t) + \bar{\theta}(x,t) \qquad |\bar{\theta}(x,t)| \ll 1 \tag{92}$$

94

Since $\tilde{\theta}(x,t)$ is small, we can linearize the resulting eqtn. with (92) substituted into (86), to get the following result for a __stationary__ soliton $(v=0)$: We write $\tilde{\theta}(x,t)$ as
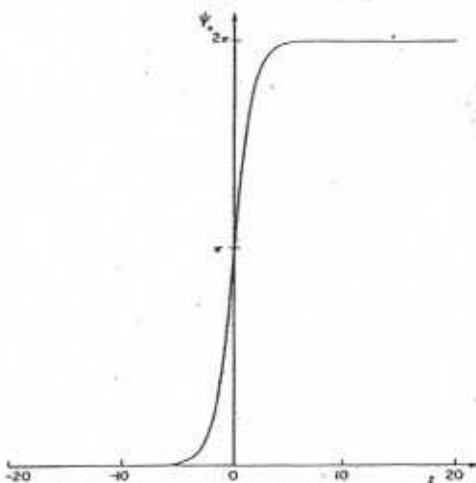
$$\tilde{\theta}(x,t) = \chi(r)\, e^{-i\omega t} \tag{93}$$

and immediately find that

$$c_0^2 \frac{d^2}{dx^2}\chi(x) + \left[\omega^2 - \omega_0^2\left(1 - 2\,\mathrm{sech}^2 q_0 x\right)\right]\chi(x) = 0 \tag{94}$$

where $q_0 = \omega_0/c_0$. This is just a Schrödinger-type eqtn., with soltns:

(a) $\qquad \chi_0(x) = 2q_0\,\mathrm{sech}\,q_0 x \qquad\qquad\qquad \Omega_0 = 0$

(b) $\chi_q(x) = \frac{1}{\sqrt{2\pi}}\left(\frac{c_0}{\omega_q}\right)e^{iqx}\left[q + iq_0\tanh q_0 x\right] \qquad \omega_q^2 = \omega_0^2 + c_0^2 q^2$ $\qquad\Big\}$ (95)

PROFILE OF THE 1-d SOLITON SOLUTION OF EQTN (95), AS A FUNCTION OF THE DIMENSIONLESS VARIABLE $z = q_0 x$.

Now the first of these 2 solutions is for the soliton itself - the so-called "zero mode". We shall see how this achieves its full flowering when we go to higher dimensions - right now we just think of it as a zero-energy bound state for quasiparticles.

The 2nd set of quasiparticle modes has the same energy as before, but they are excluded from the soliton now - they are orthogonal to the bound state:

$$\int dx\, \chi_q(x)\,\chi_{q'}(x) = \delta(q-q')$$
$$\int dx\, \chi_q(x)\,\chi_0(x) = 0 \qquad\qquad \Big\} \quad (96)$$

Notice moreover that a quasiparticle wave going through the soliton suffers a phase shift

$$\delta_q = \pi\frac{q}{|q|} - 2\tan^{-1}(q/q_0) \tag{97}$$

but is otherwise not scattered by it. Note also that we can generalize all this to a finite wall velocity by "Lorentz-boosting" (94)-(96); the problem is Lorentz-invariant.

Now let us go to 3 dimensions, & consider the "Bloch wall" problem, in which we have an easy-axis anisotropy, and in the continuum approximation, an effective Hamiltonian:

$$\mathcal{H}_{eff} = \tfrac{1}{2}\int d^3r \left\{ \bar{J}\left(\nabla\underline{M}(r,t)\right)^2 + \bar{K}_z M_z^2(r,t) - \hbar\gamma\,\underline{M}(r,t)\cdot\left(\underline{H}_0 + \underline{H}_{dm}(r,t)\right)\right\} \tag{98}$$

where we define $\bar{J} = J/(g^2\mu_B^2 a_0^3)$, $\bar{K} = K/g^2\mu_B^2 a_0^3$, and all other quantities appeared previously in (47) and (48); in fact we have just rewritten (47).

In this system we will assume that $\bar{K} > 0$, so that $\underline{M}(r)$ prefers to lie $\perp \hat{z}$. Now the planar Bloch wall solution is obtained by a simple generalization of the 1-d soliton discussion. Let us assume a flat wall moving along the z-direction, with the magnetisation lying essentially in the x-y plane. We can add a very small anisotropy which tends to orient the magnetisation in the x-y plane - we will make this preferred axis the $\hat{x}$-axis, so that our final anisotropy term is

$$H_k = -\frac{1}{2}\int d^3r\left(\bar{K}_z M_z^2(\underline{r}) + \bar{K}_y M_y^2(\underline{r})\right) \left.\begin{array}{c}\\ \\ \end{array}\right\} \quad (99)$$
$$\bar{K}_z \gg \bar{K}_y > 0.$$

The wall configuration we are thinking of is shown in the Fig. below. If the wall is stationary then there will be no wall magnetisation in the $\hat{z}$-direction, ie, all the spins will stay in the wall plane. This is not just because of the anisotropy. The wall is kept flat by the demagnetisation field, since a flat wall has no surface poles. Any curvature of the wall creates such poles, ie, allows dipolar fields to come out of the wall, thereby increasing its energy.

If the wall begins to move, it is impossible to prevent a small component of magnetisation from "leaking" out of the wall – this is because all spins in the wall must turn over from up to down as the wall passes through them. To lowest approximation, they must do this in a field which is in the wall plane (in the absence of any external field); but their motion then creates a torque which forces them to point partly out of the plane. The solution to this rather complex self-consistency problem gives a magnetisation profile, for a wall of +ve chirality, of

(a)
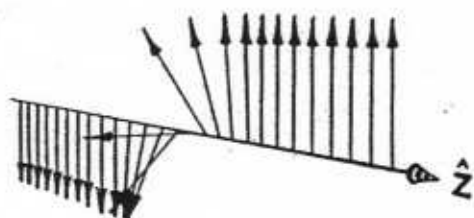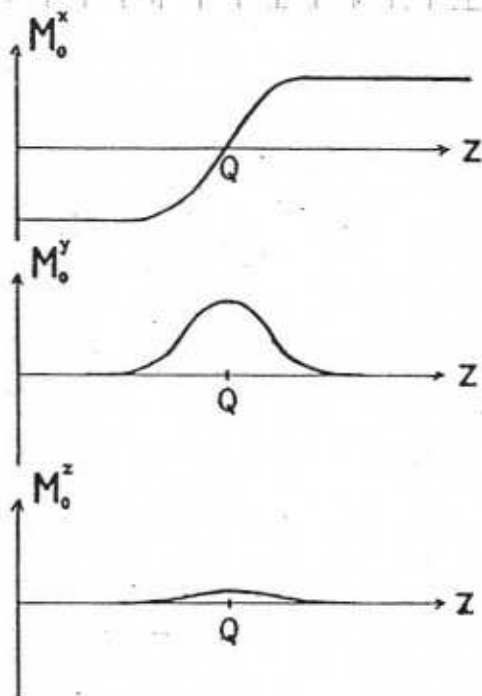
(a)   (b)

The basic planar Bloch wall configuration. In (a) the spin configuration is shown along a line which moves perpendicular to the wall, and through it (i.e., along $\hat{z}$). In (b), graphs are plotted for M_0^x, M_0^y, and M_0^z, along this same line, for a slowly moving wall.

$$M_W^x(\underline{r},t) = M_0\cos\theta(\underline{z}) = M_0\tanh\left(\frac{z-Q(t)}{\lambda}\right) \left.\begin{array}{c}\\ \\ \\ \\ \\ \end{array}\right.$$

$$M_W^y(\underline{r},t) = M_0\sin\theta(z)\cos\phi(z) = M_0\left(1-\frac{\dot{Q}^2}{8c_0^2}\right)\text{sech}\left(\frac{z-Q(t)}{\lambda}\right) \left.\begin{array}{c}\\ \\ \end{array}\right\} \quad (100)$$

$$M_W^z(\underline{r},t) = M_0\sin\theta(z)\sin\phi(z) = M_0\frac{\dot{Q}}{8c_0}\text{sech}\left(\frac{z-Q(t)}{\lambda}\right) \left.\begin{array}{c}\\ \\ \\ \end{array}\right.$$

where we have used a set of spherical coordinates with θ measured from the x-axis. The wall thickness λ is given by

$$\lambda = \left(\frac{J}{K}\right)^{1/2}a_0 \quad (101)$$

and the "Walker velocity" is

$$c_0 = 4\pi\gamma\lambda \quad (102)$$

The wall has an inertial mass, which can be calculated by looking at the extra energy obtained from the interaction between M_W^z and the demagnetization field when the wall is moving. This gives an energy $\frac{1}{2} m_W \dot{Q}^2$, where

$$m_W = A_W \left(\frac{2}{\mu_0 \gamma^2} \right) \frac{1}{\lambda} \qquad (103)$$

Finally, the energy of the wall is

$$E_W = \sigma_W A_W = 4 (\bar{J}\bar{K})^{\frac{1}{2}} A_W \qquad (104)$$

where σ_W is the energy per unit area, and A_W the wall area.

The Bloch wall is just one example of a magnetic domain wall — many others exist, depending on the crystal symmetry. Domain walls like this also interact with magnons, in just the same way that we saw for the 1-d Sine-Gordon soliton. We may summarize the results as follows:

(i) We define a magnetisation profile $M(\underline{r},t) = (M_W(\underline{r},t) + \delta M(\underline{r},t))$, and then quantize the components $\delta \underline{M}, \delta \underline{M}$ using a Holstein-Primakoff representation. The resulting magnons, in a continuum theory, are then described by magnon field operators $b(\underline{r},t)$, $b^+(\underline{r},t)$, which in the presence of a single wall at $z = \underline{Q}$ is described by an energy

$$\mathcal{H}_m^{(2)} = \int d^3 r \left[\Delta_0^2 \lambda^2 |\nabla_r b(\underline{r},t)|^2 + (U(z) + 4\pi\hbar\gamma M_0) b^+(\underline{r},t) b(\underline{r},t) \right] \quad \Bigg\} \quad (105)$$

$$U(z) = \Delta_0 \left[1 - 2 \, \text{sech}^2 \left(\frac{z - Q(t)}{\lambda} \right) \right]$$

where the energy gap is

$$\Delta_0 = 2\hbar\gamma \bar{K}_z / M_0 \qquad (106)$$

and comes from the easy axis anisotropy. A general solution to the equation of motion for $b(\underline{r},t)$ which results from (105) can then be written as (for a stationary wall):

$$b(\underline{r},t) = b(\underline{r}) e^{-i\omega t} \qquad b^+(\underline{r},t) = b^+(\underline{r}) e^{i\omega t} \qquad (107)$$

with

$$b(\underline{r}) = \sum_K \Phi_K(\underline{r}) b_W^+ + \sum_q \psi_q(\underline{r}) b_B^+ \qquad (108)$$

and with amplitudes

$$\Phi_K(\underline{r}) = \frac{1}{(\lambda A_W)^{\frac{1}{2}}} e^{iK \cdot \rho} \, \text{sech} \left(\frac{z - Q}{\lambda} \right) \qquad (109)$$
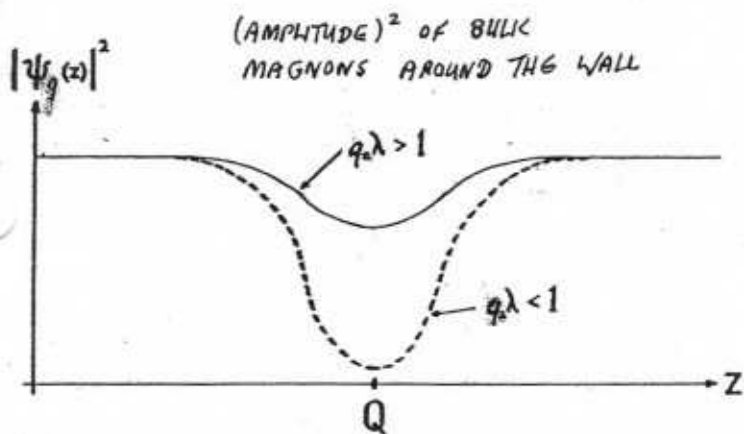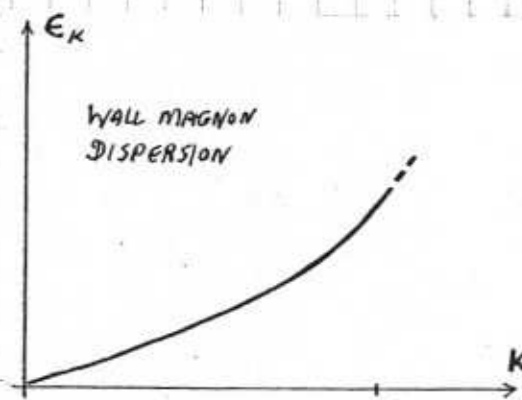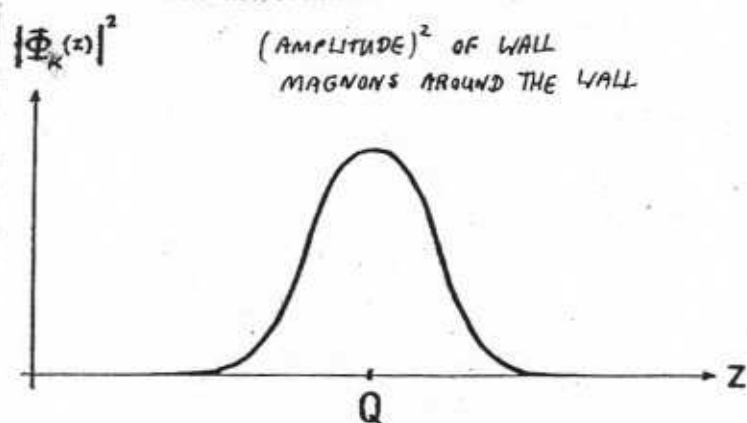
$$\psi_q(\underline{r}) = e^{iq \cdot r} \frac{1}{(1 + \lambda^2 q_z^2)^{\frac{1}{2}}} \left[\tanh \left(\frac{z - Q}{\lambda} \right) - i q_z \lambda \right] \qquad (110)$$

where $\rho = (x,y)$ is a vector describing position in the wall plane. The magnon field has divided into 2 sectors, one confined to the wall, with amplitude $\Phi_K(\underline{r})$ and wave vector K in the wall plane, and one defined throughout the bulk system, with amplitude $\psi_q(\underline{r})$ and wave-vector q.

The energy spectrum of these modes also comes out of this calculation; one finds:

$$\omega_q^2 = (\Delta_0 + \alpha q^2)(\Delta_0 + \alpha q^2 + 4\pi \hbar \gamma M_0) \qquad \text{(bulk modes)}$$

$$\varepsilon_\kappa^2 = \alpha \kappa (\alpha \kappa + 4\pi \hbar \gamma M_0) \qquad \text{(wall modes)} \qquad \qquad (111)$$

In the Fig. below we plot the (amplitudes)^2 and the energies of these modes - note how high-momentum modes are much less seriously affected than the long-wavelength bulk modes by the presence of the wall.

(AMPLITUDE)^2 OF WALL MAGNONS AROUND THE WALL

$|\Phi_\kappa(z)|^2$

WALL MAGNON DISPERSION

ε_κ

(AMPLITUDE)^2 OF BULK MAGNONS AROUND THE WALL

$|\psi_q(z)|^2$

$q_a \lambda > 1$

$q_a \lambda < 1$

BULK MAGNON DISPERSION

ω_q
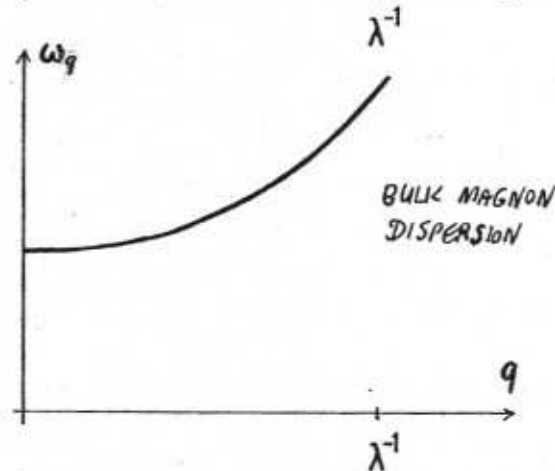
There is a semi-classical interpretation of these quantized wall modes, which in the quantum theory are magnon bound states. In this interpretation, they correspond to wave-like flexural oscillations of the wall, with very small amplitude.

One can summarize the results of all this in the form of an effective Hamiltonian for the (wall + magnon) system, as follows:

$$\mathcal{H}_{eff} = \frac{1}{2} m_W \dot{Q}^2 + \mathcal{H}_m^{eff}$$

$$\mathcal{H}_m^{eff} = \mathcal{H}_m^{(2)} + \mathcal{H}_m^{(3)} + \mathcal{H}_m^{(4)} + \cdots \qquad \qquad (112)$$

where $\mathcal{H}_m^{(n)}$ describes the coupling between n magnons and the wall - the term we have just been discussing involves a quadratic form in the magnon operators, so that $n = 2$.

The form of these higher couplings is very complicated, and quite beyond the scope of these lectures. We will refer to them again, however, when we come to look at large-scale quantum phenomena in magnetic systems. We see from this formalism, incidentally, that the dynamics of real domain walls in a magnetic system is liable to be very complex, since it will involve interactions between

the wall, the bulk magnons, and the wall magnons. The dissipation caused by all of these processes when a wall is moving is essentially a transfer of energy & momentum from the wall into the wall & bulk modes. In principle this can cause instabilities of the wall shape, if too much energy is pumped into the wall magnons. Note that the wall magnons and bulk magnons are coupled, both directly at higher orders and via the wall, so eventually all of the energy will pass to the bulk modes.
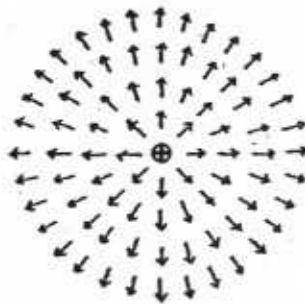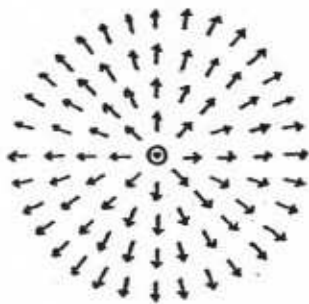
(i)

(ii)

(iii)

(iv)

(v)

(vi)
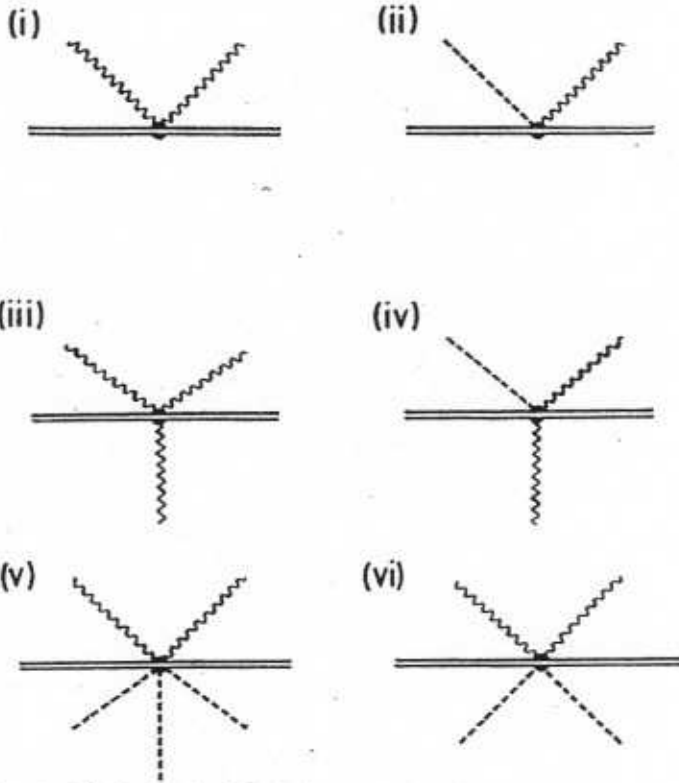
SCATTERING VERTICES INVOLVING A FM DOMAIN WALL (DOUBLE LINE), BULK MAGNONS (WAVY LINES) AND WALL MAGNONS (HATCHED LINE). PROCESSES (i) & (ii) ARE INCLUDED IN $\mathcal{H}_m^{(2)}$ IN EQTN. (105).

The problem of interacting magnons is inherently non-linear, which is what makes it so complex. The non-linearity stems in the formalism from the form of the HP expansion, with the square-root. Ultimately the non-linearity, and the square root in the HP operator representation of spin, arises from the constraint that we cannot have an unlimited bosonic occupation of any site, or of any particular magnon mode. Such constraints always need to non-trivial interactions in a field theory.

Domain walls are not the only solitonic modes in a system with the simple $O(3)$ FM order parameter. One can also have line-like (vortex) solutions, which can either exist in an "easy-plane" system, where the magnetisation vector likes to lie in the plane because of a positive $K_2 S_z^2$ term in the anisotropy, or they can be found inside domain walls themselves.

The vortex solutions are interesting, because they provide a nice illustration a non-trivial topological quantum number which is conserved. Suppose we define the "gyrovector" $G(r)$, with components

$p=1 \quad q=1$

$p=-1 \quad q=1$

2-d VORTEX or "MERON" CONFIGS

$p=1 \quad q=-1$

$p=-1 \quad q=-1$

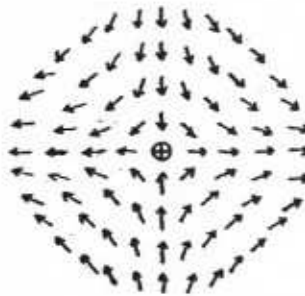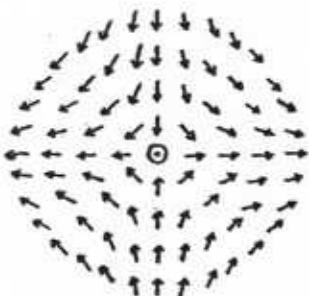$$G^i(r) = \epsilon^{ijk} \epsilon_{abc}\, \hat{m}^a\, \nabla_j\, m^b\, \nabla_k\, m^c \qquad (113)$$

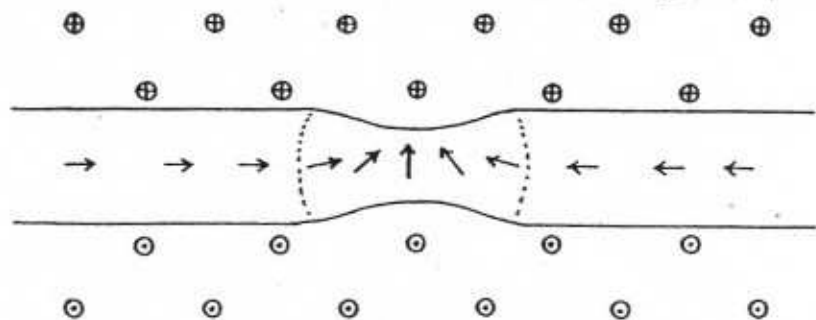This vector measures a kind of density of "splay" at a given point. We can also write:

$$G(r) = (\nabla\theta(r) \times \nabla\phi(r))\sin\theta(r) \qquad (114)$$

where $m = M(r)/M_0$ is a unit vector in the direction of the magnetisation, and θ, ϕ are polar coordinates of

ABOVE: BLOCH LINE IN A DOMAIN WALL

RIGHT: A BLOCH POINT

$m(r)$. We can define also a topological charge

$$q(r) = \epsilon^{ij} \epsilon_{abc} \, m^a \nabla_i m^b \nabla_j m^c \Big\}$$

$$\equiv \epsilon^{ij} \, m \cdot (\nabla_i m \times \nabla_j m) \Big\} \quad (11)$$

and the associated "Skyrmion charge", or "Pontryagin index":

$$Q = \frac{1}{8\pi} \int d^D r \; q(r) \qquad (116)$$

The skyrmion charge is a quantity, like the winding number, which must take integer values and which is conserved for a system, unless we are allowed to somehow take charge in and out of the system.

In the case of an easy plane system, one can easily show that for a vortex at $r = r_j$,

$$Q_j = P_j q_j = \pm 1 \Big\}$$

$$P_j = \pm 1 \qquad q_j = \pm 1 \Big\} \quad (117)$$

where the core charge P_j indicates the direction of $m(r)$ in the core (along $\pm z$) and q_j is the winding number. In fact for a simple easy axis vortex, with the effective Hamiltonian in (98) (and assuming H_o and H_{dm} can be ignored) one has a magnetisation profile

$$\cos \theta(r) = p \, e^{-r^2/2\lambda} \Big\}$$

$$\phi(r) = q \tan^{-1}(y/x) \Big\} \quad (118)$$

One can also classify Bloch points by their Pontryagin index $\mathcal{P} = \pm 1$. As one might expect, the dynamics of these objects is not simple. Magnetic vortices have properties somewhat similar to superfluid vortices (including a "Magnus force"), but the moment one includes coupling to magnons, things become rather complex. The same is true of Bloch points.

Even domain walls have interesting topological properties. Thus we notice in the picture on p.95 that the sense of twist of $m(r)$ as one passes through the wall has one of 2 possible chiralities. In a simple treatment, the chirality of the wall is unimportant to its properties, but in fact some environments (eg, transverse phonons) can distinguish between the two.

This should raise in your minds the question of how these solitons will behave if they are treated fully quantum-mechanically. In fact their topological properties generally survive, but one can imagine tunneling processes which take one from one topological configuration to another. More generally, those objects like walls or lines which up to now we have given a semi-classical description must ultimately be described quantum-mechanically, and this opens up the way to a host of remarkable phenomena, to be described later on.

C.3.2. SPIN WAVES IN ANTIFERROMAGNETS

Most of the theory of the antiferromagnetic state (AFM) is a straightforward adaptation of what we already learned for the FM state. However there is one interesting conceptual question associated with the existence of the AFM state, which is most easily examined once we have determined the spectrum of AFM magnons. Note that AFM systems also possess soliton excitations, but they are hard to observe and I will not discuss them here.

(a) AFM spin waves / magnons : The FM order parameter and ground state are in one respect very simple. The FM ground state is written as

$$|0\rangle_{FM} = \prod_{j=1}^{N} c_{j\uparrow} |VAC\rangle \qquad (spin\text{-}\tfrac{1}{2}) \tag{119}$$

and if we assume the simple exchange Hamiltonian

$$\left. \begin{aligned} \mathcal{H} &= \tfrac{1}{2} \sum_{ij} J_{ij} \, \underline{S}_i \cdot \underline{S}_j \\ &\equiv \sum_{ij} J_{ij} \left(\hat{P}_{ij} - \tfrac{1}{2} \right) \end{aligned} \right\} \tag{120}$$

where $\hat{P}_{ij}$ is the Dirac exchange operator, then we see that the order parameter of the system is conserved :

$$\dot{\underline{S}}_{tot} = \frac{d}{dt} \sum_j \underline{S}_j (t) = \frac{-i}{\hbar} [\underline{S}_{tot}, \mathcal{H}] = 0 \qquad (FM) \tag{121}.$$

We also saw that in the presence of dipolar interactions this conservation law was no longer necessarily obeyed. The same is true of the AFM state, which we write as

$$|0\rangle_{AFM} = \prod_{i \in A} \prod_{j \in B} c_{i\uparrow}^{+} c_{j\downarrow}^{+} |VAC\rangle \qquad (spin\text{-}\tfrac{1}{2}) \tag{122}$$

where we divide the system into 2 sublattices. The macroscopic order parameter in question is now the Néel vector $\underline{N}$, defined as

$$\underline{N} = \left(\sum_{i \in A} \underline{S}_j - \sum_{j \in B} \underline{S}_j \right) \tag{123}$$

and it is easy to verify that

$$\dot{\underline{N}}(t) = -\frac{2}{\hbar} \sum_{i \in A} \sum_{j \in B} (\underline{S}_i \times \underline{S}_j) \tag{124}$$

At first glance this seems to be a harmless result, because <u>classically</u>, $\underline{S}_i \times \underline{S}_j = 0$ for the AFM state. But this conclusion is <u>wrong</u> ; eqtn (124) is an operator eqtn, and it is clear that the RHS, acting on the state $|0\rangle_{AFM}$, does not give zero! We could have expected this already just by noting that the exchange Hamiltonian clearly has matrix elements between states with $\underline{N} = \hat{z} N_0$ and $\underline{N} = -\hat{z} N_0$, since the exchange operator $\hat{P}_{ij}$ exchanges spins between sub-lattices A and B.

Thus, just as in the case of a dipolar FM, we see that there is a rather clear paradox - how can we define a physically meaningful order parameter if it is not conserved ?

We will return to this question below and analyze it properly. However to understand it properly we first need to look at what one gets using a naive calculation of the spin wave spectrum of the system. There are various ways of doing this. The most simple conceptually is to define HP operators separately for the 2 sublattices, and then calculate their coupled dynamics. In an equivalent but

formally simpler calculation, we make the following formal transformation on the spin operators:

$$\text{sub-lattice } A: \qquad \underline{S}_i \to \underline{S}_i$$

$$\text{sub-lattice } B: \qquad S_j^z \to -S_j^z \qquad S_j^y \to -S_j^y \qquad S_j^x \to S_j^x$$

so that

$$\text{sub-lattice } B: \qquad S_j^+ \to S_j^- \qquad S_j^- \to S_j^+ \qquad\qquad (126)$$

and the Hamiltonian is transformed to (using $S_j^z \approx S - S_j^- S_j^+/2S$ for small deviations):

$$\mathcal{H}' = -\tfrac{1}{2} J \sum_{<ij>} \left(S_i^z S_j^z + S_i^y S_j^y - S_i^x S_j^x \right)$$

$$\approx -\tfrac{N}{2} J Z S^2 + \tfrac{1}{2} \sum_{<ij>} \left[\left(S_i^- S_i^+ + S_j^- S_j^+ \right) + \left(S_i^+ S_j^+ + S_i^- S_j^- \right) \right]$$

where Z is the coordination number of the lattice. Converting to HP operators & Fourier transforming we get

$$\mathcal{H}' = -\tfrac{N}{2} J Z S^2 + \tfrac{1}{2} J S \sum_q \left[Z \left(b_q^+ b_q + b_{-q}^+ b_{-q} \right) + \sum_{<ij>} e^{iq \cdot r_{ij}} \left(b_q b_{-q} + b_q^+ b_{-q}^+ \right) \right] \qquad (128)$$

Thus we are faced with exactly the same problem as before, and we can deal with it in the same way, using the following HP/Bogoliubov transformation:

$$\underline{b}_q = \hat{U}_q \underline{\beta}_q \qquad\qquad \underline{\beta}_q = \hat{U}_q^{-1} \underline{b}_q$$

with

$$U_q = \begin{pmatrix} u_q & -v_q \\ -v_q & u_q \end{pmatrix}_{4\times4} \qquad U_q^{-1} = \begin{pmatrix} u_q & v_q \\ v_q & u_q \end{pmatrix}_{4\times4}$$

and

$$u_q^2 - v_q^2 = 1$$

with the 4-d vector the same as in (92); and we can if we wish parametrise the coefficients as

$$u_q = \cosh \theta_q/2$$

$$v_q = \sinh \theta_q/2 \qquad\qquad \tanh \theta_q = \tfrac{1}{Z} \sum_{<ij>} e^{iq \cdot r_{ij}} \qquad (130)$$

We now have the Hamiltonian in the form

$$\mathcal{H}' = -\tfrac{N}{2} J Z S^2 - J Z N S + \sum_q \hbar \omega_q \beta_q^+ \beta_q \qquad\qquad (131)$$

$$\omega_q = J S Z \left[1 - \tanh^2 \theta_q \right]^{1/2} \equiv J S \left[Z^2 - \left(\sum_{<ij>} e^{iq \cdot r_{ij}} \right)^2 \right]^{1/2}$$

$$\xrightarrow[q a_0 \ll 1]{} J Z S (q a_0) \equiv c_s q \qquad\qquad (132)$$

Thus we derive the well-known result that a Heisenberg AFM has a spin wave spectrum with ω_q linear in q (whereas the Heisenberg FM has a spectrum $\omega_q \sim q^2$, i.e., quadratic in q).

Note that if we add an external field and/or spin anisotropy, the spin wave again becomes gapped. In fact it is fairly easy to show that for an AFM with exchange anisotropy, in the form of a Hamiltonian
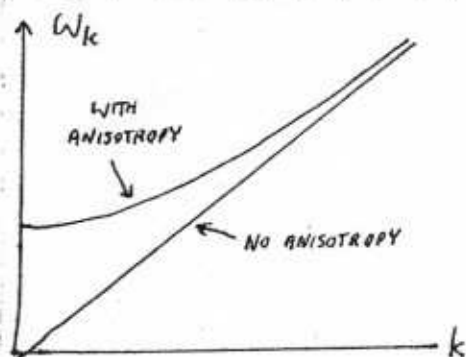
$$\mathcal{H} = \frac{1}{2}\sum_{<ij>}\left[J_z S_i^z S_j^z + J_\perp(S_i^x S_j^x + S_i^y S_j^y)\right] + K_2\sum_j (S_j^z)^2 \tag{133}$$

with $K_2 > 0$, we get the new spectrum

$$\omega_q^2 = \omega_0^2 + C_s^2 q^2 \tag{134}$$

with

$$\left. \begin{aligned} \omega_0^2 &= (g\mu_B)^2\left[(H_J + H_K)^2 - \frac{J_\perp^2}{J_z^2}H_J^2\right] \\ &\sim 2(g\mu_B)^2 H_J H_K \end{aligned} \right\}$$

where we have

$$\left. \begin{aligned} H_J &= Jz S/g\mu_B \\ H_K &= 2K_2 S/g\mu_B \end{aligned} \right\} \tag{136}$$

The interesting thing to note here is how much more sensitive the AFM gap is to anisotropy than the FM gap. The FM magnon spectrum for the isotropic Heisenberg model is already quadratic at low q; adding an anisotropy energy $g\mu_B H_K$ simply raises the spectrum bodily by this amount. However in an AFM system, even a tiny anisotropy energy $g\mu_B H_K$ bounces the gap up to a value $\sim g\mu_B\sqrt{H_J H_K}$. For example, in K_2NiF_4, $J \sim 10$ meV but $K \sim 0.02$ meV, but still the gap $\omega_0 \sim 2.2$ meV.

(b) <u>Quantum Fluctuations in the Néel state</u>: One can see already how the existence of spin wave excitations lowers the energy of the Néel AFM below its classical value. The classical ground state energy is

$$E_0^{class} = -\frac{N}{2}Jz S^2 \tag{137}$$

and the result (131) lowers this by another $Jz SN$. This is analogous to the kinetic reduction of energy when we switch on hopping in the Hubbard model. It is interesting to look at the corresponding reduction in the staggered spin density — one finds that

$$\left. \begin{aligned} \frac{1}{N}\langle N\rangle &\equiv \frac{1}{N}\left\langle \sum_{i\in A}\hat{S}_i^z - \sum_{j\in B}\hat{S}_j^z\right\rangle = S - \frac{2}{N}\sum_q V_q^2 \\ &= S - \frac{1}{N}\sum_q\left[\frac{1}{(1-\tanh^2\theta_q)^{1/2}} - 1\right] \end{aligned} \right\} \tag{138}$$

so that we get a reduction $\Delta N \sim \int\frac{d^D q}{q}$ in the magnitude of the Néel vector per site.

This reduction of $\underline{N}$ is our first consistency check on the validity of a spin wave expansion about the classical Néel state. It tells us immediately that the whole idea fails when $D=1$, i.e., we cannot expect a Néel state to be physically meaningful in 1 dimension.

THE MAGNON SPECTRUM FOR THE ANTIFERROMAGNET.